

# 16

## Elements of Cardiac Function

### LEARNING OBJECTIVES

Upon completion of this chapter, the student should be able to answer the following questions:

1. How does the action potential contribute to excitability and contraction in heart muscle?
2. What is automaticity, and how does it differ from excitability? How do derangements of these properties contribute to arrhythmias?
3. What is the structural basis of the electrocardiogram?
4. What are preload and afterload and how do they regulate contraction of the heart?
5. What is the local control theory of cardiac excitation-contraction coupling?
6. What changes occur in atrial and ventricular pressures and volumes during a cardiac cycle, and what is their temporal relation to the electrocardiogram?
7. How does the relation between end-diastolic volume and left ventricular developed pressure define the Frank-Starling law of the heart and regulate the force of cardiac contraction?
8. What is the pressure-volume loop of the left ventricle, and how does it define changes in left ventricular function?
9. How is cardiac metabolism linked to O<sup>2</sup> consumption, and how are these processes affected by changes in cardiac work?

### Overview of Cardiac Function

The human heart typically beats over 3 billion times during an average lifetime, accomplishing a truly extraordinary amount of physical work. Essential to this task is the ability to adjust the rate of beating, the strength of contraction, and the rate of relaxation. Efficient ejection of blood into arteries requires precise timing of electrical activation and contraction of the ventricles, as provided by specialized pacemaker tissue and a conduction system. The cellular processes that comprise excitation-contraction (E-C) coupling produce a change in cytoplasmic [Ca<sup>++</sup>] of the cardiac myocytes that activates the contractile proteins (actin, myosin). E-C coupling processes are regulated by hormones and the autonomic nervous system. The output of the heart is also affected by conditions in the systemic vasculature, such as total peripheral vascular resistance and venous capacitance. Finally, the need for constant and considerable metabolic energy is associated with a high reliance on oxidative phosphorylation of available metabolic substrates.

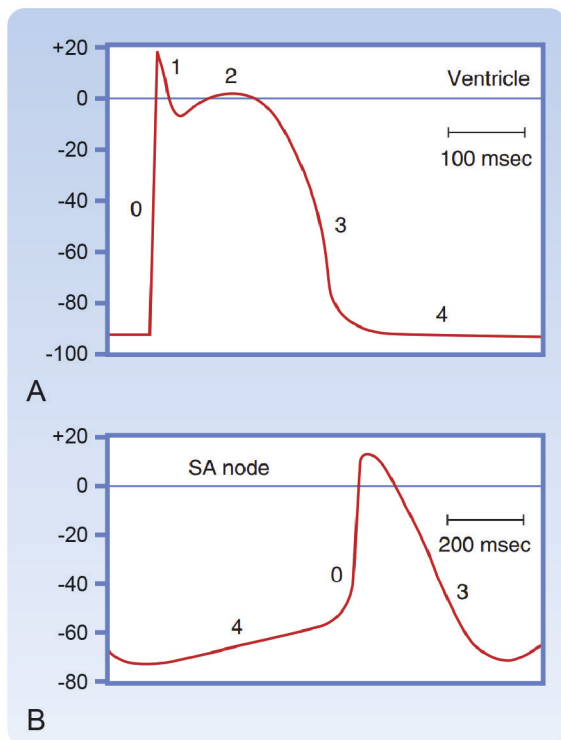
### Electrical Properties of the Heart

Cardiac myocytes, like neurons, are excitable cells capable of generating action potentials. However, the primary function of the heart is to pump blood throughout the circulatory system. For this to occur, an orderly sequence of events must take place at a given interval. This is accomplished through the initiation of an action potential and the propagation of this impulse throughout the heart. The cardiac action potential is important not only because it is the trigger that initiates contraction of individual myocytes through the process of E-C coupling, but also because it synchronizes the contraction of the entire heart as it is conducted from cell to cell. Furthermore, while the heart possesses the property of intrinsic automaticity, it is continually under the influence of both intrinsic and extrinsic mechanisms that modulate its activity to meet the demands of the body. Therefore, altering the electrical properties of the heart is an important means by which cardiac function can be controlled. In this section, the electrical properties of cardiac cells and tissues are described. In addition, how these electrical properties account for the **electrocardiogram (ECG)** is discussed. The coupling of electrical and mechanical activity of cardiac cells is considered in a later section.

### Cardiac Action Potentials

The human heart contains billions of cardiac myocytes, and although they are all capable of generating an action potential, not all action potentials are alike. The actual configuration of the action potential is related to the functional role of the myocyte in which it occurs. However, in general, cardiac myocytes can be categorized as exhibiting either **fast-response** or **slow-response** action potentials. Examples of each are illustrated in Fig. 16.1.

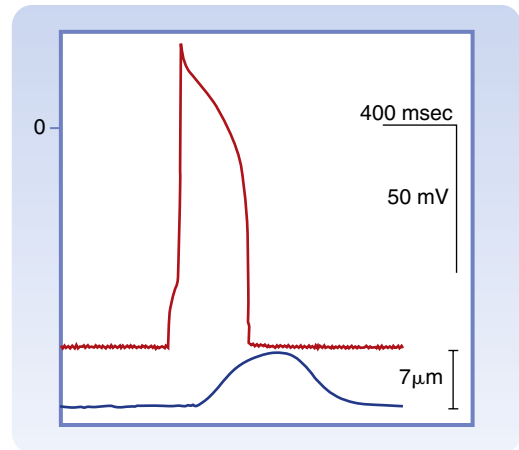
Fast-response action potentials are found in **atrial and ventricular myocytes**, which make up the bulk of the contractile cells found in the heart. Fast-response action potentials are also found in myocytes like those that make up **Purkinje fibers**, which are part of the specialized conducting system responsible for transmitting electrical impulses rapidly to all areas of the ventricular myocardium. A fast-response action potential can be divided into five phases: upstroke (phase 0), initial repolarization (phase 1), plateau (phase 2), final repolarization (phase 3), and resting



• **Fig. 16.1** Examples of typical **(A)** fast-response (ventricular) and **(B)** slow-response (sinoatrial node) action potentials. Action potential phases are labeled (see text for details). Note: compared to fast-response cells, in slow-response cells the action potential upstroke (phase 0) is less steep, the amplitude is smaller, there is no initial repolarization (phase 1) or plateau (phase 2), and the diastolic membrane potential (phase 4) is less negative. (From Hoffman BF, Cranefield PF. *Electrophysiology of the Heart*. New York: McGraw-Hill; 1960.)

membrane potential (phase 4). These action potentials have several other key characteristics. First, as the name implies, they exhibit a rapid change in membrane potential during the upstroke (phase 0). This facilitates rapid propagation of impulses from cell to cell. These action potentials also exhibit a pronounced plateau (phase 2), which gives them the characteristic long duration (200–400 msec). Another important property is that during diastole (phase 4), which is when the heart is relaxed or at rest, the membrane potential is quite negative (approximately  $-90$  mV). The relationship between the fast-response action potential and contraction of a ventricular myocyte is shown in Fig. 16.2. Rapid depolarization (phase 0) precedes cell shortening, and completion of repolarization occurs just before peak shortening. Relaxation of the muscle takes place mainly during phase 4 of the action potential. The duration of contraction usually parallels the duration of the action potential.

Slow-response action potentials are found in myocytes that make up the **sinoatrial (SA) node**, which is the normal pacemaker region of the heart, and the **atrioventricular (AV) node**, which is the specialized tissue that conducts electrical impulses from the atria to the ventricles. These action potentials have just three phases: upstroke (phase 0), final repolarization (phase 3), and diastole (phase 4). A key feature of these action potentials is the slow upstroke velocity (phase 0).



• **Fig. 16.2** Temporal relationship between the changes in transmembrane potential (*top trace*) and cell shortening (*bottom trace*) in a single ventricular myocyte. The value of 0 mV membrane potential is indicated by “0.” (From Pappano A. unpublished record, 1995.)

This contributes to slow conduction of impulses, which is particularly important in the AV node, which contributes to the delay between contraction of the atria and ventricles. After reaching a peak, slow-response action potentials begin to gradually repolarize (phase 3). There are no initial repolarization or plateau phases. Furthermore, the membrane potential during diastole (phase 4) is more depolarized (less negative) than that found in fast-response cells, and it never stabilizes at a fixed level. Once the membrane reaches its most negative value, called the **maximum diastolic potential**, it begins to spontaneously depolarize.

### Ionic Basis of Membrane Potential

The actual membrane potential of a cardiac myocyte, like any excitable cell, is a function of the unequal distribution of ions across the plasma membrane. The ions that are most important in determining the membrane potential of a cardiac myocyte are  $K^+$ ,  $Na^+$ , and  $Ca^{++}$ , and the typical intracellular and extracellular concentrations of these ions are listed in Table 16.1. Even though the concentration gradient for each of these ions is large, that alone does not determine whether they will diffuse across the membrane and contribute to an action potential. Because of their charged nature, the movement of ions is also affected by the membrane potential ( $V_M$ ) of the cell. The potential difference that offsets or balances the concentration gradient of an ion is referred to as the **equilibrium potential** ( $E_{ion}$ ) for that ion, and it can be calculated using the Nernst equation, as described in Chapter 1. The equilibrium potentials for  $K^+$ ,  $Na^+$ , and  $Ca^{++}$  in a typical cardiac myocyte are included in Table 16.1. Thus, the potential for any ion to move across the plasma membrane is determined by the difference between the membrane potential and the equilibrium potential for that ion ( $V_M - E_{ion}$ ). This is referred to as the **electrochemical gradient** or **driving force**.

Even in the presence of a significant driving force, an ion cannot affect the membrane potential of a cell unless there

**TABLE 16.1** Intracellular and Extracellular Ion Concentrations and Equilibrium Potentials in Cardiac Muscle Cells

Ion	Extracellular Concentrations (mmol/L)	Intracellular Concentrations (mmol/L)*	Equilibrium Potential (mV)
Na <sup>+</sup>	145	10	71
K <sup>+</sup>	4	135	-93
Ca <sup>++</sup>	2	10 <sup>-4</sup>	129

The intracellular concentrations are estimates of the free concentrations in cytoplasm.

Data from Ten Eick RE, et al. *Prog Cardiovasc Dis.* 1981;24:157.

is a means for it to cross the membrane. Ions are unable to freely diffuse across the lipid membrane of a cell on their own. This process relies on the presence of ion channels, which are membrane proteins that form aqueous pores providing a pathway for passive transport. Ultimately, the actual contribution any ion makes to the membrane potential depends on the relative permeability or conductance of the membrane to that ion, as described by the **chord conductance equation** (discussed in [Chapter 2](#)):

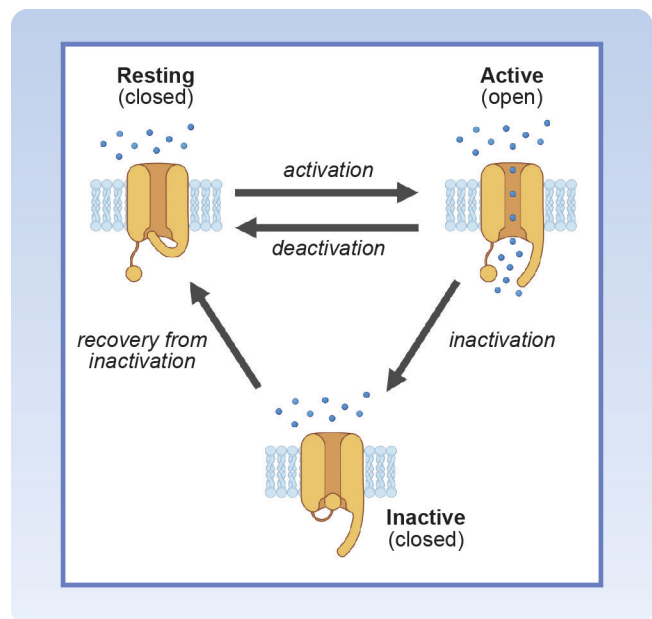
$$V_M = \frac{g_K}{g_M} E_K + \frac{g_{Na}}{g_M} E_{Na} + \frac{g_{Ca}}{g_M} E_{Ca}$$

This relationship says that the size of the contribution that any ion makes to the membrane potential is determined by the relative magnitude of the conductance of the membrane to that ion ( $g_{ion}$ ), expressed as a fraction of the total membrane conductance to all ions ( $g_M$ ), multiplied by the equilibrium potential for that ion. Put another way,  $V_M$  is simply a weighted average of the equilibrium potentials of the ions that the membrane is permeable to, where the weighting factor for each ion is the fraction of the total membrane conductance attributable to that ion. The bottom line is that  $V_M$  will move toward the equilibrium potential of the ion to which the membrane has the greatest conductance.

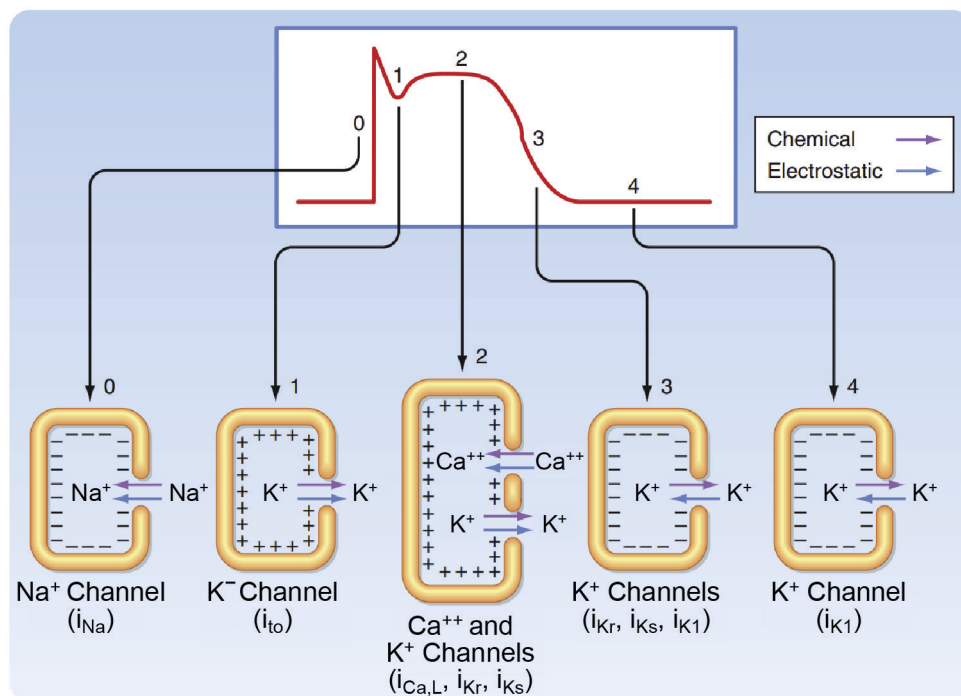
In a simple example that illustrates how this relationship works, if the membrane is permeable to only one type of ion ( $g_{ion}/g_M = 1$ ), then the membrane potential will approach the equilibrium potential for that ion. This is close to the situation that exists in a ventricular myocyte at rest (phase 4), where the conductance of the membrane is primarily due to K<sup>+</sup> ( $g_K/g_M \approx 1$ ). The membrane has only a very low permeability to either Na<sup>+</sup> or Ca<sup>++</sup> at that time. As a result, the resting membrane potential of a ventricular myocyte is very negative because it closely follows the equilibrium potential for K<sup>+</sup> ( $E_K$ ). However, during the upstroke of the ventricular action potential (phase 0), this situation reverses. The conductance of the membrane to Na<sup>+</sup> increases, and the conductance to K<sup>+</sup> decreases. As a result, the membrane potential depolarizes as it moves away from  $E_K$  and toward the equilibrium potential for Na<sup>+</sup> ( $E_{Na}$ ). Using this basic principle, the ionic basis of an action potential can then be explained if one knows what types of ion channels are present and the factors that influence the opening and closing, or **gating**, of those channels.

Most cardiac ion channels are voltage-dependent, which means their gating is affected by changes in membrane potential ([Fig. 16.3](#)). **Activation** is the gating process a

channel goes through when transitioning from a resting (closed) state to an active (open) state. When open, the conductance of the membrane to ions that are permeable through the channel can then affect the membrane potential. Channels can return to their resting closed state by one of two general mechanisms. The first involves a reversal of activation, through a process called **deactivation**. The second involves a process called **inactivation**. A channel that undergoes inactivation is closed, and therefore cannot contribute to the membrane potential. However, an inactivated channel cannot be reactivated, or reopened, unless it first returns to its resting state through a process called **recovery from inactivation**. All these steps are voltage-dependent. A key to understanding the ionic basis of the cardiac action potential is remembering which channels open and close through a process that involves activation and deactivation (i.e., inward rectifier and delayed rectifier K<sup>+</sup> channels),



• **Fig. 16.3** Cardiac ion channel gating schemes. Channel **activation** is the process of going from a resting (closed) state to an active (open) state. After opening, some types of ion channels close by returning directly to their resting state through a process of **deactivation**. Other types of ion channels close by undergoing the process of **inactivation**. Inactivated channels typically cannot be reactivated or reopened unless they first return to the resting state through the process of **recovery from inactivation**. All of these processes are time- and voltage-dependent.



• **Fig. 16.4** Conductance mechanisms that contribute to fast-response (ventricular) action potentials. **Phase 0**, the upstroke is due to a rapid increase in  $\text{Na}^+$  conductance caused by activation of channels that generate the voltage-dependent  $\text{Na}^+$  current ( $i_{\text{Na}}$ ). **Phase 1**, during initial repolarization  $\text{Na}^+$  channels close and there is a transient increase in  $\text{K}^+$  conductance due to channels that generate a transient outward  $\text{K}^+$  current ( $i_{\text{to}}$ ). **Phase 2**, the plateau is due to an increase in  $\text{Ca}^{++}$  conductance caused by activation of channels that generate the L-type  $\text{Ca}^{++}$  current ( $i_{\text{Ca,L}}$ ). There is also a gradual increase in  $\text{K}^+$  conductance due to activation of channels that generate the rapid ( $i_{\text{Kr}}$ ) and slow delayed rectifier ( $i_{\text{Ks}}$ ) currents. **Phase 3**,  $\text{Ca}^{++}$  channels close, while the  $\text{K}^+$  conductance continues to increase initially due to  $i_{\text{Kr}}$  and  $i_{\text{Ks}}$  channels and later to channels that generate the inward rectifier  $\text{K}^+$  ( $i_{\text{K1}}$ ) current. **Phase 4**, the resting membrane potential is due to the large resting  $\text{K}^+$  conductance due to  $i_{\text{K1}}$  channels. See text for details.

and which channels open and close through a process that involves activation, inactivation, and recovery from inactivation (i.e.,  $\text{Na}^+$ ,  $\text{Ca}^{++}$ , and transient outward  $\text{K}^+$  channels).

### Fast-Response (Ventricular) Action Potentials Upstroke (Phase 0)

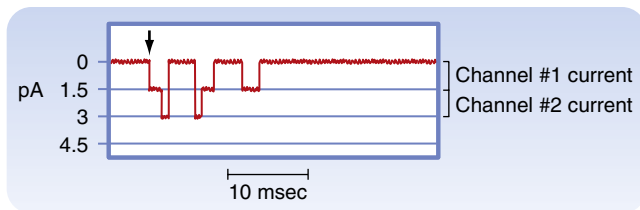
The upstroke of a ventricular action potential is normally initiated by depolarization of the membrane by an electrical impulse propagating from an adjacent cell. This causes activation of voltage-dependent  $\text{Na}^+$  channels. If enough of these channels open, the resulting increase in  $g_{\text{Na}}$  (Fig. 16.4) will cause the membrane potential to move toward  $E_{\text{Na}}$ , resulting in further depolarization. This, in turn, activates even more  $\text{Na}^+$  channels, facilitating an even greater increase in  $g_{\text{Na}}$  and a more rapid movement of the membrane potential toward  $E_{\text{Na}}$ . This type of positive feedback response, together with the fact that these  $\text{Na}^+$  channels respond to changes in membrane potential extremely rapidly, explains the fast depolarization of the membrane during the upstroke of a ventricular action potential. However, after opening, these  $\text{Na}^+$  channels quickly close by inactivating, and they cannot reopen until they recover from inactivation, which only occurs after the membrane repolarizes. It is important to understand that both activation and inactivation of these

$\text{Na}^+$  channels are caused by membrane depolarization, and both processes are very rapid. Activation occurs over a time course of a few microseconds; inactivation occurs over a time course of a few milliseconds.



### AT THE CELLULAR LEVEL

The ionic current conducted through individual membrane channels can be measured with the patch clamp technique. Channels open and close repeatedly in what often appears to be a random manner. This process is illustrated in Fig. 16.5, which shows the current flowing through  $\text{Na}^+$  channels in a myocardial cell. In this experiment the membrane potential was initially held constant or “clamped” at  $-85$  mV, where these channels exist in a resting state. At the time point indicated by the arrow, the potential was suddenly changed to  $-45$  mV to activate these channels, and the membrane potential was held there for the remainder of the recording. Immediately after the membrane was depolarized, one channel opened (1.5 pA in amplitude) and then a second (3 pA total current from both channels). These channels then proceeded to open and close multiple times before finally entering an inactivated state, where they remained closed. When viewed individually, the opening and closing of ion channels appears to be random. However, when the activity of an entire population of channels in a cell is added together, the behavior is quite predictable.



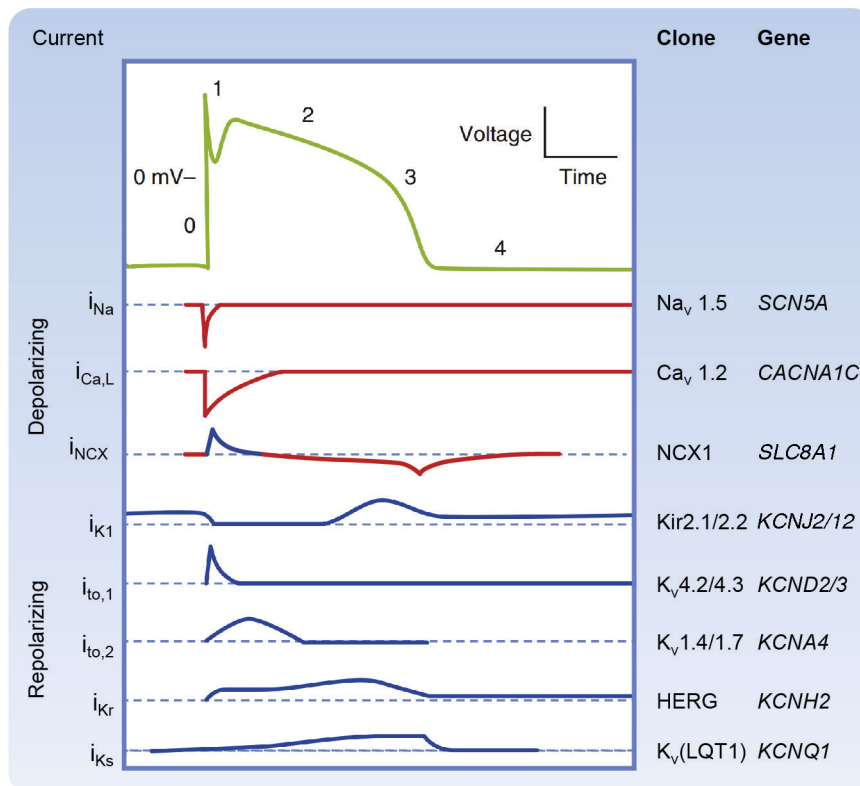
• **Fig. 16.5** Current (in picoamperes [pA]) through two individual  $\text{Na}^+$  channels recorded in a cardiac myocyte using the patch clamp technique. Membrane voltage was held at  $-85$  mV and then abruptly changed to  $-45$  mV (at the time indicated by the arrow), where it was held for the remainder of the recording. (Redrawn from Cachelin AB, et al. *J Physiol.* 1983;340:389.)

Depolarization of the membrane potential during the upstroke of the action potential also causes a decrease in the background  $\text{K}^+$  conductance that is responsible for the resting membrane potential of ventricular myocytes. This large resting  $\text{K}^+$  conductance is due to the activity of a specific type of  $\text{K}^+$  channel, one that generates the **inward rectifier  $\text{K}^+$  current ( $I_{\text{K1}}$ )** (Fig. 16.6). The term *inward rectification* simply refers to the fact that these are voltage-dependent ion channels that are activated as the membrane potential is made more negative (Fig. 16.7). As a result, they can generate an inward current carried by  $\text{K}^+$

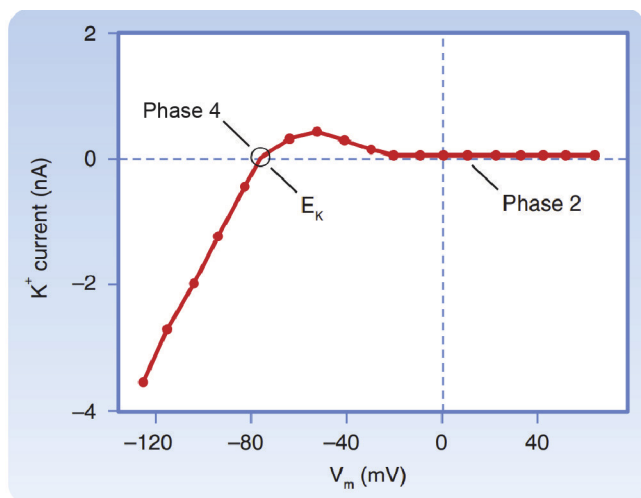
when the membrane potential is more negative than  $E_{\text{K}}$ , because of the inward driving force. At membrane potentials more positive than  $E_{\text{K}}$ , when the driving force would be expected to cause an outward movement of  $\text{K}^+$  ions, there is actually very little current because these channels close due to a deactivation-like process. This facilitates depolarization during the upstroke by decreasing  $g_{\text{K}}$ , allowing the membrane potential to move away from  $E_{\text{K}}$ . These channels are unusual in that the gating is due to the block and unblock of the channel pore by intracellular  $\text{Mg}^{++}$  and positively charged molecules called polyamines. This is unlike other channels, where the voltage dependence is due to gating mechanisms that are intrinsic to the channel protein itself.

### Initial Repolarization (Phase 1)

After the action potential reaches its peak, there is a brief period of limited repolarization that results in a notch between the upstroke and the beginning of the plateau (see Fig. 16.1). This is facilitated in part by the rapid decrease in  $g_{\text{Na}}$  caused by voltage-dependent inactivation of the  $\text{Na}^+$  channels responsible for the upstroke. The prominence of the initial repolarization phase can be quite variable. In cells where it is most noticeable, the notch is largely due to a transient increase in  $g_{\text{K}}$  caused by



• **Fig. 16.6** Molecular basis for the ion currents contributing to fast-response (ventricular) action potentials. Depolarizing inward currents (red) include the voltage-dependent  $\text{Na}^+$  ( $i_{\text{Na}}$ ) and L-type  $\text{Ca}^{++}$  ( $i_{\text{Ca,L}}$ ) currents. Repolarizing outward currents (blue) include the transient outward  $\text{K}^+$  currents ( $i_{\text{to,1}}$  and  $i_{\text{to,2}}$ ), rapid and slow delayed rectifier  $\text{K}^+$  currents ( $i_{\text{Kr}}$  and  $i_{\text{Ks}}$ ), and the inward rectifier  $\text{K}^+$  current ( $i_{\text{K1}}$ ). Note: current generated by the  $\text{Na}/\text{Ca}$  exchanger ( $i_{\text{NCX}}$ ) can be both depolarizing and repolarizing. The clones and genes underlying these currents are included. (Redrawn from Tomaselli G, Marbán E. *Cardiovasc Res.* 1999;42:270.)



• **Fig. 16.7** Plot of inward rectifier  $K^+$  current recorded from a ventricular myocyte at various membrane potentials. Negative values along the vertical axis represent inward currents; positive values represent outward currents. The current is inward when the membrane potential ( $V_M$ ) is more negative than the equilibrium potential for  $K^+$  ( $E_K$ ) and outward when  $V_M$  is more positive than  $E_K$ . The point at which the plot intersects the x-axis is the reversal potential (*open circle*). Note that  $V_M$  during phase 4 of the ventricular action potential coincides with the reversal potential for this current. (Redrawn from Giles WR, Imaizumi Y. *J Physiol [Lond]*. 1988;405:123.)

voltage-dependent activation and subsequent inactivation of  $K^+$  channels that generate a **transient outward current** ( $I_{to}$ ). There are at least two components to this current. They are conducted by  $K^+$  channels that generate  $I_{to,1}$  and  $I_{to,2}$  (Fig. 16.6).

### Plateau (Phase 2)

The membrane of a fast-response cell does not return to its resting potential following initial repolarization because the depolarization that occurs during the upstroke also causes an increase in  $Ca^{++}$  conductance ( $g_{Ca}$ ) (Fig. 6.4). In ventricular myocytes, this is due to the activation of channels that generate an **L-type  $Ca^{++}$  current** ( $I_{Ca,L}$ ) (Fig. 16.6), which depolarizes the cell by attempting to move the membrane potential to  $E_{Ca}$ . The voltage-dependent behavior of these channels is like that of the  $Na^+$  channels responsible for the upstroke. They are activated by membrane depolarization, and after opening they undergo inactivation. However, there are two important differences. First, these  $Ca^{++}$  channels require the membrane potential to be more depolarized to activate. Second, they respond more slowly to changes in membrane potential: They activate over a time course of a millisecond and inactivate over a time course of tens to hundreds of milliseconds. The influx of  $Ca^{++}$  that occurs with the activation of  $I_{Ca,L}$  channels also triggers myocyte contraction through a process that is discussed in the section “Excitation-Contraction Coupling” (see also Chapter 13). The prolonged increase in  $g_{Ca}$  due to slow inactivation of these channels is the primary mechanism responsible for keeping the membrane depolarized during the plateau.



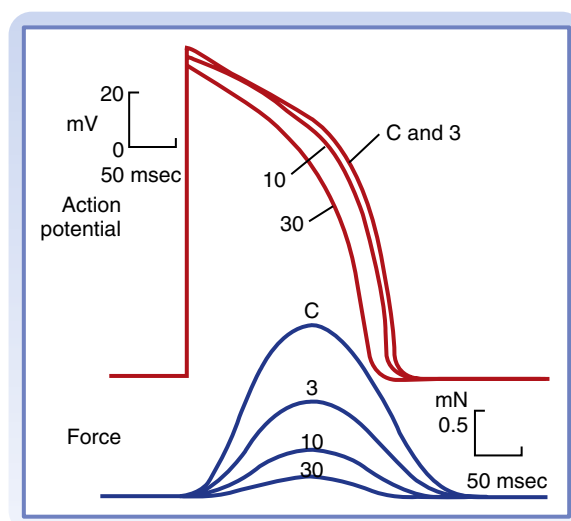
## AT THE CELLULAR LEVEL

The autonomic nervous system regulates cardiac contractility in part through changes in L-type  $Ca^{++}$  channel activity. The sympathetic neurotransmitter norepinephrine acts by stimulating  $\beta$ -adrenergic receptors found in the plasma membrane of cardiac myocytes. This interaction activates the membrane-bound enzyme adenylate cyclase, which then stimulates the production of cyclic adenosine monophosphate (cAMP; see Chapter 13). The rise in cAMP activates protein kinase A, which in turn causes a phosphorylation-dependent increase in channel activity, augmenting the influx of  $Ca^{++}$  into the cell. Conversely, the parasympathetic neurotransmitter acetylcholine can antagonize this effect by acting through muscarinic receptors to inhibit the production of cAMP by adenylate cyclase.



## IN THE CLINIC

Calcium channel antagonists such as verapamil, amlodipine, and diltiazem are drugs that block L-type  $Ca^{++}$  channels. These compounds can inhibit the influx of  $Ca^{++}$  into cardiac myocytes. This can result in a decrease in ventricular action potential duration as well as the strength of contraction (see Fig. 16.8). Blocking these channels can also decrease action potential firing frequency in the SA node as well as the speed of impulse propagation through the AV node. Calcium channel antagonists can also depress the contraction of vascular smooth muscle and thereby induce generalized vasodilation. This diminished vascular resistance reduces the counterforce (afterload) that opposes the propulsion of blood from the ventricles into the arterial system, as explained in Chapter 17. Hence, vasodilator drugs such as the calcium channel antagonists are often referred to as *afterload-reducing drugs*.



• **Fig. 16.8** Effects of diltiazem, a calcium channel antagonist, on the action potentials (in millivolts [mV]) and isometric contractile forces (in millinewtons [mN]) recorded from a papillary muscle *in vitro*. The tracings were recorded under control conditions (C) and in the presence of diltiazem at concentrations of 3, 10, and 30  $\mu\text{mol/L}$ . (Redrawn from Hirth C, et al. *J Mol Cell Cardiol*. 1983;15:799.)

Even though the driving force for  $K^+$  is significant at depolarized membrane potentials,  $g_K$  is quite low during much of the plateau. This is because  $I_{K1}$  channels open during phase 4 are deactivated during phase 0 and most  $I_{to}$  channels activated during phase 1 have inactivated. This explains why the membrane potential during phase 2 of the ventricular action potential is maintained between  $E_{Ca}$  and  $E_K$ . The reduction in  $g_K$  minimizes the amount of  $Ca^{++}$  that needs to flow into the cell in order to maintain depolarization. It also minimizes the amount of  $K^+$  that would otherwise flow out of the cell during the plateau. Both effects reduce the energy required to maintain the gradients for these ions through active transport mechanisms.

### Final Repolarization (Phase 3)

The end of the plateau and beginning of final repolarization of the fast-response action potential comes about when the balance between the  $Ca^{++}$  and  $K^+$  conductance of the membrane shifts back toward  $g_K$  (Fig. 16.4). There is a decrease in  $g_{Ca}$  due to the time- and voltage-dependent inactivation of the L-type  $Ca^{++}$  channels. There is also an increase in  $g_K$  due to the time- and voltage-dependent activation of channels that generate a **delayed rectifier  $K^+$  current ( $I_K$ )**. These  $K^+$  channels are activated when the membrane depolarizes to potentials like those that activate the  $Ca^{++}$  channels. However, an important distinction is that, as their name implies, delayed rectifier  $K^+$  channels activate very slowly, even more slowly than the  $Ca^{++}$  channels. Therefore, the increase in  $g_K$  due to opening of these channels does not become significant until the end of phase 2. There are also multiple types of delayed rectifier  $K^+$  channels. The two types most prominent in ventricular myocytes generate a **rapidly activating delayed rectifier  $K^+$  current ( $I_{Kr}$ )** and a **slowly activating delayed rectifier  $K^+$  current ( $I_{Ks}$ )** (Fig. 16.6). Both contribute to an increase in  $g_K$  that drives the membrane potential back toward  $E_K$ . As the membrane potential becomes more negative, this causes these

channels to close by deactivating late in phase 3. However,  $g_K$  does not decrease. In fact, it continues to increase, because at the same time,  $I_{K1}$  channels begin to reactivate bringing the membrane back to its resting potential near  $E_K$ .

### Resting Membrane Potential (Phase 4)

As described previously, the resting membrane conductance of a ventricular myocyte is dominated by its permeability to  $K^+$  (Fig. 16.4). As a result, the membrane potential during phase 4 closely follows  $E_K$ . Because  $g_K$  is so large, it very effectively stabilizes the membrane, preventing spurious depolarization, which might otherwise lead to the generation of arrhythmias. At the resting membrane potential there is actually very little movement of  $K^+$  because the driving force is minimal. There is also very little movement of  $Na^+$  and  $Ca^{++}$  because the conductance of the membrane to these ions is very small, even though the inward driving force is quite large.

## Slow-Response (SA Node) Action Potentials

### Upstroke (Phase 0)

The upstroke of slow-response action potentials is due to the activity of L-type  $Ca^{++}$  channels (Fig. 16.9). The increase in  $g_{Ca}$  caused by activation of these channels causes the membrane potential to depolarize, as it moves toward  $E_{Ca}$ . Unlike fast-response action potentials, where  $Na^+$  channels are involved, the rate of change in the membrane potential during the upstroke of the action potential in an SA node cell is much slower. This is because L-type  $Ca^{++}$  channels activate much more slowly than  $Na^+$  channels and the channel density is lower.

### Final Repolarization (Phase 3)

As mentioned earlier, there is no pronounced plateau phase in a slow-response action potential. However, action potential duration is determined by a similar process in both fast- and slow-response cells: a shift in the balance between  $g_{Ca}$  and  $g_K$ . There is a gradual decrease in  $g_{Ca}$  as the L-type  $Ca^{++}$  channels responsible for the upstroke slowly inactivate, and there is a gradual increase in  $g_K$  due to activation of delayed rectifier  $K^+$  channels (Fig. 16.9). The increase in  $g_K$  causes the cell to repolarize until it eventually reaches its maximum diastolic potential.

### Diastole (Phase 4)

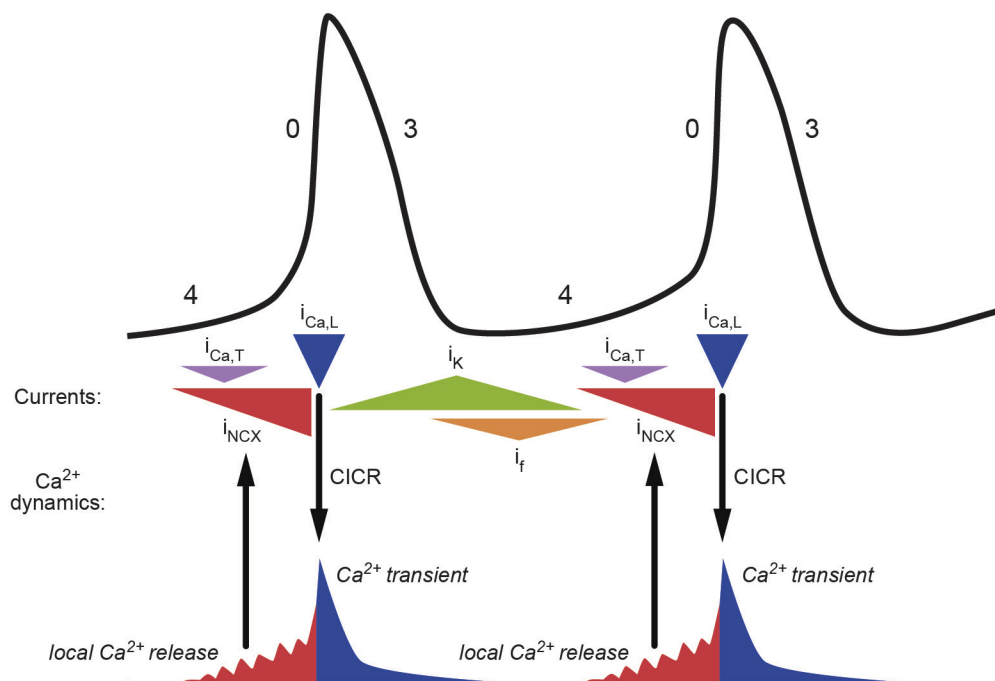
The maximum diastolic potential during phase 4 of the slow-response action potential in an SA node cell is less negative ( $-50$  to  $-70$  mV) than the resting membrane potential of a ventricular myocyte. This can be explained by the fact that SA node cells have a lower background  $g_K$ , which is due to  $K^+$  channels that generate an **acetylcholine (ACh)-activated  $K^+$  current ( $I_{K,ACh}$ )**. The lower background  $K^+$  conductance makes it easier for these cells to be depolarized by the activity of other ion channels and transporters.

One mechanism that contributes to spontaneous depolarization during phase 4 actually begins during phase 3. The



## AT THE CELLULAR LEVEL

Cardiac ion channels associate with various cellular proteins to form macromolecular complexes. These interactions are involved in many aspects of ion channel function, including trafficking, gating, and post-translational modification. For example, the L-type  $Ca^{++}$  channel ( $Ca_v1.2$ ) exists as a complex consisting of  $\alpha_1$ ,  $\beta$ ,  $\alpha_2\delta$ , and  $\gamma$  subunits. While the  $\alpha_1$  subunit can function as an ion channel on its own, the  $\beta$  and  $\gamma$  subunits affect the voltage-dependent properties of the channel, and the  $\beta$  and  $\alpha_2\delta$  subunits promote trafficking of the channel to the plasma membrane. The  $\alpha_1$  subunit also interacts with various signaling proteins, including calmodulin, which is involved in regulation of channel inactivation by intracellular  $Ca^{++}$ , as well as A-kinase anchoring proteins, which act as scaffolds to bind various components of the protein kinase A signaling pathway. This multimeric complex also interacts with other membrane proteins including caveolin-3, which facilitates interactions with the stimulatory G protein  $G_s$ , adenylate cyclase, and  $\beta$ -adrenergic receptors, all of which are involved in sympathetic regulation of this channel by the autonomic nervous system.



• **Fig. 16.9** Conductance mechanisms contributing to slow-response (sinoatrial node) action potentials. **Phase 0**, the upstroke is due to an increase in  $\text{Ca}^{2+}$  conductance caused by activation of channels that generate the L-type  $\text{Ca}^{2+}$  current ( $i_{\text{Ca,L}}$ ). Note, this triggers a  $\text{Ca}^{2+}$  transient due to  $\text{Ca}^{2+}$ -induced  $\text{Ca}^{2+}$  release (CICR). **Phase 3**, final repolarization occurs when the  $\text{Ca}^{2+}$  conductance decreases due to  $i_{\text{Ca,L}}$  inactivation and the  $\text{K}^{+}$  conductance increases due to activation channels that generate delayed rectifier  $\text{K}^{+}$  current ( $i_{\text{K}}$ ). **Phase 4**, spontaneous depolarization is due to (1) a gradual decrease in  $\text{K}^{+}$  conductance due to deactivation of  $i_{\text{K}}$ , (2) an increase in  $\text{Na}^{+}$  conductance due to channels that generate the pacemaker current ( $i_{\text{f}}$ ), (3) an increase in  $\text{Ca}^{2+}$  conductance due to channels that generate the T-type  $\text{Ca}^{2+}$  current ( $i_{\text{Ca,T}}$ ), and (4) inward current generated by the  $\text{Na}/\text{Ca}$  exchanger ( $i_{\text{NCX}}$ ), which is activated by spontaneous local  $\text{Ca}^{2+}$  release from the sarcoplasmic reticulum. (Redrawn from Lakatta EG, et al. *Circ Res.* 2010;106:659.) See text for details.

delayed rectifier  $\text{K}^{+}$  channels that contribute to final repolarization begin to close by deactivating as the membrane potential becomes more negative (Fig. 16.9). However, this gating process is slow. The result is a time-dependent decrease in  $g_{\text{K}}$  during phase 4, which allows the membrane potential to slowly move away from  $E_{\text{K}}$ , or depolarize.

Depolarization during phase 4 is also facilitated by the activation of channels that generate a **pacemaker** or **funny current** ( $i_{\text{f}}$ ). These are called “funny” channels because they activate upon hyperpolarization of the membrane, which was viewed as unusual at the time they were originally discovered. As such, these channels are closed when the membrane is depolarized during the action potential, but activate or open upon repolarization during phase 4 (Fig. 16.9). Pacemaker channels are also unusual because they are permeable to both  $\text{Na}^{+}$  and  $\text{K}^{+}$ . So, when they are open, they cause the membrane to move toward their equilibrium potential, which is between  $E_{\text{K}}$  and  $E_{\text{Na}}$  ( $-15$  mV). Because this is more positive than the maximum diastolic potential, the result is a net inward current carried by  $\text{Na}^{+}$  moving down its electrochemical gradient.

The combination of factors described above eventually depolarizes the membrane enough to cause a brief increase in  $g_{\text{Ca}}$  due to the activation of channels that generate a **T-type  $\text{Ca}^{2+}$  current** ( $i_{\text{Ca,T}}$ ) (Fig. 16.9). These channels activate upon membrane depolarization and then inactivate,

similar to L-type  $\text{Ca}^{2+}$  channels. However, there are two main differences. T-type  $\text{Ca}^{2+}$  channels activate at more negative membrane potentials, and they activate and inactivate much more rapidly.

In addition to the effects of the time- and voltage-dependent ion channels described earlier in the chapter, SA node cells spontaneously release  $\text{Ca}^{2+}$  from the sarcoplasmic reticulum (SR) into the cytoplasm. The resulting rise in intracellular  $\text{Ca}^{2+}$  near the plasma membrane activates the  $\text{Na}/\text{Ca}$  exchanger (NCX), which couples the movement of extracellular  $\text{Na}^{+}$  down its electrochemical gradient into the cell to the movement of intracellular  $\text{Ca}^{2+}$  out of the cell. Because this process involves three  $\text{Na}^{+}$  ions moving in for each  $\text{Ca}^{2+}$  ion that moves out, the result is a net inward current ( $i_{\text{NCX}}$ ). This contributes to spontaneous depolarization late during phase 4 (Fig. 16.9).

### Excitability of Cardiac Myocytes

The ability to initiate an action potential in response to a stimulus is a characteristic of any excitable cell. Yet, for this to happen, the stimulus must depolarize the membrane to a threshold potential, the absolute value of which varies depending on the cell type and the timing. The threshold for initiating an action potential that can be propagated within a cell and from cell to cell in cardiac tissue depends on (1) whether



## AT THE CELLULAR LEVEL

Changes in serum  $[K^+]$  can have significant effects on the cardiac action potential and the electrical properties of the heart. For example, an increase in serum  $[K^+]$  (*hyperkalemia*) will depolarize the resting membrane potential, and a decrease in serum  $[K^+]$  (*hypokalemia*) can hyperpolarize the resting membrane potential (see Fig. 16.10). These responses can be easily explained by the effect that changing the extracellular  $K^+$  concentration has on  $E_K$ . However, changes in serum  $[K^+]$  can have what appear to be paradoxical effects on action potential duration if one only considers what happens to  $E_K$ . Remember, the chord conductance equation tells us that membrane potential is a function of the conductance of the membrane to an ion, as well as its equilibrium potential. It turns out that changes in extracellular  $[K^+]$  also affect the  $K^+$  conductance of the membrane associated with delayed and inward rectifier  $K^+$  channels: Increasing extracellular  $[K^+]$  increases  $g_K$  and decreasing extracellular  $[K^+]$  decreases  $g_K$ . The changes in  $g_K$  have a greater effect on action potential duration than the changes in  $E_K$ . As a result, hyperkalemia reduces action potential duration and hypokalemia prolongs action potential duration.



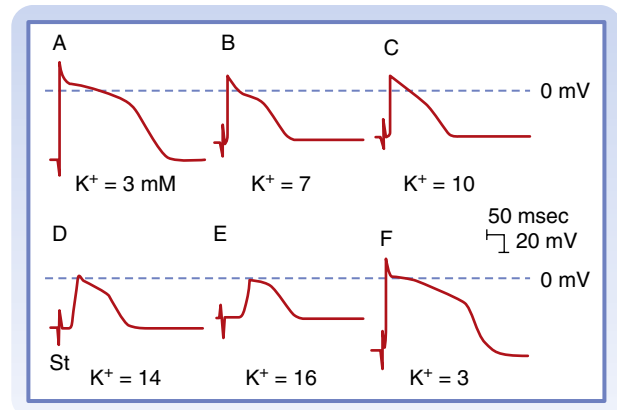
## IN THE CLINIC

The experimentally induced changes in transmembrane potential shown in Fig. 16.10 mimic those that may take place in the cardiac tissue of patients with coronary artery disease. When regional myocardial blood flow is diminished, the supply of  $O_2$  and metabolic substrates delivered to the ischemic tissues is insufficient. The  $Na^+,K^+$ -ATPase in the membrane of cardiac myocytes requires considerable metabolic energy to maintain the normal transmembrane gradients of  $Na^+$  and  $K^+$ . When blood flow is inadequate, the activity of  $Na^+,K^+$ -ATPase is impaired, and the affected myocytes gain excess  $Na^+$  and lose excess  $K^+$  to the surrounding interstitial space. This can critically disturb conduction of electrical impulses by causing fast-response cells to produce slow-response-like action potentials. The increase in  $[K^+]$  in the extracellular space causes a shift in  $E_K$ , resulting in depolarization of the resting membrane potential of these cells. This leads to inactivation of voltage-dependent  $Na^+$  channels that normally contribute to the upstroke. As a result, the upstroke may be slowed (as illustrated in Fig. 16.10) or even blocked. This often contributes to the generation of arrhythmias.

fast- or slow-response action potentials are involved and (2) precisely when during the cardiac cycle the stimulus arrives.

### Fast-Response Cells

In fast-response cells, excitability depends on the availability of voltage-dependent  $Na^+$  channels to generate the upstroke of the action potential. Once a fast-response action potential has been initiated, the depolarized cell cannot be re-excited until it has at least partially repolarized. This is because the  $Na^+$  channels, which inactivated immediately following the upstroke, must recover from inactivation before they can reopen. This is a time- and voltage-dependent process that occurs at more negative membrane potentials. The interval from the

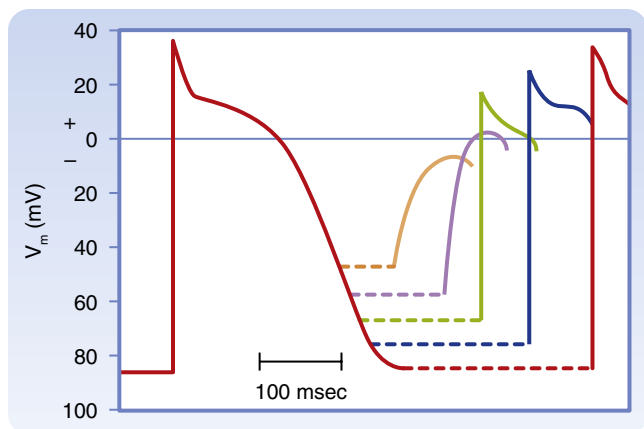


• **Fig. 16.10** Effect of changes in extracellular  $[K^+]$  on action potentials recorded from a Purkinje fiber. The stimulus artifact (St in tracing D) appears as a biphasic spike to the left of the upstroke of the action potential. The horizontal dashed lines near the peaks of the action potentials denote 0 mV. When extracellular  $[K^+]$  is 3 mM (tracings A and F), the resting membrane potential ( $V_M$ ) is  $-82$  mV, and the slope of phase 0 is steep. At the end of phase 0, the overshoot attains a value of  $+30$  mV. Hence, the action potential amplitude is 112 mV. The distance from the stimulus artifact to the beginning of phase 0 is inversely proportional to the conduction velocity. When extracellular  $[K^+]$  is increased gradually to 16 mM (tracings B to E), resting  $V_M$  becomes progressively less negative. At the same time, the amplitude and duration of the action potential and the steepness of the upstroke all diminish. As a consequence, conduction velocity decreases progressively. At extracellular  $[K^+]$  levels of 14 and 16 mM (tracings D and E), the resting  $V_M$  attains levels sufficient to inactivate all the fast sodium channels and leads to the characteristic slow-response action potentials. (From Myerburg RJ, Lazzara R. In: Fisch E, ed. *Complex Electrocardiography*. Philadelphia: FA Davis; 1973.)

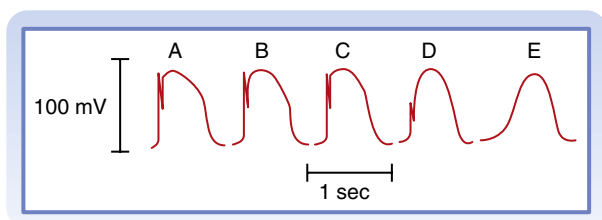
beginning of the action potential until the cell can generate at least some type of action potential is called the **effective refractory period**. This extends approximately midway through repolarization, during phase 3. At that point, enough  $Na^+$  channels have typically recovered from inactivation to restore some degree of excitability. However, fast-response cells are not fully excitable until they have completely repolarized. The time between the end of the effective refractory period and complete repolarization is referred to as the **relative refractory period**. When a response is evoked during the relative refractory period, its properties vary as a function of the membrane potential at the time the stimulus arrived (Fig. 16.11). This reflects the difference in the number of  $Na^+$  channels that have recovered from inactivation and are available to contribute to the upstroke. The earlier in the relative refractory period that the fast-response cell is stimulated, the slower the upstroke velocity and the smaller the amplitude of the resulting action potential. Consequently, conduction velocity also decreases. This effect can be mimicked by pharmacologically blocking  $Na^+$  channels with the drug tetrodotoxin (Fig. 16.12). The result is a slow-response-like action potential, due to activation of L-type  $Ca^{++}$  channels.

### Slow-Response Cells

In slow-response cells, excitability depends on the availability of the L-type  $Ca^{++}$  channels that generate the upstroke

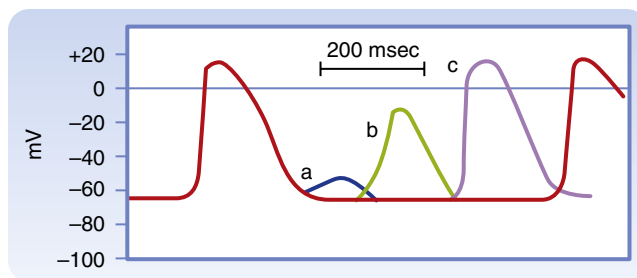


• **Fig. 16.11** Changes in action potential amplitude and upstroke slope as action potentials are initiated at different stages of the relative refractory period of the preceding excitation. (Redrawn from Rosen MR, et al. *Am Heart J.* 1974;88:380.)



• **Fig. 16.12** Effect of blocking  $\text{Na}^+$  channels with tetrodotoxin on action potentials recorded in a Purkinje fiber. The concentrations of tetrodotoxin were 0 mol/L in tracing A,  $3 \times 10^{-9}$  mol/L in tracing B,  $3 \times 10^{-7}$  mol/L in tracing C, and  $3 \times 10^{-6}$  mol/L in tracings D and E; E was recorded later than D. (Redrawn from Carmeliet E, Vereecke J. *Pflügers Arch.* 1969;313:300.)

of the action potential. In these cells, the relative refractory period frequently extends well beyond phase 3. Even after the cell has completely repolarized, it may be difficult to evoke a propagated response for some time. This characteristic of slow-response cells is called **postrepolarization refractoriness**. Refractoriness of a slow-response cell is due to L-type  $\text{Ca}^{++}$  channel inactivation, and normal excitability does not return until these channels have recovered. Just like  $\text{Na}^+$  channels in fast-response cells, recovery from inactivation of  $\text{Ca}^{++}$  channels in slow-response cells is a time- and voltage-dependent process. However, it occurs much more slowly, which explains the long refractory period duration. The amplitude and upstroke velocity of slow-response action potentials progressively improve the later the stimulus arrives in the relative refractory period (Fig. 16.13). The fact that recovery of full excitability extends well beyond the point of complete repolarization is particularly important property of slow-response cells found in the AV node. The long refractory period makes it difficult for a premature stimulus arriving from the atria to be conducted to the ventricles. It can also lead to AV node conduction block. In some situations, the AV node may be able to conduct only a fraction of the impulses that arrive from the atria.



• **Fig. 16.13** Effects of excitation at various times after the initiation of an action potential in a slow-response fiber. In this fiber, excitation very late in phase 3 (or early in phase 4) induces a small, nonpropagated (local) response (wave a). Later in phase 4, a propagated response (wave b) can be elicited, but its amplitude is small and the upstroke is not very steep; this response is conducted very slowly. Still later in phase 4, full excitability is regained, and the response (wave c) displays normal characteristics. (Modified from Singer DH, et al. *Prog Cardio-vasc Dis.* 1981;24:97.)

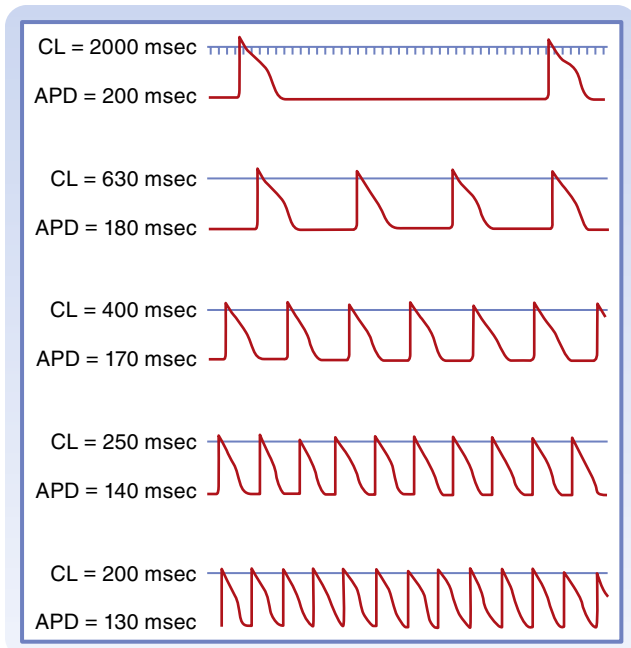


## IN THE CLINIC

In a patient who has occasional premature atrial depolarizations (see Fig. 16.28), the timing of these early beats may determine their clinical consequence. If they occur late in the relative refractory period of the preceding depolarization or after full repolarization, the premature depolarization is inconsequential. However, if the premature depolarizations originate early in the relative refractory period of the ventricles, conduction of the premature impulse from the site of origin is slowed, and hence a cardiac impulse is more likely to re-excite some myocardial region through which it had passed previously (a phenomenon known as *reentry*). If that reentry is irregular (i.e., if ventricular fibrillation ensues), the heart cannot pump effectively, and death may result.

### Frequency-Dependent Effects on Excitability

Excitability of a cardiac myocyte can also be affected by changes in cycle length, or the time between successive action potentials. This is because of the effect that cycle length has on action potential duration. As a result, changes in pacing frequency or heart rate are often important factors in the initiation or termination of certain arrhythmias (irregular heart rhythms). The changes in action potential duration produced by stepwise reductions in cycle length from 2000 to 200 msec in a Purkinje fiber are shown in Fig. 16.14. Note that as cycle length diminishes, the duration of the action potential decreases. This direct correlation between action potential duration and cycle length can be explained by changes in  $g_K$  that involve delayed rectifier  $\text{K}^+$  ( $\text{I}_K$ ) channels. These channels, which normally activate very slowly during the plateau of the action potential, also deactivate or close very slowly following repolarization. As the cycle length progressively decreases, so does the amount of time between action potentials, resulting in insufficient time for these channels to close. Consequently, there is an accumulation of channels that remain activated. The result is an increase in  $g_K$  during the plateau, which results in earlier repolarization and shorter action potential duration.



• **Fig. 16.14** Effect of changes in cycle length (CL) on the action potential duration (APD) of Purkinje fibers. (Modified from Singer D, Ten Eick RE. *Am J Cardiol.* 1971;28:381.)

### Propagation of Cardiac Impulses

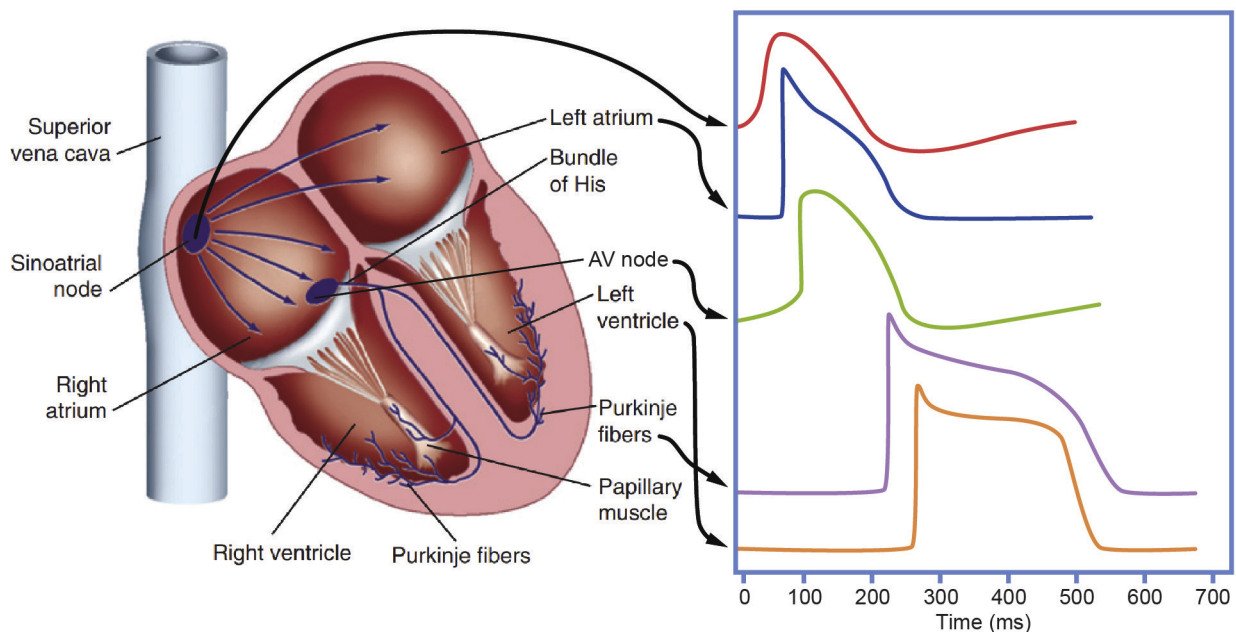
Each heartbeat starts with an electrical impulse that is generated in the SA node and then conducted throughout the atria. The impulse arriving from the atria is then slowed as it passes through the AV node to the His-Purkinje system, where it speeds up again, synchronizing the spread of

electrical activity across the entire subendocardial surface of the ventricles. From there, the wave of excitation is conducted from cell to cell throughout the ventricular myocardium. Electrical activity initiated by the SA node and conducted throughout the heart in this manner (Fig. 16.15) at regular intervals is referred to as *normal sinus rhythm*, and it typically occurs at a frequency between 60 and 100 beats/minute. Maintaining this rate, rhythm, and conduction pattern is essential to ensuring that the heart contracts in a coordinated manner, effectively pumping blood throughout the body.

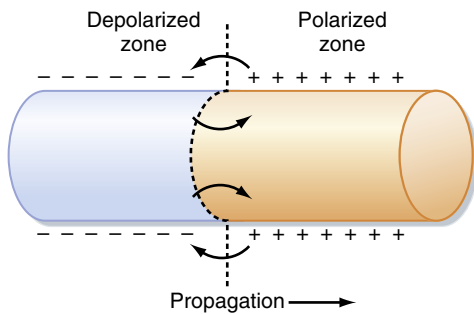
### Passive Properties

There are several factors that affect the speed and direction of impulse propagation throughout the heart. One set of these factors relates to the passive or cable properties of the cells and tissues. An action potential traveling from cell to cell along a cardiac muscle fiber is propagated by local circuit currents, much as it does in nerve and skeletal muscle fibers (see Chapter 5). These local currents, which are generated as the membrane is depolarized during the upstroke, flow along the inside of a cell, or from cell to cell, depolarizing adjacent areas of membrane or cells (Fig. 16.16). As a result, the speed with which an action potential is propagated is affected by both intracellular and intercellular resistances to this local current flow.

The degree of (intracellular) resistance within a cell determines how far from the site of stimulation current will flow. The lower the intracellular resistance, the farther the current will reach and the faster the action potential will be propagated. Therefore, cells with a larger diameter and



• **Fig. 16.15** Conduction of electrical activity throughout the heart. Note the change in shape of the action potential as the impulse travels from the sinoatrial node through the atria, atrioventricular node, Purkinje fibers, and ventricular myocardium. See text for details.



• **Fig. 16.16** The role of local currents in the propagation of a wave of excitation down a cardiac fiber.

less complex morphology, such as those found in Purkinje fibers, can conduct impulses faster, and smaller cells, like those found in the AV node, will tend to conduct impulses more slowly.

The spread of an impulse from cell to cell is facilitated by the fact that cardiac myocytes are electrically coupled to one another via gap junctions (see Chapter 6). Gap junctions are rather nonselective in their permeability to ions, and they create a low electrical (intercellular) resistance pathway that allows ionic current to pass from one cell to the next. Therefore, areas of the heart that have a greater number of gap junctions connecting adjacent cells can propagate impulses faster. For example, gap junction density is higher in Purkinje fibers and lower in certain regions of the AV node.

Where gap junctions are positioned in a cell can also affect the direction of impulse propagation. For example, in ventricular myocytes, which are long cylindrical cells, gap junctions are preferentially located in the intercalated disks that connect cells end-to-end, rather than side-to-side. This facilitates the (isotropic) propagation of impulses more readily in the direction of the long axis of the muscle cells, which are arranged to form fibers that wrap the chambers of the ventricles. This ensures that impulses propagate in an organized and orderly fashion, resulting in coordinated contraction of the heart.

### Active Properties

The conduction velocity along a fiber also varies directly with the action potential amplitude and the rate of change of the membrane potential ( $dV_M/dt$ ) during phase 0. The action potential amplitude is the potential difference between fully depolarized and fully polarized regions of the cell. The magnitude of the local current generated is proportional to this potential difference (see Chapter 5). These local currents are responsible for depolarizing the adjacent resting portion of the cell or fiber to its threshold potential. The greater the potential difference between the polarized and depolarized regions (i.e., the greater the action potential amplitude), the more effectively local stimuli can depolarize adjacent parts of the membrane and the more rapidly the wave of depolarization is propagated down the fiber. The rate of change in membrane potential during phase 0 is also an important determinant of conduction velocity. If the active portion of

a fiber depolarizes gradually, the local currents generated between resting and neighboring depolarized regions are small. The resting region adjacent to the active zone is depolarized gradually, and more time is therefore required for each new section of the fiber to reach threshold. For these reasons, fast-response action potentials propagate more quickly than slow-response action potentials.

Conduction velocity can also be influenced by changes in the resting membrane potential, especially in fast-response tissues. Depolarization of the resting potential inactivates the voltage-dependent  $\text{Na}^+$  channels, decreasing both action potential amplitude and  $dV_M/dt$ , which results in a slowing of conduction velocity. This effect can be observed when the resting potential is depolarized by an increase in extracellular  $[\text{K}^+]$  (see Fig. 16.10). It is also reflected in the response to premature excitation of a cell during the relative refractory period. Both situations can lead to slowed impulse propagation, which can contribute to the development of arrhythmias.

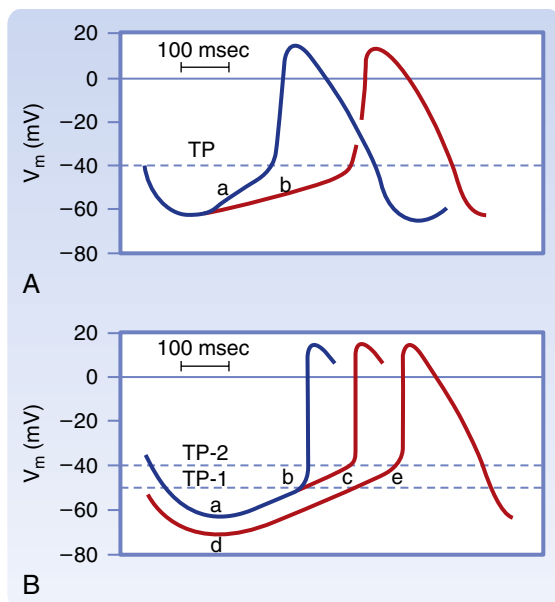
## Normal Sinus Rhythm

### Initiation of the Heartbeat

Initiation of each heartbeat is a characteristic intrinsic to the heart itself. Specific cell types within the heart possess the property of automaticity or the ability to spontaneously depolarize during diastole and initiate a propagated impulse. This behavior is most commonly associated with slow-response action potentials found in cells that make up the SA node, as described earlier. However, it is also observed in cells whose primary function is normally associated with conducting impulses from one region of the heart to another. This includes cells in the AV node, which elicit slow-response action potentials, as well as cells in the Purkinje network, which elicit fast-response action potentials.

Although multiple cell types have the potential to act as pacemakers for the heart, initiation of the heartbeat normally starts in the SA node because the cells there exhibit an intrinsic rate of firing (60–100 beats/minute) that is faster than that observed in the AV node (40–55 beats/minute) or Purkinje fibers (25–50 beats/minute). So, an impulse that originates in the SA node will reach these other latent pacemakers, triggering them to fire an action potential before they can do so on their own.

There are three main factors that affect the rate of spontaneous firing (Fig. 16.17). They include: (1) the rate of spontaneous depolarization during phase 4, (2) the maximal maximum diastolic potential during phase 4, and (3) the threshold potential. Assuming two cells have the same maximum diastolic potential, the cell with the fastest rate of spontaneous depolarization will reach the threshold for initiating an action potential first, and thus fire at a faster rate. Alternatively, if these two cells spontaneously depolarize at the same rate during phase 4, the cell that starts from a more depolarized maximum diastolic potential is likely to reach threshold sooner and fire at a faster intrinsic rate.



• **Fig. 16.17** Mechanisms involved in the changes in frequency of pacemaker firing. **A**, A reduction in the slope (from wave a to wave b) of slow diastolic depolarization diminishes the firing frequency. **TP**, Threshold potential. **B**, An increase in the threshold potential (from TP-1 to TP-2) or an increase in the magnitude of the maximum diastolic potential (from wave segments a to d) also diminishes the firing frequency. (From Hoffman BF, Cranefield PF. *Electrophysiology of the Heart*. New York: McGraw-Hill; 1960.)

Finally, if these two cells have the same maximum diastolic potential and the same rate of phase 4 depolarization, then the cell that has a lower threshold potential is likely to initiate an upstroke first and exhibit the fastest intrinsic rate of firing.

## Sinoatrial Node

As noted, the region of the mammalian heart that ordinarily generates impulses at the greatest frequency is the sinoatrial (SA) node; it is the main cardiac pacemaker. Detailed mapping of the electrical potentials on the surface of the right atrium has revealed that two or three sites of automaticity, located 1 or 2 cm from the SA node itself, serve along with the SA node as an atrial pacemaker complex. Sometimes these loci initiate impulses simultaneously. Other times the site of earliest excitation shifts from locus to locus, depending on certain conditions, such as the level of autonomic neural activity.

In humans, the SA node is approximately 8 mm long and 2 mm thick, and it lies posteriorly in the groove at the junction between the superior vena cava and the right atrium. The sinus node artery runs lengthwise through the center of the node. The SA node contains two principal cell types: (1) small, round cells that have few organelles and myofibrils; and (2) slender, elongated cells that are intermediate in appearance between the round and “ordinary” atrial myocardial cells. The round cells are probably the pacemaker cells; the slender, elongated cells probably conduct the impulses within the node and to the nodal margins.



## IN THE CLINIC

The frequency of pacemaker firing is controlled by the activity of both divisions of the autonomic nervous system. Sympathetic stimulation increases heart rate by enhancing the rate of spontaneous depolarization during phase 4 of the slow-response action potential in SA node cells. This is due to  $\beta$ -adrenergic receptor production of cAMP, which can then directly act on  $I_f$  pacemaker channels to increase their activity. The production of cAMP can also activate protein kinase A, enhancing the spontaneous release of  $Ca^{++}$  from the SR and increasing the contribution of  $I_{NCX}$  to phase 4 depolarization. These effects contribute to the increase in heart rate associated with stress and exercise.

Parasympathetic stimulation decreases heart rate by at least two mechanisms. First, it reduces the slope of diastolic depolarization during phase 4 of the slow-response action potential through muscarinic receptor inhibition of cAMP production, reversing the effects it has on  $I_f$  pacemaker channel activity and spontaneous  $Ca^{++}$  release. Second, muscarinic receptor activation shifts the maximum diastolic potential in a hyperpolarizing direction by activating  $I_{K,ACh}$  channels and increasing  $g_K$ . All of these effects contribute to the slowing of heart rate and subsequent decrease in cardiac output associated with vagal nerve stimulation. An extreme example is vasovagal syncope, a brief period of lightheadedness or loss of consciousness caused by an intense burst of vagal activity. This type of syncope is a reflex response to pain or to certain psychological stimuli. The autonomic neural effects on cardiac cells are described in greater detail in [Chapter 18](#).

Effects of the autonomic nervous system on pacemaking activity are not necessarily associated with changes the threshold level of pacemaker cells. However, drugs that directly inhibit L-type  $Ca^{++}$  channels can slow heart rate by reducing the number of  $Ca^{++}$  channels available to contribute to the upstroke. As a result, it takes pacemaker cells longer to depolarize to threshold, or the point where enough  $Ca^{++}$  channels are activated to initiate an action potential.



## AT THE CELLULAR LEVEL

The so-called funny current ( $I_f$ ) in cardiac SA node cells is activated by hyperpolarization and gated by cyclic nucleotides, and its channel is designated HCN. There are four members of the HCN gene family, and such channels are also found in central nervous system neurons that generate action potentials repetitively. Transmembrane segment 4 ( $S_4$ ) of HCN has many positively charged amino acids that act as voltage sensors, which are also present in voltage-gated  $Na^+$ ,  $K^+$ , and  $Ca^{++}$  channels. The dominant channel expressed in the heart is derived from the *HCN4* gene. Mutations in amino acids in  $S_4$  and in the  $S_4$ -to- $S_5$  linker cause marked changes in the voltage dependence of activation in such a way that greater hyperpolarization is needed to open the channel. This effect is like that of acetylcholine, and it has been predicted that the occurrence of such mutations in the human heart could underlie sinus bradycardia and sick sinus syndrome.



## IN THE CLINIC

Regions of the heart other than the SA node may initiate beats in special circumstances. Such sites are called *ectopic foci* or *ectopic pacemakers*. Ectopic foci may become pacemakers when (1) their own rhythmicity becomes enhanced, (2) the rhythmicity of the higher order pacemakers becomes depressed, or (3) all conduction pathways between the ectopic focus and regions with greater rhythmicity become blocked. Ectopic pacemakers may act as a safety mechanism when normal pacemaking centers fail. However, if an ectopic center fires while the normal pacemaking center still functions, the ectopic activity may induce either sporadic rhythm disturbances, such as premature depolarizations, or continuous rhythm disturbances, such as paroxysmal tachycardias (see the section “Ectopic Tachycardias”).

## Atrial Conduction

From the SA node, the cardiac impulse spreads radially throughout the right atrium (see Fig. 16.15) along ordinary atrial myocardial fibers at a conduction velocity of approximately 1 m/sec. A specialized pathway, the anterior interatrial myocardial band (or Bachmann’s bundle), conducts the SA node impulse directly to the left atrium. The wave of excitation proceeds inferiorly through the right atrium and ultimately reaches the AV node, which is normally the sole entry route of the cardiac impulse to the ventricles.



## IN THE CLINIC

Some people have accessory AV pathways. Because these pathways often serve as a part of a reentry loop (see the section “Reentry”), they can be associated with serious cardiac rhythm disturbances. Wolff-Parkinson-White syndrome, a congenital disturbance, is the most common clinical disorder in which a bypass tract of myocardial fibers becomes an accessory pathway between the atria and ventricles. Ordinarily, the syndrome causes no functional abnormality. The disturbance is easily detected on an ECG because a portion of the ventricle is excited via the bypass tract before the remainder of the ventricle is excited via the AV node and the His-Purkinje system. This pre-excitation appears as a bizarre configuration in the ventricular (QRS) complex of the ECG. On occasion, however, a reentry loop develops in which the atrial impulse travels to the ventricles via one of the two AV pathways (AV node or bypass tract) and then back to the atria through the other of these two pathways. Continuous circling around the loop leads to a very rapid rhythm (supraventricular tachycardia). This rapid rhythm may be incapacitating because it might not allow sufficient time for ventricular filling. Transient block of the AV node by an intravenous injection of adenosine, which mimics the effects of vagal nerve stimulation, or by a reflexive increase in vagal activity (by pressing on the neck over the carotid sinus region) usually abolishes the tachycardia and restores a normal sinus rhythm.

The action potential of atrial myocytes has a plateau (phase 2) that is briefer and less developed, and repolarization (phase 3) is slower than in a typical ventricular

myocyte (see Fig. 16.15). The decrease in the duration and amplitude of the plateau is due to the presence of an **ultra-rapid delayed rectifier K<sup>+</sup> current (I<sub>Kur</sub>)**. The specific type of delayed rectifier K<sup>+</sup> channel responsible for this current results in a more rapid increase in g<sub>K</sub> during phase 2. Slower repolarization during phase 3 may be explained by a lower density of I<sub>K1</sub> K<sup>+</sup> channels.

Atrial myocytes express I<sub>K<sub>ACh</sub></sub> channels, like those found in slow-response cells in the SA and AV nodes. In the presence of vagal nerve stimulation, activation of these channels contributes to a further shortening of the atrial action potential duration. This results in the atria being more vulnerable to premature excitation and reentrant arrhythmias.

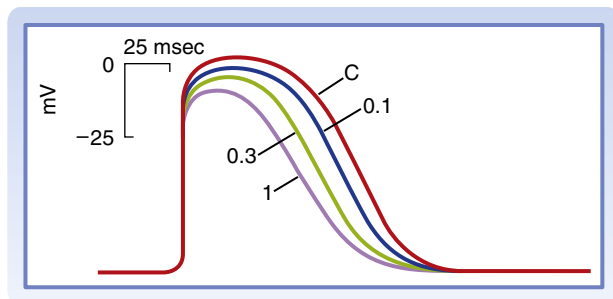
## Atrioventricular Conduction

The wave of atrial excitation reaches the ventricles via the AV node. In adult humans, this node is approximately 15 mm long, 10 mm wide, and 3 mm thick. The node is situated posteriorly on the right side of the interatrial septum near the ostium of the coronary sinus. The AV node contains the same two cell types as the SA node, but the round cells in the AV node are less abundant and the elongated cells predominate.

The AV node is made up of three functional regions: (1) the atrionodal (AN) region, or the transitional zone between the atrium and the remainder of the node; (2) the nodal (N) region, or the midportion of the AV node; and (3) the nodal-His (NH) region, or the zone in which nodal fibers gradually merge with the **bundle of His**, which is the upper portion of the specialized conducting system for the ventricles (see Fig. 16.15). Normally, the AV node and the bundle of His are the only pathways along which the cardiac impulse travels from atria to ventricles.

Several features of AV conduction are of physiological and clinical significance. The principal delay in conduction of impulses from the atria to the ventricles occurs in the AN and N regions of the AV node. Conduction velocity is slower in the N region than in the AN region. However, the path length is substantially greater in the AN region than in the N region. Conduction times through the AN and N regions account for the delay between the start of the P wave (the electrical manifestation of atrial excitation) and the QRS complex (the electrical manifestation of ventricular excitation) on an ECG (see the section “Scalar Electrocardiography”). In terms of function, the delay between atrial and ventricular excitation enables optimal ventricular filling during atrial contraction.

In the N region, slow-response action potentials prevail (see Fig. 16.15). The maximum diastolic potential is approximately -60 mV, the upstroke velocity is slow, and the conduction velocity is approximately 0.05 m/sec. Tetrodotoxin, which blocks the voltage-dependent Na<sup>+</sup> channels, has virtually no effect on action potentials in this region (or on any other slow-response fibers). Conversely, calcium channel antagonists decrease the amplitude and duration of the action potentials (Fig. 16.18) and depress AV conduction.



• **Fig. 16.18** Membrane potentials recorded from an atrioventricular node cell under control conditions (C) and in the presence of the calcium channel antagonist diltiazem at concentrations of 0.1, 0.3, and 1  $\mu\text{mol/L}$ . (Redrawn from Hirth C, et al. *J Mol Cell Cardiol.* 1983;15:799.)

Like other slow-response action potentials, the relative refractory period of cells in the N region extends well beyond the period of complete repolarization; that is, these cells display postrepolarization refractoriness (see Fig. 16.13). As heart rate increases, the time between successive atrial depolarizations is decreased, and conduction through the AV junction slows. Abnormal prolongation of the AV conduction time is called a *first-degree AV block* (see the section “Atrioventricular Conduction Blocks”). Most of the prolongation of AV conduction induced by an increase of atrial frequency takes place in the N region of the AV node.

Impulses tend to be blocked in the AV node at stimulation frequencies that are easily conducted in other regions of the heart. If the atria are depolarized at a high repetition rate, only a fraction (e.g., half) of the atrial impulses might be conducted through the AV junction to the ventricles. The conduction pattern in which only a fraction of the atrial impulses are conducted to the ventricles is called a *second-degree AV block* (see the section “Atrioventricular Conduction Blocks”). This type of block may protect the ventricles from contracting when the filling time between contractions is inadequate.

Conduction can occur in the retrograde (reverse) direction through the AV node. However, the conduction time is significantly longer, and the impulse is blocked at lower repetition rates when the impulse is conducted in the retrograde instead of the antegrade (normal or forward) direction. In addition, the AV node is a common site for reentry (see the section “Reentry”).

As in the SA node, the autonomic nervous system regulates AV conduction. Weak vagal activity may simply prolong the AV conduction time. Thus for any given atrial cycle length, the atrium-to-His or atrium-to-ventricle conduction time is prolonged by vagal stimulation. Stronger vagal activity may cause some or all of the impulses arriving from the atria to be blocked in the node. The conduction pattern in which none of the atrial impulses reaches the ventricles is called a *third-degree, or complete, AV block* (see the section “Atrioventricular Conduction Blocks”). The vagally induced delay or absence of conduction through the AV node occurs mainly in the N region. This effect of vagal stimulation reflects the action of acetylcholine to hyperpolarize the

membrane of the conducting fibers in the N region due to the activation of  $I_{K,ACH}$ . The greater the hyperpolarization at the time of arrival of the atrial impulse, the more impaired AV conduction becomes. Slowing of conduction is also associated with vagal inhibition of  $I_{Ca,L}$ , which slows action potential upstroke and conduction velocity.

Cardiac sympathetic nerves, in contrast, facilitate AV conduction. They decrease AV conduction time and enhance the rhythmicity of latent pacemakers in the AV junction. Norepinephrine released from sympathetic nerves increases the amplitude and slope of the upstroke of AV nodal action potentials, principally in the AN and N regions of the node, due to the stimulation of  $I_{Ca,L}$ .

## Ventricular Conduction

The bundle of His passes subendocardially down the right side of the interventricular septum for approximately 1 cm and then divides into the right and left bundle branches (see Fig. 16.15). The right bundle branch, a direct continuation of the bundle of His, proceeds down the right side of the interventricular septum. The left bundle branch, which is considerably thicker than the right, arises almost perpendicular from the bundle of His and perforates the interventricular septum. On the subendocardial surface of the left side of the interventricular septum, the left bundle branch splits into a thin anterior division and a thick posterior division.



### IN THE CLINIC

Conduction of impulses in the right or left bundle branch or in either division of the left bundle branch may be impaired. Conduction block may develop in one or more of these conduction pathways as a consequence of coronary artery disease or degenerative processes associated with aging, and they give rise to characteristic ECG patterns. Block of either of the main bundle branches is known as *right or left bundle branch block*. Block of either division of the left bundle branch is called *left anterior or left posterior hemiblock*.

The right bundle branch and the two divisions of the left bundle branch ultimately subdivide into a complex network of Purkinje fibers that spread out over the subendocardial surfaces of both ventricles. Purkinje fibers have abundant, linearly arranged sarcomeres, as do myocytes. However, the transverse (T) tubular system, which is well developed in myocytes, is absent in the Purkinje fibers of many species. Myocytes found in Purkinje fibers also have a diameter (70–80  $\mu\text{m}$ ) that is significantly greater than that of ventricular myocytes (10–15  $\mu\text{m}$ ). These factors decrease intracellular resistance, contributing to a conduction velocity (1–4 m/sec) that is faster than that found anywhere else in the heart, which enables rapid activation of the entire endocardial surface of the ventricles.

Although action potentials recorded from Purkinje fibers resemble those of ordinary ventricular myocardial fibers, the duration tends to be longer. The resulting increase in

refractory period duration helps to ensure that any premature atrial impulses arriving via the AV node are blocked. This function of protecting the ventricles against the effects of premature atrial depolarization is especially pronounced at slow heart rates, where Purkinje fiber action potential duration is prolonged (see Fig. 16.14). In contrast to Purkinje fibers, the effective refractory period of AV node cells does not change appreciably over the normal range of heart rates and actually increases at very rapid heart rates. Therefore, when the atrium is excited at high rates, it is the AV node that normally protects the ventricles from these excessively high frequencies.

Purkinje fibers can also act as latent pacemakers. This is due to the presence of  $I_f$  channels, which result in spontaneous depolarization during phase 4 of the fast-response action potential found in these cells.

Impulses arriving from the AV node first excite the papillary muscles and interventricular septum (except the basal portion). The activation wave spreads into the substance of the septum from both its left and right endocardial surfaces. Early contraction of the septum makes it more rigid and allows it to serve as an anchor point for contraction of the remaining ventricular myocardium. Furthermore, early contraction of the papillary muscles prevents eversion of the AV valves into the atria during ventricular systole.

The endocardial surfaces of both ventricles are activated rapidly, but the wave of excitation spreads from endocardium to epicardium at a slower velocity ( $\approx 0.3$  to  $0.4$  m/sec). The epicardial surface of the right ventricle is activated earlier than that of the left ventricle (LV) because the right ventricular wall is thinner than the left. In addition, the apical and central epicardial regions of both ventricles are activated earlier than their respective basal regions. The last portions of the ventricles to be excited are the posterior basal epicardial regions and a small zone in the basal portion of the interventricular septum.

## Arrhythmogenic Mechanisms

An arrhythmia is any change in electrical activity that alters the normal sinus rhythm of the heart. Invariably this involves disturbances in the initiation and/or propagation of normal electrical activity. This may be due to alterations in normal pacemaking and conduction mechanisms already discussed. It may also involve aberrant mechanisms, such as those described below.

### Triggered Activity

Arrhythmias due to alterations in the initiation of electrical activity may involve changes in normal function of the SA node or latent pacemakers found in the AV node or ventricular conducting system (Purkinje fibers), as discussed earlier. Impulses may also be triggered by abnormal electrical activity in other cell types. Such triggered activity is caused by **afterdepolarizations**, of which two types are recognized: **early afterdepolarizations (EADs)** and **delayed**

**afterdepolarizations (DADs)**. EADs typically occur during repolarization (phase 3), whereas DADs occur after repolarization is complete (phase 4).

### Early Afterdepolarizations

EADs are usually triggered by factors that prolong the action potential duration. When the prolongation occurs in ventricular myocytes, there is often a corresponding increase in the QT interval of the ECG. This can be caused by genetic mutations in various ion channels associated with congenital long QT syndrome. Many drugs can also prolong ventricular action potential duration, producing “acquired” long QT syndrome.

The direct correlation between action potential duration and the susceptibility to EADs may be related to  $Ca^{++}$  channel recovery from inactivation. When action potentials are prolonged,  $Ca^{++}$  channels that inactivated during the action potential plateau have time to recover from inactivation and thus may be reactivated before the cell fully repolarizes. This secondary activation is believed to trigger EADs.



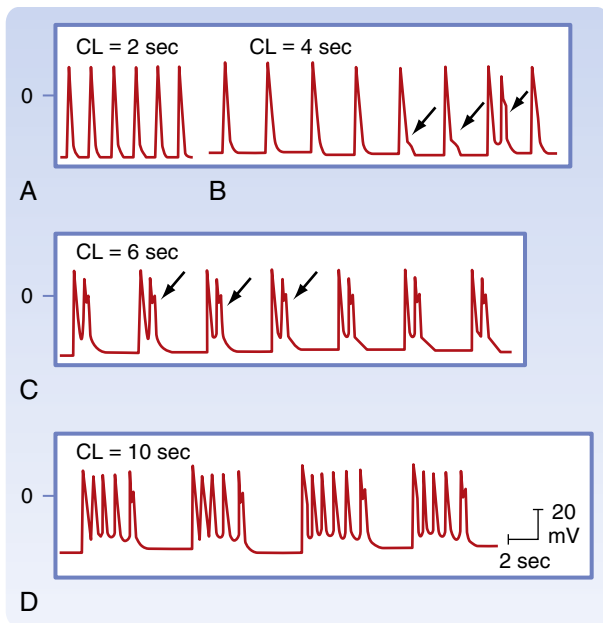
## AT THE CELLULAR LEVEL

In some individuals, the interval between the QRS complex and the T wave is abnormally prolonged, a condition termed *long QT syndrome* (Fig. 16.31). This is due to prolongation of the ventricular action potential. Several *congenital* forms of long QT syndrome have been identified in human subjects. These can be attributed to ion channel defects that produce either a decrease in outward repolarizing current (loss of function) or an increase in depolarizing inward current (gain of function). Genetic studies have identified well over 1000 different mutations in at least 15 gene products associated with congenital long QT syndrome. Examples include mutations affecting the *HERG* ( $I_{Kr}$  channel) gene located on chromosome 7, the *KCNQ1* ( $I_{Ks}$  channel) gene located on chromosome 11, and the *SCN5A* ( $I_{Na}$  channel) gene located on chromosome 3. A number of drugs (antiarrhythmic as well as nonantiarrhythmic agents) can produce *acquired* long QT syndrome in normal individuals. This is almost always due to block of the rapid delayed rectifier ( $I_{Kr}$  or *HERG*)  $K^+$  channel.



## IN THE CLINIC

The significance of EADs is associated with congenital and drug-induced long QT syndrome. As the ventricular action potential lengthens, EADs occur and cause triggered automaticity. In the ECG, this problem appears as polymorphic ventricular tachycardia, also called *torsades de pointes*. These episodes can be self-limiting, but in some instances they progress to ventricular fibrillation and sudden death. Hypokalemia and bradycardia (see Fig. 16.19), both of which lead to an increase in action potential duration, are common factors contributing to the precipitation of these arrhythmias. Therefore, restoring extracellular  $K^+$  to normal levels and increasing heart rate are two approaches used to prevent or treat this type of arrhythmia.



• **Fig. 16.19** Effect of pacing at different cycle lengths (*CL*) on early afterdepolarizations (EADs) in a Purkinje fiber treated with cesium, which prolongs action potential duration by blocking  $g_{K^+}$ . **A**, When the fiber is paced at a faster frequency, action potential duration is shortened and no EADs are observed. **B**, When the pacing frequency is slowed, action potential duration increases and EADs begin to appear (arrows). Note, the third EAD reaches threshold and triggers an action potential. **C**, Further slowing the pacing frequency produces EADs that trigger an action potential after each driven depolarization. **D**, Triggered action potentials eventually occur in salvos. (Modified from Damiano BP, Rosen M. *Circulation*. 1984;69:1013.)

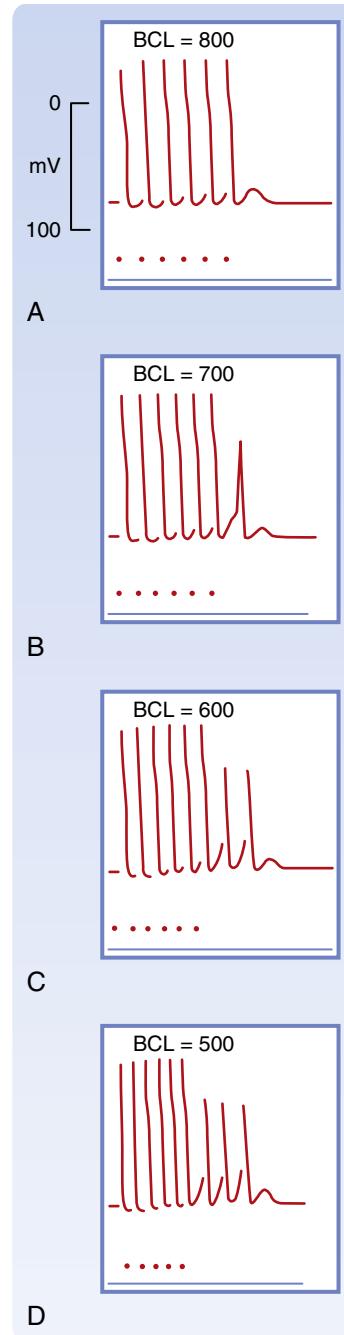
### Delayed Afterdepolarizations

In contrast to EADs, DADs are more likely to occur under conditions where there is excess accumulation of  $Ca^{++}$  in the SR. This can happen when the heart rate is high (Fig. 16.20). It can also be caused by cardiac glycosides, excess sympathetic stimulation, and myocardial ischemia. DADs are a result of spontaneous release of  $Ca^{++}$  from the SR into the cytoplasm of the cell. The increase in cytoplasmic  $Ca^{++}$  results in activation of  $I_{NCX}$  that depolarizes the membrane.

### Reentry

In certain conditions, a cardiac impulse may re-excite a region of the myocardium through which it has previously passed. This phenomenon, known as *reentry*, is responsible for most clinically significant arrhythmias. The reentry may be ordered or random. In ordered reentry, the impulse traverses a fixed anatomical path, whereas in random reentry, the path continues to change.

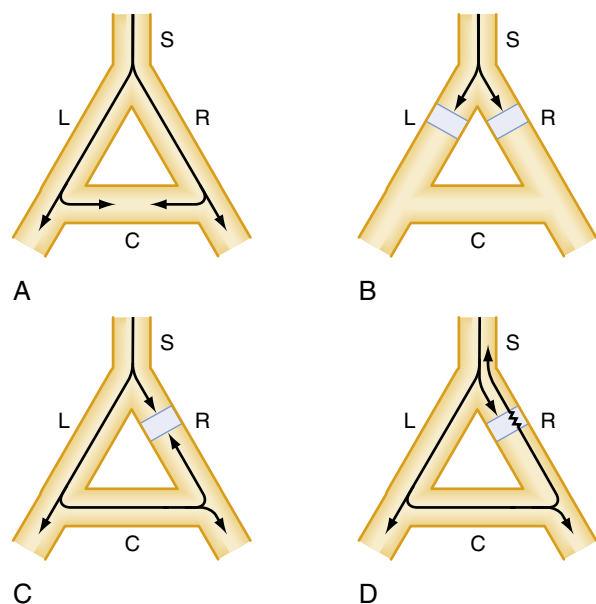
Conditions necessary for reentry to occur are illustrated in Fig. 16.21. In each of the four panels, a single bundle of cardiac fibers splits into a left and right branch, with a connecting bundle that runs between the two branches. Normally, an impulse moving down the single bundle splits and is conducted along the left and right branches (see Fig. 16.21A). As the two impulses reach the connecting



• **Fig. 16.20** Delayed after depolarizations in Purkinje fibers following  $Na^+/K^+$ -ATPase inhibition with a cardiac glycoside to facilitate  $Ca^{++}$  loading of the sarcoplasmic reticulum. After exposure to the glycoside, sequences of six driven beats (denoted by the dots) were each produced at a basic cycle length (*BCL*) of 800 (**A**), 700 (**B**), 600 (**C**), and 500 (**D**) msec. Note that delayed depolarizations occurred following the driven beats and that these afterpotentials reached threshold after the last driven beat in **B** to **D**. (From Ferrier GR, et al. *Circ Res*. 1973;32:600.)

bundle they enter from both sides, but then become extinguished at the point of collision, because each has run into tissue that is refractory.

Fig. 16.21B shows that the impulse cannot complete the circuit if an area of conduction block exists in both the left and right branches of the fiber bundle. However, if an area of conduction block exists in only one branch



• **Fig. 16.21** The role of *unidirectional* block in reentry. **A**, An excitation wave traveling down a single bundle (S) of fibers continues down the left (L) and right (R) branches. The depolarization wave enters the connecting branch (C) from both ends and the two wave fronts are extinguished when they collide. **B**, The wave is blocked in the L and R branches. **C**, A bidirectional block exists in the R branch. **D**, A unidirectional block exists in the R branch. The antegrade impulse is blocked, but the retrograde impulse is conducted through and reenters the S bundle.

(Fig. 16.21C), the impulse can propagate down the unaffected branch, enter the connecting bundle, and continue to propagate around the circuit until it reaches the affected area and stops. This is an area of *bidirectional block*.

A necessary condition for reentry is that some point in the loop must be able to conduct an impulse in one direction but not the other. This phenomenon is called *unidirectional block*. As shown in Fig. 16.21D, the impulse that travels down one branch of the fiber is blocked when it attempts to enter an affected area from the antegrade direction. However, the impulse that travels down the other branch, which is unaffected, can continue around the circuit. Yet, when it reaches the affected area, this time from the opposite direction, the tissue is now excitable. As a result, the impulse can continue, reentering the previously excited tissue and conducting an impulse in the retrograde direction.

Why is the antegrade impulse blocked but not the retrograde impulse? The reason is that the affected area is refractory to excitation when the initial impulse arrives, but with the added time it takes it to return from the opposite direction, the tissue is no longer refractory. Although unidirectional block is a necessary condition for reentry, it alone is not enough. For reentry to occur, the effective refractory period in the area of unidirectional block must be shorter in duration than the conduction time around the loop.

The functional characteristics of the various components of the reentry loops responsible for specific cardiac arrhythmias are diverse. Some loops are large and involve entire specialized conduction bundles, whereas others are

microscopic. The loop may include myocardial fibers, specialized conducting fibers, nodal cells, and junctional tissues in almost any conceivable arrangement. In addition, the various cardiac cells in the loop may be normal or abnormal.

## Electrocardiography

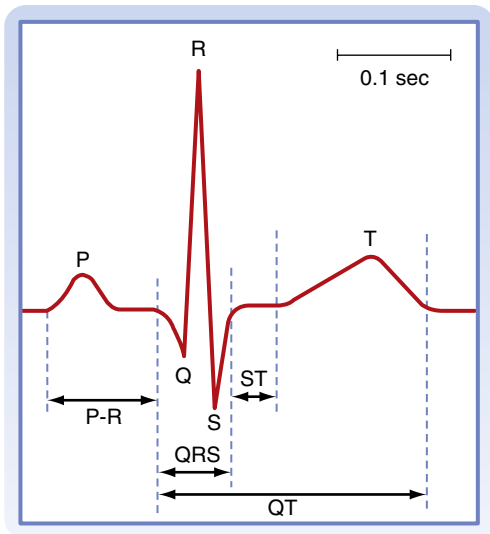
The **ECG** enables physicians to infer the course of cardiac electrical impulses by recording the variations in electrical potential at various loci on the surface of the body. By analyzing the details of these fluctuations in electrical potential, the physician gains valuable insight into (1) the anatomical orientation of the heart; (2) the relative sizes of its chambers; (3) various disturbances in rhythm and conduction; (4) the extent, location, and progress of ischemic damage to the myocardium; (5) the effects of altered electrolyte concentrations; and (6) the influence of certain drugs (notably digitalis, antiarrhythmic agents, and calcium channel antagonists). Because electrocardiography is an extensive and complex discipline, only the elementary principles are considered in this section.

## Scalar Electrocardiography

In electrocardiography, a lead is the electrical connection from the patient's skin to a recording device (**electrocardiograph**) that measures the electrical activity of the heart. The system of leads used to record routine ECGs is oriented in certain planes of the body. The diverse electrical events that exist in the heart at any moment can be represented by a three-dimensional vector (a quantity with magnitude and direction). A system of recording leads oriented in a given plane detects only the projection of the three-dimensional vector on that plane. The potential difference between two recording electrodes represents the projection of the vector on the line between the two leads. Components of vectors projected on such lines are not vectors but scalar quantities (having magnitude but not direction). Hence, a recording of changes in the difference in potential between two points on the skin surface over time is called a *scalar ECG*.

A scalar ECG detects temporal changes in the electrical potential between some point on the surface of the skin and an indifferent electrode or between pairs of points on the skin surface. The cardiac impulse progresses through the heart in a complex three-dimensional pattern. Hence, the precise configuration of the ECG varies from individual to individual, and in any given individual, the pattern varies with the anatomical location of the leads. The graphic display of the electrical impulse recorded in an ECG is called a *tracing*.

In general, a tracing consists of P, QRS, and T waves (Fig. 16.22). The P wave reflects the spread of depolarization through the atria, the QRS wave (or complex) reflects depolarization of the ventricles, and the T wave represents repolarization of the ventricles (repolarization of the atria occurs during ventricular depolarization, and is therefore masked).

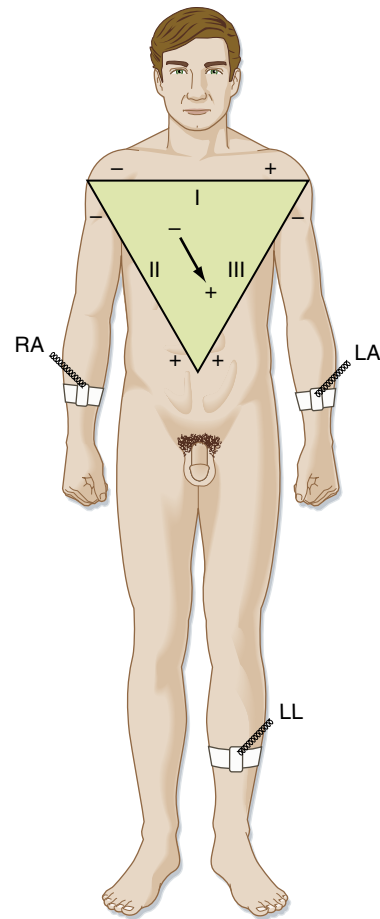


• **Fig. 16.22** Important deflections and intervals of a typical scalar electrocardiogram.

The PR interval (or more precisely, the PQ interval) is a measure of the time from the onset of atrial activation to the onset of ventricular activation; it normally ranges from 0.12 to 0.20 second. A large fraction of this time involves passage of the impulse through the AV conduction system. Pathological prolongations of the PR interval are associated with disturbances in AV conduction. Such disturbances may be produced by inflammatory, circulatory, pharmacological, or neuronal mechanisms.

The configuration and amplitude of the QRS complex vary considerably among individuals. The duration is usually between 0.06 and 0.10 second. An abnormally prolonged QRS complex may indicate a block in the normal conduction pathways through the ventricles (such as a block of the left or right bundle branch). During the ST interval, the entire ventricular myocardium is depolarized. Therefore, the ST segment normally lies on the isoelectric line. Any appreciable deviation of the ST segment from the isoelectric line may indicate ischemic damage to the myocardium. The QT interval, sometimes referred to as the period of “electrical systole” of the ventricles, is closely correlated with the mean action potential duration of the ventricular myocytes. The duration of the QT interval is approximately 0.4 second, but it varies inversely with the heart rate, mainly because the duration of the myocardial cell’s action potential varies inversely with the heart rate (see Fig. 16.14).

In most leads, the T wave is deflected in the same direction from the isoelectric line as the major component of the QRS complex, although biphasic (i.e., oppositely directed) T waves are perfectly normal in certain leads. Deviation of the T wave and QRS complex in the same direction from the isoelectric line indicates that the repolarization process is proceeding in a direction counter to that of the depolarization process. T waves that are abnormal either in direction or in amplitude may indicate myocardial damage, electrolyte disturbances, or cardiac hypertrophy.

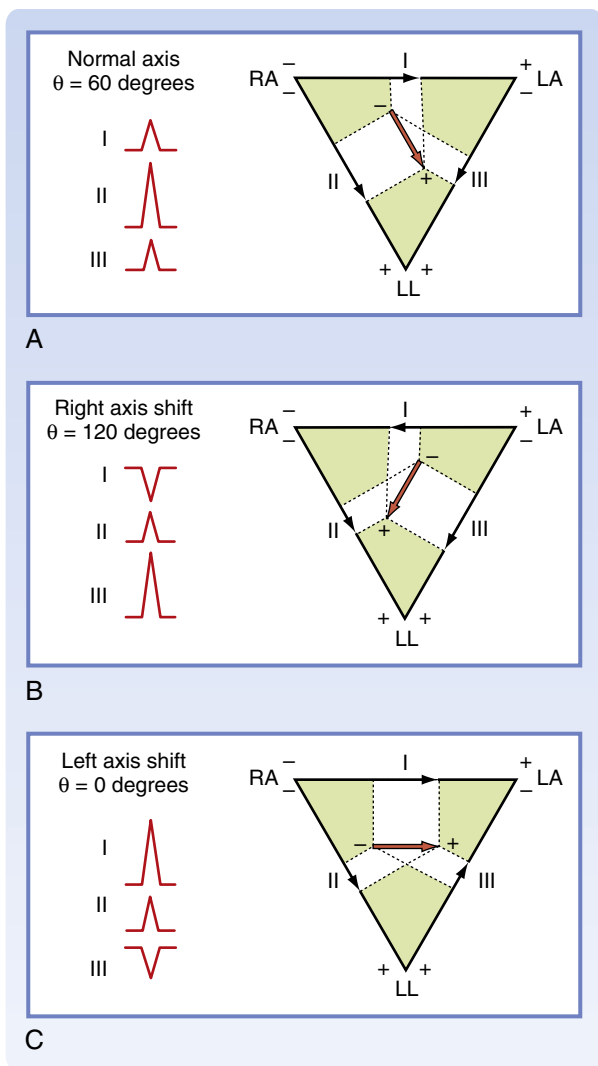


• **Fig. 16.23** Einthoven's triangle, illustrating the electrocardiographic connections for standard limb leads I, II, and III.

### Standard Limb Leads

The original ECG lead system was devised by Willem Einthoven at the beginning of the 20th century. In this system, the vector sum of all cardiac electrical activity at any moment is called the **resultant cardiac vector**. This directional electrical force is considered to lie in the center of an equilateral triangle whose apices are located in the left and right shoulders and the pubic region (Fig. 16.23). This triangle, called **Einthoven's triangle**, is oriented in the frontal plane of the body. Hence, only the projection of the resultant cardiac vector on the frontal plane is detected by this system of leads. For convenience, the electrodes are connected to the right and left forearms rather than to the corresponding shoulders because the arms represent simple electrical extensions of leads from the shoulders. Similarly, the leg represents an extension of the lead system from the pubis, and thus the third electrode is generally connected to an ankle (usually the left one).

Certain conventions dictate the manner in which these standard limb leads are connected to the electrocardiograph. Lead I records the potential difference between the left arm and the right arm. The connections are such that when the potential at the left arm ( $V_{LA}$ ) exceeds the potential at the right arm ( $V_{RA}$ ), the tracing is deflected upward



• **Fig. 16.24** Magnitude and direction of the QRS complexes in limb leads I, II, and III when the mean electrical axis ( $\theta$ ) is 60 degrees (**A**), 120 degrees (**B**), and 0 degrees (**C**).

from the isoelectric line. In **Fig. 16.23** and **Fig. 16.24**, this arrangement of connections for lead I is designated by a plus sign at the left arm and by a minus sign at the right arm. Lead II records the potential difference between the right arm and the left leg, and the tracing is deflected upward when the potential at the left leg ( $V_{LL}$ ) exceeds  $V_{RA}$ . Finally, lead III registers the potential difference between the left arm and the left leg, and the tracing is deflected upward when  $V_{LL}$  exceeds  $V_{LA}$ . These connections were chosen arbitrarily so that the QRS complexes are upright in all three standard limb leads in most normal individuals.

If the frontal projection of a resultant cardiac vector at some moment is represented by an arrow (tail negative, head positive), as in **Fig. 16.23**, the potential difference,  $V_{LA} - V_{RA}$ , recorded in lead I is represented by the component of the vector projected along the horizontal line between the left arm and the right arm, also shown in **Fig. 16.23**. If the vector makes an angle ( $\theta$ ) of 60 degrees with the horizontal line (as in **Fig. 16.24A**), the deflection

recorded in lead I is upward because the positive arrowhead lies closer to the left arm than to the right arm. The deflection in lead II is also upright because the arrowhead lies closer to the left leg than to the right arm. The magnitude of the lead II deflection is greater than that in lead I because in this example, the direction of the vector parallels that of lead II; therefore, the magnitude of the projection on lead II exceeds that on lead I. Similarly, in lead III, the deflection is upright and its magnitude equals that in lead I.

If the vector in **Fig. 16.23A** is the result of electrical events that occur during the peak of the QRS complex, the orientation of this vector is said to represent the mean electrical axis of the heart in the frontal plane. The positive rotatory direction of this axis is assumed to be in the clockwise direction from the horizontal plane (contrary to the usual mathematical convention). In normal individuals, the average mean electrical axis is approximately +60 degrees (as in **Fig. 16.24A**). Therefore, QRS complexes are usually upright in all three leads and largest in lead II.

If the mean electrical axis shifts substantially to the right (as in **Fig. 16.24B**, in which  $\theta = 120$  degrees), projections of the QRS complexes on the standard leads change considerably. In this case, the largest upright deflection is in lead III, and the deflection in lead I is inverted because the arrowhead is closer to the right arm than to the left arm. Such a shift is termed *right axis deviation* and occurs with hypertrophy (i.e., increased thickness) of the right ventricle. When the axis shifts to the left, as occurs with hypertrophy of the LV (see **Fig. 16.24C**, where  $\theta = 0$  degrees), the largest upright deflection is in lead I, and the QRS complex in lead III is inverted.

In addition to limb leads I, II, and III, other limb leads that are also oriented in the frontal plane are routinely recorded in patients. These leads are (1) **aVR**, for which the right arm is defined as the positive lead and the middle of the heart is defined as the negative lead (i.e., the left arm and ankle leads are connected together); (2) **aVL**, for which the left arm is the positive lead and the middle of the heart is defined as the negative lead (i.e., the right arm and ankle leads are connected together); and (3) **aVF**, for which the ankle (foot) lead is defined as positive and the middle of the heart is defined as the negative lead (i.e., the two arm leads are connected together). The axes of these leads form angles of +90 degrees for aVF, -30 degrees for aVL, and -150 degrees for aVR (all with respect to the horizontal axis).

Leads can also be applied to the surface of the chest, so-called **precordial leads**, to determine the projections of the cardiac vector on the sagittal and transverse planes of the body. These precordial leads are recorded from six selected points on the anterior and lateral surfaces of the chest in the vicinity of the heart. The leads extend from the right border of the sternum in the fourth intercostal space (lead  $V_1$ ) to under the left arm (midaxillary line) in the fifth intercostal space (lead  $V_6$ ). Each precordial lead ( $V_1$  to  $V_6$ ) is defined as a positive lead, whereas the middle of

the heart is defined as the negative lead. Detailed analysis of the ECG, as detected by the various lead systems just described, is beyond the scope of this book. Interested students are referred to textbooks on electrocardiography for more information.



## IN THE CLINIC

Changes in the mean electrical axis may occur if the anatomical position of the heart is altered or if the relative mass of the right and left ventricles is abnormal, as it is in certain cardiovascular disturbances. For example, the axis tends to shift toward the left (more horizontal) in short, obese or stocky individuals and toward the right (more vertical) in tall, thin persons. In addition, in left or right ventricular hypertrophy (increased myocardial mass of either ventricle), the axis shifts toward the hypertrophied side.

## Arrhythmias

Cardiac arrhythmias are disturbances in either impulse initiation or impulse propagation. Disturbances in impulse initiation include those that arise from the SA node and those that originate from various ectopic foci. The principal

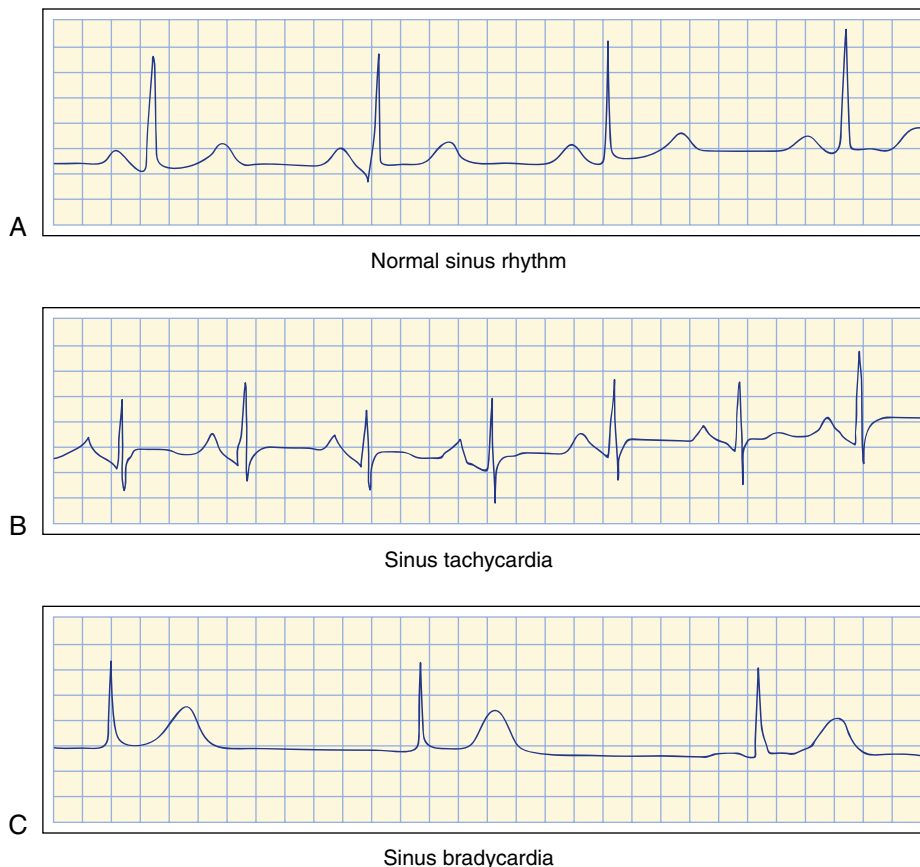
disturbances in impulse propagation are reentrant rhythms and conduction blocks.

## Altered Sinoatrial Rhythms

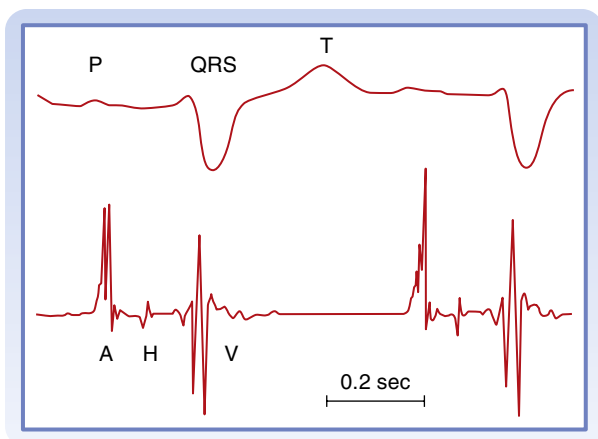
Mechanisms that vary the firing frequency of cardiac pacemaker cells were described previously. Changes in the firing rate of the SA node are usually produced by cardiac autonomic nerves. When the firing rate of the SA node is decreased, the heart rate also decreases (**bradycardia**). Conversely, increased SA node firing results in elevation of the heart rate (**tachycardia**). Examples of ECGs of sinus tachycardia and sinus bradycardia are shown in Fig. 16.25. The P, QRS, and T deflections are all normal, but duration of the cardiac cycle (the PP interval) is altered. The changes in cardiac frequency are characteristically gradual. A rhythmic variation of the PP interval at the respiratory frequency (i.e., a respiratory sinus arrhythmia) is a normal, common occurrence (see Fig. 18.7).

## Atrioventricular Conduction Blocks

Various physiological, pharmacological, and pathological processes can impede transmission of an impulse through the AV node. The site of block can be localized more precisely by an ECG of the His bundle (Fig. 16.26). To obtain such



• **Fig. 16.25** Electrocardiographic tracings of heart rhythms. **A**, Normal sinus rhythm. **B**, Sinus tachycardia. **C**, Sinus bradycardia.



• **Fig. 16.26** Electrocardiogram of the His bundle (*lower tracing, retouched*) and lead II recording of the scalar electrocardiogram (*upper tracing*). The deflection H, which represents conduction of the impulse over the bundle of His, is clearly visible between the atrial (A) and the ventricular (V) deflections. The conduction time from the atria to the bundle of His is denoted by the A-H interval; that from the bundle of His to the ventricles, by the H-V interval. (Courtesy of Dr. J. Edelstein.)

tracings, an electrode catheter is inserted into a peripheral vein and advanced centrally into the right side of the heart until the electrode lies in the AV junctional region. When the electrode is properly positioned, a distinct deflection (H in Fig. 16.26) is registered as the cardiac impulse passes through the bundle of His. The time intervals required for propagation from the atrium to the bundle of His and from



## IN THE CLINIC

Three degrees of AV block can be distinguished, as shown in Fig. 16.27. First-degree AV block is characterized by a prolonged PR interval. In most cases of first-degree block, the atrium-to-His interval is prolonged and the His-to-ventricle interval is normal. Hence, the delay in a first-degree AV block is located above the His bundle (i.e., in the AV node). In second-degree AV block, all QRS complexes are preceded by P waves, but not all P waves are followed by QRS complexes. The ratio of P waves to QRS complexes is usually the ratio of two small integers (such as 2:1, 3:1, or 3:2). The site of block may be located above or below the His bundle. A block below the bundle is usually more serious than one above the bundle because the former is more likely to evolve into a third-degree block. An artificial pacemaker is frequently implanted when the block is below the bundle. Third-degree AV block is often referred to as *complete heart block* because the impulse is completely unable to traverse the AV conduction pathway from atria to ventricles. The most common sites of complete block are distal to the bundle of His. In complete heart block, the atrial and ventricular rhythms are entirely independent. Because of the slow ventricular rhythm that results, the volume of blood pumped by the heart is often inadequate, especially during exercise. Third-degree block is frequently associated with syncope (pronounced lightheadedness), which is caused principally by insufficient cerebral blood flow. Third-degree block is one of the most common conditions that necessitate the implantation of artificial pacemakers.

the bundle of His to the ventricles (His-to-ventricle interval) may be measured accurately. Abnormal prolongation of the atrium-to-His or His-to-ventricle interval indicates block above or below the bundle of His, respectively.

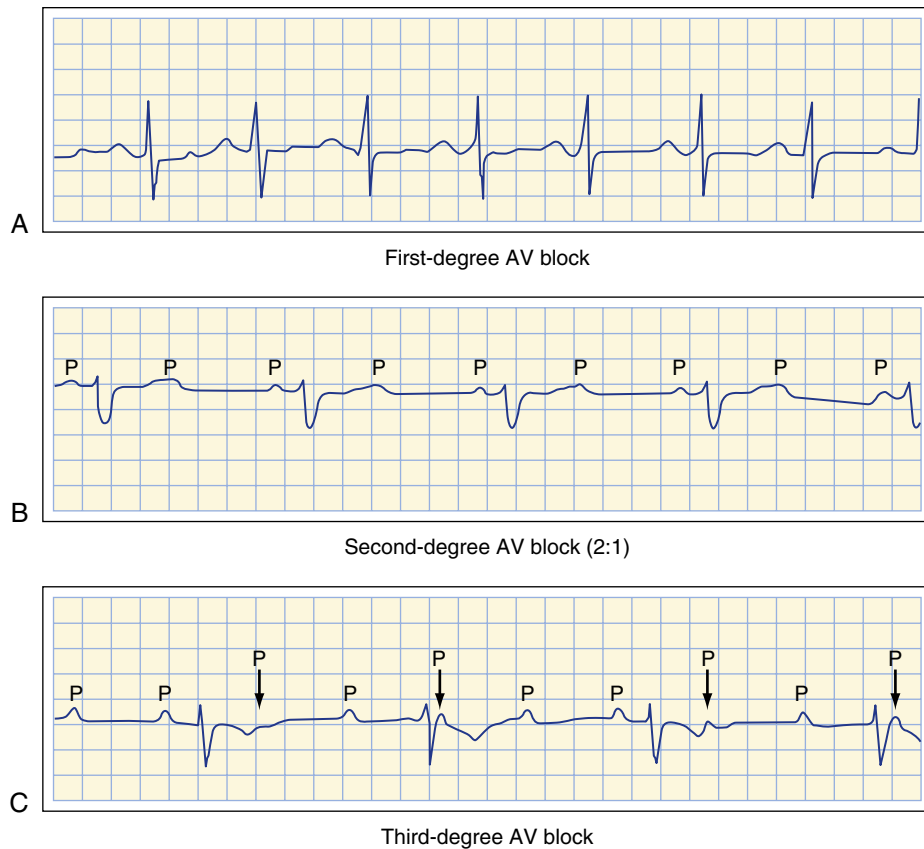
## Premature Depolarizations

Premature depolarizations occur occasionally in most normal individuals, but they arise more commonly in certain abnormal conditions. Such depolarizations may originate in the atria, AV junction, or ventricles. One type of premature depolarization follows a normally conducted depolarization at a constant time interval (the **coupling interval**). If the normal depolarization is suppressed in some way (e.g., by vagal stimulation), the premature depolarization is also abolished. Such premature depolarizations are called **coupled extrasystoles**, or simply **extrasystoles**, and they generally reflect a reentry phenomenon. A second type of premature depolarization occurs as the result of enhanced automaticity in some ectopic focus. This ectopic center may fire regularly, and a zone of tissue that conducts unidirectionally may protect this center from being depolarized by the normal cardiac impulse. If this premature depolarization occurs at a regular interval or at an integral multiple of that interval, the disturbance is called **parasytostole**.

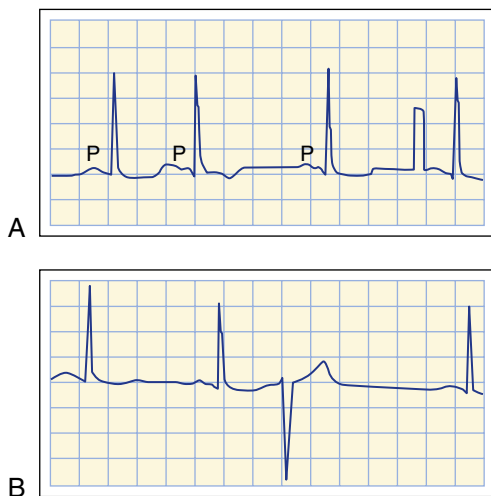
A tracing of a premature atrial depolarization is shown in Fig. 16.28A. With a premature atrial depolarization, the normal interval between beats is shortened. In addition, the configuration of the premature P wave differs from that of the other normal P waves because the course of atrial excitation, which originates at some ectopic focus in the atrium, differs from the normal spread of excitation, which originates at the SA node. The QRS complex of the premature depolarization is generally normal because the ventricular excitation spreads over the usual pathways.

A tracing of a premature ventricular depolarization is shown in Fig. 16.28B. Propagation of the impulse is abnormal, and the configuration of the QRS complex and T wave is entirely different from the normal ventricular deflections because the premature excitation originates at some ectopic focus in the ventricles. The time interval between the premature QRS complex and the preceding normal QRS complex is shortened, whereas the interval after the premature QRS complex and the next normal QRS complex is prolonged by a compensatory pause. The interval from the QRS complex just before the premature excitation to the QRS complex just after it is virtually equal to the duration of two normal cardiac cycles.

As noted, a compensatory pause usually follows a premature ventricular depolarization. This pause occurs because the ectopic ventricular impulse does not disturb the natural rhythm of the SA node. There are two possible reasons for this: The ectopic ventricular impulse is not conducted in a retrograde direction through the AV conduction system, or the SA node had already fired at its natural interval before the ectopic impulse could have reached and depolarized it prematurely. Likewise, the SA nodal impulse generated just



• **Fig. 16.27** Atrioventricular (AV) blocks. **A**, First-degree block; the PR interval is 0.28 seconds (normal, <0.20 seconds). **B**, Second-degree block (ratio of P waves to QRS complexes, 2:1). **C**, Third-degree block; note the dissociation between the P waves and the QRS complexes.



• **Fig. 16.28** Premature atrial depolarization and premature ventricular depolarization. The premature atrial depolarization (**A**; second beat) is characterized by an inverted P wave (just below the second “P”) and normal QRS complexes and T waves. The interval after the premature atrial depolarization is not much longer than the usual interval between beats. The brief rectangular deflection just before the last atrial depolarization is a standardization signal. The premature ventricular depolarization (**B**) is characterized by bizarre, inverted QRS complexes and elevated T waves and is followed by a compensatory pause.

before or after the ventricular extrasystole generally does not affect the ventricle because the AV junction and perhaps

also the ventricles are still refractory from the premature ventricular excitation.

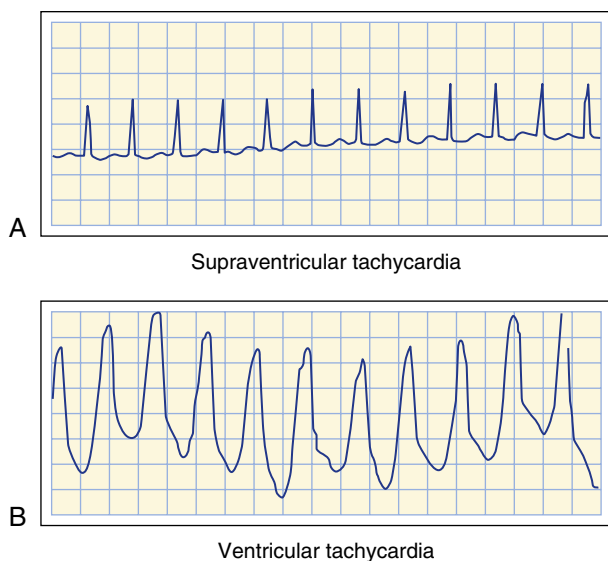


## IN THE CLINIC

Paroxysmal tachycardias that originate either in the atria or in the AV junctional tissues ([Fig. 16.29A](#)) are usually indistinguishable, and therefore the term *paroxysmal supraventricular tachycardia* refers to both types. In this tachycardia, the impulse often circles a reentry loop that includes atrial and AV junctional tissue. The QRS complexes are frequently normal because ventricular activation proceeds over the usual pathways. As its name implies, paroxysmal ventricular tachycardia originates from an ectopic focus in the ventricles. The ECG is characterized by repeated bizarre QRS complexes that reflect the abnormal intraventricular impulse conduction (see [Fig. 16.29B](#)). Paroxysmal ventricular tachycardia is much more ominous than supraventricular tachycardia because the former is frequently a precursor of ventricular fibrillation, a lethal arrhythmia described in the next section.

## Ectopic Tachycardias

In contrast to the gradual rate changes that characterize sinus tachycardia, tachycardias that originate from an ectopic focus typically begin and end abruptly. Such ectopic tachycardias are generally called **paroxysmal tachycardias**.



• **Fig. 16.29** Paroxysmal tachycardias. **A**, Supraventricular tachycardia; P waves precede each QRS complex. **B**, Ventricular tachycardia; P waves not readily observed.

Episodes of paroxysmal tachycardia may persist for only a few beats or for many hours or days, and episodes often recur. Paroxysmal tachycardias may result from (1) rapid firing of an ectopic pacemaker, (2) triggered activity secondary to afterpotentials that reach threshold, or (3) an impulse that circles a reentry loop repetitively.

## Fibrillation

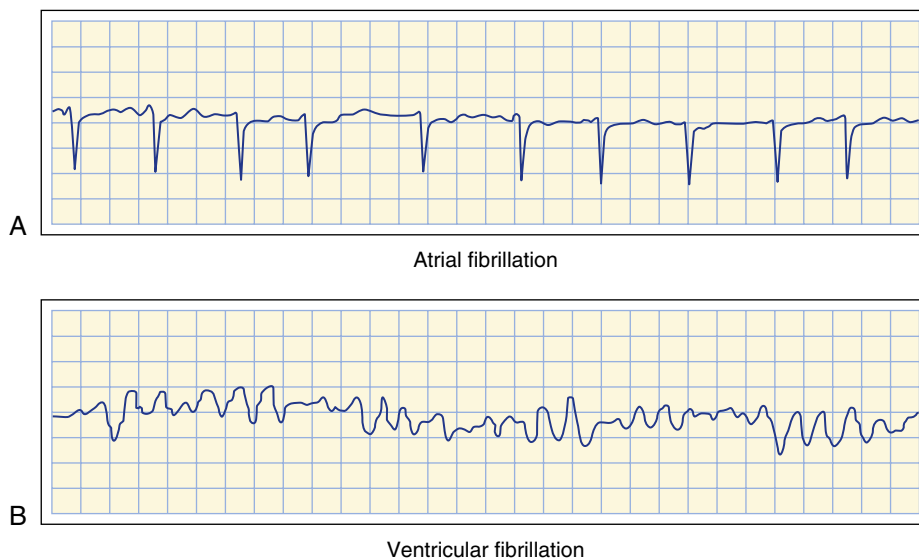
Under certain conditions, cardiac muscle undergoes an irregular type of contraction that is ineffectual in propelling blood. Such an arrhythmia is termed **fibrillation**, and the disturbance may involve either the atria or the ventricles. Fibrillation probably represents a reentry phenomenon in which the reentry loop fragments into multiple, irregular circuits.

The electrocardiographic changes in atrial fibrillation are shown in [Fig. 16.30A](#). This arrhythmia occurs in various types of chronic heart disease. The atria do not contract and relax sequentially during each cardiac cycle, and thus they do not contribute to ventricular filling. Instead, the atria undergo a continuous, uncoordinated rippling motion. P waves do not appear on the ECG; instead, the tracing shows continuous irregular fluctuations in potential called *f waves*. The AV node is activated at intervals that may vary considerably from cycle to cycle. Hence, no constant interval occurs between successive QRS complexes or between successive ventricular contractions. Because the strength of ventricular contraction depends on the interval between beats (see [Chapter 18](#)), the volume and rhythm of the pulse are irregular. In many affected patients, the atrial reentry loop and the pattern of AV conduction are more regular than they are in atrial fibrillation. The rhythm is then referred to as *atrial flutter*.



## IN THE CLINIC

Atrial fibrillation and flutter are not usually life-threatening; some people with these disturbances can function normally. However, because the atria do not contract and relax rhythmically, blood clots tend to form in the atria. Such clots, if dislodged, may then travel to the pulmonary or systemic vascular beds. Patients with atrial fibrillation or flutter are generally treated with anticoagulant drugs such as coumadin to prevent the formation of such clots. Ventricular fibrillation, in contrast, leads to loss of consciousness within a few seconds. The irregular, continuous, uncoordinated twitching of the ventricular muscle fibers pumps no blood. Death ensues unless immediate resuscitation is achieved or the rhythm spontaneously reverts to normal, which rarely occurs. Ventricular fibrillation may supervene when the entire ventricle, or some portion of it, is deprived of its normal blood supply. It may also occur as a result of electrocution or in response to certain drugs and anesthetics. On the ECG (see [Fig. 16.30B](#)), the fluctuations in potential are highly irregular.



• **Fig. 16.30** Atrial (**A**) and ventricular (**B**) fibrillation.

Ventricular fibrillation is often initiated when a premature impulse arrives during the vulnerable period of the cardiac cycle. This period coincides with the downslope of the T wave on the ECG. During this period, the excitability of cardiac cells varies spatially. Some fibers are still in their effective refractory periods, others have almost fully recovered their excitability, and still others are able to conduct impulses, but only at very slow conduction velocities. As a consequence, the action potentials are propagated over the chambers in many irregular wavelets that travel along circuitous paths and at various conduction velocities. As a region of cardiac cells becomes excitable again, it is ultimately activated by one of the wave fronts traveling around the chamber. Hence, the process is self-sustaining.

Atrial fibrillation may be changed to a normal sinus rhythm by drugs that prolong the refractory period. As the cardiac impulse completes the reentry loop, it may then encounter refractory myocardial fibers. When atrial fibrillation does not respond adequately to drugs, electrical defibrillation may be used to correct this condition.

Dramatic therapy is required for ventricular fibrillation. Conversion to a normal sinus rhythm is accomplished by means of a strong electrical current that places the entire myocardium briefly in a refractory state. Techniques have been developed to administer the current safely through the intact chest wall. In successful cases, the SA node again takes over the normal pacemaker function for the entire heart.

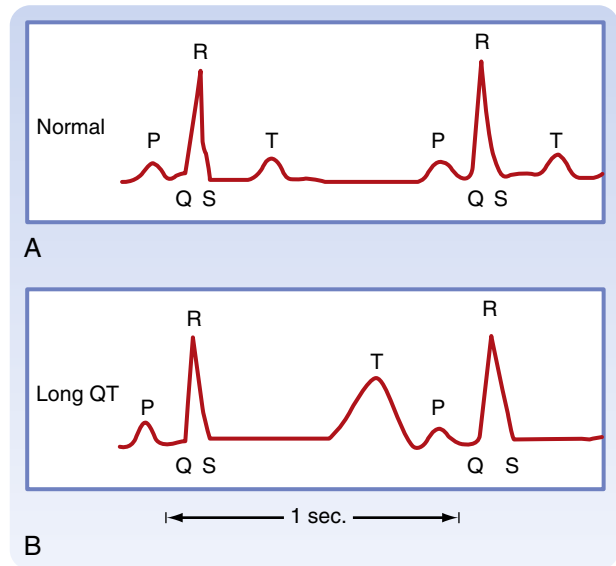


## IN THE CLINIC

Implantable cardioverter-defibrillator (ICD) devices have been developed to prevent death in patients in whom either ventricular fibrillation or paroxysmal ventricular tachycardia has suddenly developed. The former is lethal unless it is treated immediately, and the latter often leads to ventricular fibrillation and sudden death. The ICD device is implanted subcutaneously in the left subclavicular region of the chest wall. Atrial and ventricular leads enable recording of the right atrial and right ventricular electrocardiograms and provide the ability for right atrial or right ventricular pacing, or both. The defibrillation coil in the right ventricle enables the application of a strong electrical current to the ventricle and thereby usually terminates the lethal arrhythmia.

## The Cardiac Pump

The heart must always pump with enough force and volumetric output (blood flow) to (1) maintain an adequate pressure on the blood in the large arteries and (2) provide a sufficient *total* flow of blood to meet the metabolic needs of all the tissues and organs. (An adequate pressure on the blood in the large arteries ensures that each tissue or organ can regulate its own blood flow to meet its own metabolic needs, under all circumstances.) Both heart rate (discussed earlier in this chapter) and muscular contractile performance must vary to accomplish this. Variation of cardiac contraction performance is accomplished mainly by



• **Fig. 16.31** Electrocardiograms recorded from a normal subject (**A**) and from a patient with long QT syndrome (**B**).

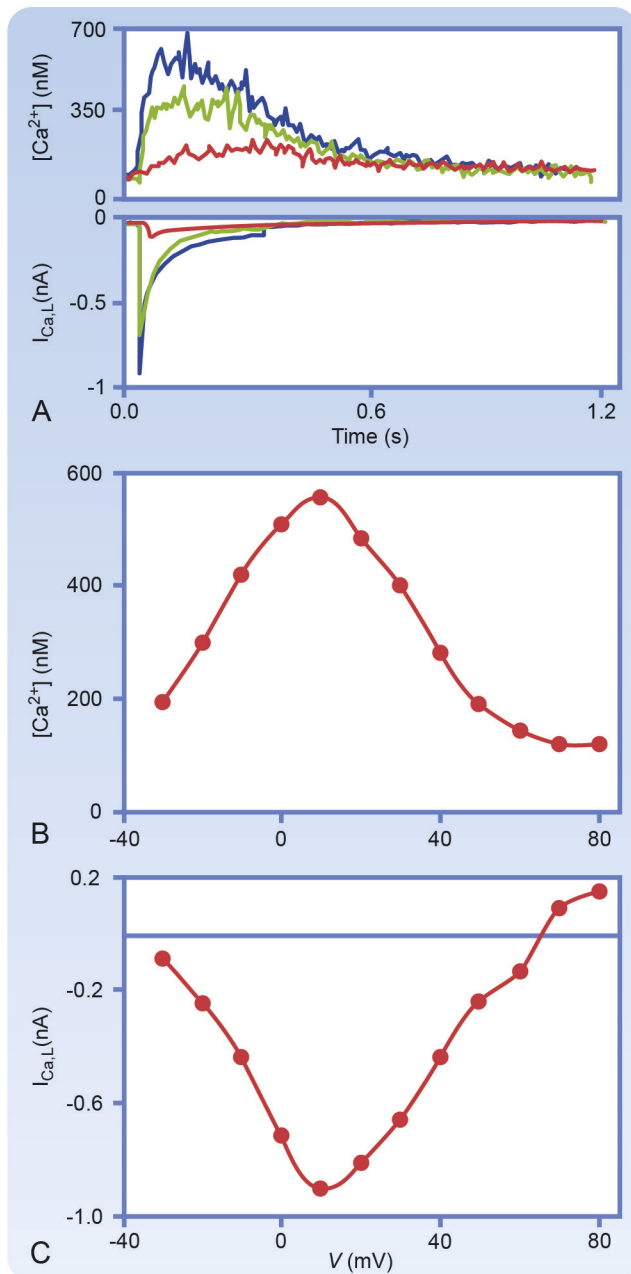
(1) regulation of E-C coupling processes (see [Chapter 13](#) and later) in all the individual myocardial cells and (2) the muscle cell's reaction to the physical forces (*viz.*, **preload** and **afterload**) that act on the intact heart during systole (contraction and ejection of blood) and diastole (relaxation and filling). E-C coupling is regulated by the nervous system and by circulating substances. Regulation by preload and afterload is the result of the heart's connections to the systemic and pulmonary vasculature, as explained later in this chapter and in [Chapters 18](#) and [19](#). In the ventricles, virtually all of the myocardial cells are activated similarly on each contraction, different to skeletal muscle, where contraction strength is modulated by varying the number of groups of tetanically activated muscle cells (*i.e.*, “recruitment,” see [Chapter 12](#)).

## Cardiac Excitation-Contraction Coupling

Within each ventricular muscle cell, the action potential causes a large and spatially uniform change in cytoplasmic  $[Ca^{++}]$ . As a result, contractile activation occurs nearly synchronously in all the sarcomeres of each cell of a particular cardiac chamber. The change in the cytoplasmic  $[Ca^{++}]$  that activates contraction is the result of  $Ca^{++}$  released from the SR and is termed the “cytoplasmic  $[Ca^{++}]$ -transient” ([Figs. 13.2](#), [13.3](#), and [16.32](#)). The size of the cytoplasmic  $[Ca^{++}]$  transient, and thus of the contraction, is determined dynamically, on a beat-to-beat basis, mainly by two cellular processes: (1) the L-type  $Ca^{++}$  current during the action potential and (2) the release of  $Ca^{++}$  from the “dyadic” ([Fig. 13.1B](#)) regions of SR.

### $Ca^{++}$ Channels and E-C Coupling

In cardiac muscle, clusters of L-type  $Ca^{++}$  channels and SR  $Ca^{++}$  release channels (RyR) are co-localized at the dyadic SR-T-tubule junction ([Figs. 13.1](#), [13.2](#), and [13.4](#)).



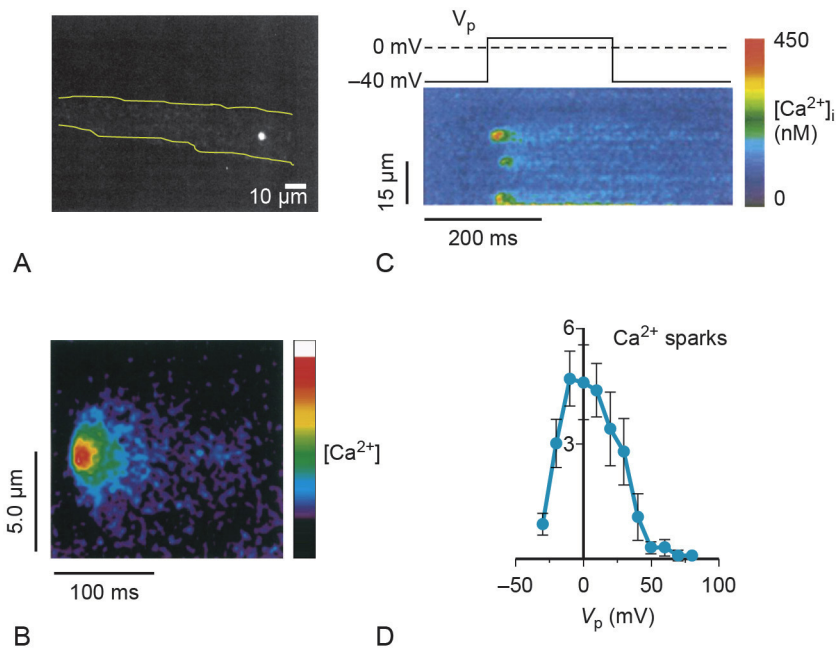
• **Fig. 16.32** L-type  $Ca^{2+}$  current and cytoplasmic  $[Ca^{2+}]$  transients elicited by voltage-clamp depolarization of ventricular myocytes. **(A)** Depolarization to  $-30$  mV (red),  $-10$  mV (green), and  $10$  mV (blue) elicits  $I_{Ca,L}$  (lower) and cytoplasmic  $[Ca^{2+}]$  transient (upper). Both  $[Ca^{2+}]$  **(B)** and current **(C)** depend on membrane voltage in a similar way. Experimental results are consistent with the idea that  $I_{Ca,L}$  controls SR  $Ca^{2+}$  release (see text). (Redrawn from Fig. 9 of Beuckelmann DJ, Wier WG. *J Physiol.* 1988;233-255.)

Abundant experimental evidence shows that  $Ca^{2+}$  entering the dyadic space via L-type  $Ca^{2+}$  channels ( $Ca_v1.2$ ) activates or “induces” the release of a much larger amount of  $Ca^{2+}$  from the SR, by activating (i.e., causing to open) the RyR. The local change in  $Ca^{2+}$  concentration ( $[Ca^{2+}]$ ) in the dyad has been found to be an elementary unit of  $Ca^{2+}$  signaling in cardiac E-C coupling and has been termed a “ $Ca^{2+}$  spark” (because these local dyadic  $Ca^{2+}$  transients were first observed experimentally as tiny flashes of light from intracellular fluorescent  $Ca^{2+}$  indicators, see Fig. 16.33).

This process by which SR  $Ca^{2+}$  release is induced by  $Ca^{2+}$  entering via L-type  $Ca^{2+}$  channels is known as “Calcium induced Calcium release,” or CICR. CICR involves positive feedback by  $Ca^{2+}$  however, and therefore has the potential to cause uncontrolled  $Ca^{2+}$  release from the SR, which would prevent the controlled regulation of cardiac contraction. Nevertheless, experimental data establish that the SR  $Ca^{2+}$  release is controlled: The explanation for this apparent paradox lies in the “local control” theory of cardiac E-C coupling. Key factors in local control of SR  $Ca^{2+}$  release are as follows: (1) A local  $[Ca^{2+}]$  much higher than normal cytoplasmic  $[Ca^{2+}]$  is required to activate the SR  $Ca^{2+}$  release channels (*viz.*, the RyR, Fig. 13.2); (2) such activation of the RyR is achieved efficaciously by  $Ca^{2+}$  entering the dyadic space through a single L-type  $Ca^{2+}$  channel ( $Ca_v1.2$ ); (3) by mechanisms in the dyad that are not yet entirely known, release is terminated; and (4) some of the released  $Ca^{2+}$  that diffuses toward a distant dyad is taken up by the SR. In summary, the longitudinal physical separation of release sites (dyads) from each other, the brevity of normal SR  $Ca^{2+}$  release flux, and the requirement for a high dyadic  $[Ca^{2+}]$  for activation of RyR, all produce a situation where  $Ca^{2+}$  released from one dyad does not normally reach the next dyad (a sarcomere length away) in sufficient concentration or rapidly enough to activate further release. Nevertheless, sufficient  $Ca^{2+}$  reaches the myofilaments within each sarcomere to bind to troponin C and activate contraction. Thus, the total  $Ca^{2+}$  released is the summation of the  $Ca^{2+}$  sparks, the number of which in the cell is related to the number of L-type  $Ca^{2+}$  channels ( $Ca_v1.2$ ) that opened and constituted the L-type  $Ca^{2+}$  current in the cell. Control of SR  $Ca^{2+}$  release, and muscular contraction, by L-type  $Ca^{2+}$  channels ( $Ca_v1.2$ ) is thus achieved.

### SR $Ca^{2+}$ Content and $Ca^{2+}$ Flux Balance

Variation of the loading of the SR with  $Ca^{2+}$  is a key element of regulation of the cardiac contraction. Increases in SR  $Ca^{2+}$  loading increase the probability and amplitude of the  $Ca^{2+}$  sparks. Nevertheless, under normal conditions, the  $Ca^{2+}$  sparks remain the elementary units of the cytoplasmic  $[Ca^{2+}]$  transient and SR  $Ca^{2+}$  release is still controlled “locally,” by the L-type  $Ca^{2+}$  channels at the dyadic junctions. Processes that will tend to increase SR  $Ca^{2+}$  content include: increased L-type  $Ca^{2+}$  current, increased SR  $Ca^{2+}$  pump (SERCA) activity, decreased  $Ca^{2+}$  extrusion via NCX, and decreased interval between beats. Opposite effects on these processes will have the opposite effect on SR  $Ca^{2+}$  content (load). These changes result in changed SR  $Ca^{2+}$  load, which will change contraction strength, but other changes must then occur to restore  $Ca^{2+}$  flux balance.  $Ca^{2+}$  flux balance is the concept that to prevent constant  $Ca^{2+}$  loss or gain, surface membrane  $Ca^{2+}$  influx must equal surface membrane  $Ca^{2+}$  efflux in any steady-state condition of heart function. This must always be true in a steady state, even though SR  $Ca^{2+}$  load may be different than in other steady state conditions, or is in a process of change (toward a new steady-state condition). As illustrated in Fig. 16.34, feedback mechanisms exist to restore  $Ca^{2+}$  flux balance after a change in sarcolemmal  $Ca^{2+}$  flux. Thus, cardiac cells can achieve a new steady state of beating, with



• **Fig. 16.33**  $\text{Ca}^{2+}$  “sparks” are the fundamental elements of the cytoplasmic  $\text{Ca}^{2+}$  transient. A few  $\text{Ca}^{2+}$  sparks occur spontaneously in resting cells, but they are triggered in large numbers by  $\text{Ca}^{2+}$  entering the dyadic space through near-by L-type  $\text{Ca}^{2+}$  channels ( $\text{Ca}_v1.2$ ) during E-C coupling. **(A)** A spontaneous  $\text{Ca}^{2+}$  spark, as recorded using an intracellular fluorescent  $\text{Ca}^{2+}$  indicator dye in a single, isolated cardiac ventricular myocyte. The cell edges are indicated in yellow; the single  $\text{Ca}^{2+}$  spark was recorded as a very small (<5 $\mu\text{m}$ ) region of elevated dye fluorescence. Modified with permission from Fig. 1 of Cheng H, Lederer WJ, Cannell MB. *Science*. 1993; 262:740-744. **(B)** A single spontaneous  $\text{Ca}^{2+}$  spark recorded with high spatial and temporal resolution. Image shows the temporal evolution of the  $\text{Ca}^{2+}$  spark along a single Z line. Redrawn from Fig. 2 of Parker I, Zang WJ, Wier WG. *J Physiol*. 1996;497.1:31-38. **(C)**  $\text{Ca}^{2+}$  sparks are triggered by voltage-clamp pulses that activate L-type  $\text{Ca}^{2+}$  channels. A  $\text{Ca}^{2+}$  channel blocker, verapamil, was used to block almost all L-type  $\text{Ca}^{2+}$  channels, thus reducing the probability of triggering  $\text{Ca}^{2+}$  sparks and revealing individual triggered sparks.  $I_{\text{Ca,L}}$  was thus too small to be recorded, but a few L-type  $\text{Ca}^{2+}$  channels opened during depolarization and a few  $\text{Ca}^{2+}$  sparks were triggered. **(D)** The voltage dependence of triggering  $\text{Ca}^{2+}$  sparks in the experiment shown in (C). The number of  $\text{Ca}^{2+}$  sparks depends on voltage in similar fashion to that of the whole-cell  $\text{Ca}^{2+}$  transient (Fig. 16.32B) and to that of the whole-cell L-type  $\text{Ca}^{2+}$  current (Fig. 16.32C). (C) and (D): Redrawn from Lopez-Lopez JR, Shacklock PS, Balke CW, Wier WG. *Science*. 1995;268:1042-1045.

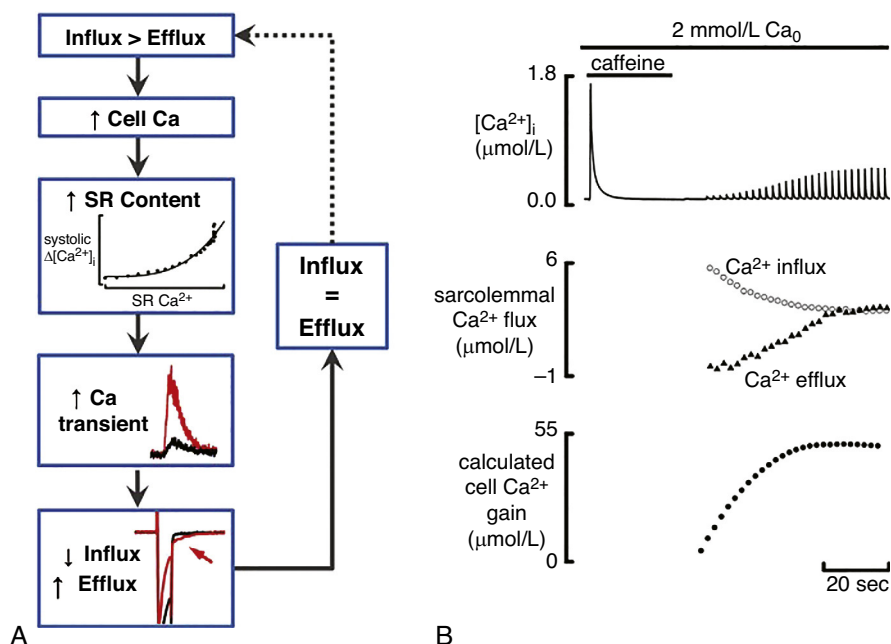
a new, changed, cytoplasmic  $\text{Ca}^{2+}$  transient, while remaining in the necessary  $\text{Ca}^{2+}$  balance. Changes in the SR  $\text{Ca}^{2+}$  load are a major component of the cardiac force-frequency relationship (Fig. 16.35, Fig. 18.14, Fig. 18.16) as well as many other normal and pathological changes in contractile performance of the heart.

In certain conditions, such as when cardiac cells are damaged and metabolically unable to extrude cytoplasmic  $\text{Ca}^{2+}$ , and cytoplasmic  $[\text{Ca}^{2+}]$  is abnormally high, the amount of  $\text{Ca}^{2+}$  in the SR becomes correspondingly high. In this case, high cytoplasmic  $[\text{Ca}^{2+}]$  (and other abnormal conditions) can result in increased frequency of “spontaneous”  $\text{Ca}^{2+}$  sparks (i.e., those that occur without being triggered by  $\text{Ca}^{2+}$  entry through an L-type  $\text{Ca}^{2+}$  channel). In this case, the change in cytoplasmic  $[\text{Ca}^{2+}]$  may reach neighboring T-tubule-SR junctions, producing a “wave” of  $[\text{Ca}^{2+}]$  change that propagates through the cell. Such  $\text{Ca}^{2+}$  waves are not normal in the myocardium and likely involved in triggered arrhythmias, such as DADs (Fig. 16.20), since the elevated  $[\text{Ca}^{2+}]$  results in increased  $\text{Ca}^{2+}$  efflux and inward (depolarizing) current through via the  $\text{Na}^+/\text{Ca}^{2+}$  exchanger (NCX) (Fig. 16.20).

### Modulation of Cardiac E-C Coupling Mechanisms

Cardiac E-C coupling mechanisms are the target of physiological regulation of the cardiovascular system. Catecholamines increase  $\text{Ca}^{2+}$  entry into the cell by phosphorylation of the  $\text{Ca}^{2+}$  channels via a cAMP-dependent protein kinase, and they also stimulate more rapid uptake of  $\text{Ca}^{2+}$  by the SR, which increases SR  $\text{Ca}^{2+}$  content. These actions of catecholamines on cardiac cells are essential to regulating heart rate, strength of contraction and rate of relaxation. For details, see Chapters 13 and 18, particularly Figures 13.3, 13.4, 18.19, and 18.20.

The  $\text{Na}^+/\text{Ca}^{2+}$  exchanger can either bring  $\text{Ca}^{2+}$  into the cell or extrude it.  $\text{Ca}^{2+}$  efflux normally occurs when  $V_m$  is negative. When  $V_m$  is positive and when cytoplasmic  $[\text{Ca}^{2+}]$  is high, the  $\text{Na}^+/\text{Ca}^{2+}$  exchanger (NCX) brings  $\text{Ca}^{2+}$  into the cell (Fig. 16.6). An increase in systolic  $\text{Ca}^{2+}$  is also achieved by increasing extracellular  $\text{Ca}^{2+}$  or decreasing the  $\text{Na}^+$  gradient across the sarcolemma. The sodium gradient can be reduced by increasing intracellular  $\text{Na}^+$  or decreasing extracellular  $\text{Na}^+$ . Cardiac glycosides increase intracellular  $\text{Na}^+$  by inhibiting the  $\text{Na}^+/\text{K}^+$  pump, which results in an accumulation of  $\text{Na}^+$  in the cells. The elevated cytosolic  $\text{Na}^+$  results in less  $\text{Ca}^{2+}$  extrusion and elevated cytoplasmic  $[\text{Ca}^{2+}]$ . More  $\text{Ca}^{2+}$  is

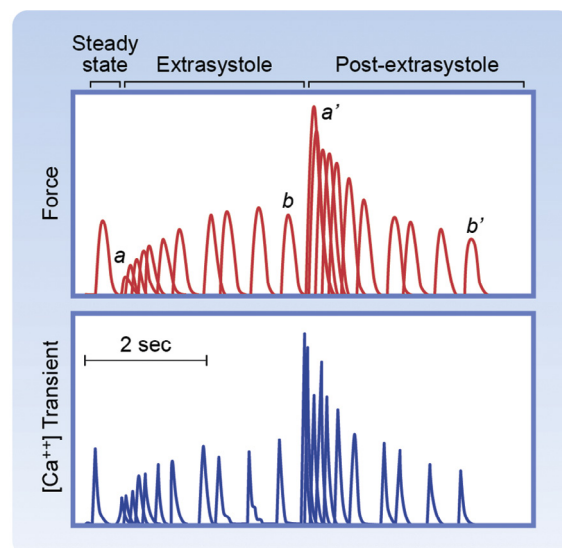


• **Fig. 16.34** Mechanisms producing calcium flux balance and controlling sarcoplasmic reticulum (SR) Ca content. **A**, Flow diagram. This illustrates recovery from a situation where influx is greater than efflux. Boxes show (from top to bottom): increase of cell Ca content leading to an increase of SR Ca; increase of the amplitude of the Ca transient (red). The bottom box shows membrane current records in response to a depolarization. The red traces show that increase in size of the Ca transient leads to faster inactivation of the L-type Ca current during the pulse and a larger sodium–calcium exchange current on repolarization (arrowed). **B**, Illustrative traces. These show (from top to bottom)  $[Ca^{2+}]_i$ ; sarcolemmal fluxes; calculated cell (and SR) Ca gain. At the start of the record, 10 mmol/L caffeine was applied to empty the SR. After removing caffeine, stimulation was commenced. Note that the recovery of the amplitude of the Ca transient is accompanied by a decrease of Ca influx and increase of efflux. (Reprinted from Trafford et al. with permission of the publisher. Copyright ©2001, American Heart Association, Inc. From Fig. 2 of Eisner DA, Caldwell JL, Kistamas K, Trafford, AW. *Circ Res*. 2017;121(2):181–195.)

then taken up and stored in the SR, and a stronger contraction can be produced. Developed tension is diminished by a reduction of extracellular  $Ca^{++}$ , by an increase in the  $Na^+$  gradient across the sarcolemma, or by administration of  $Ca^{++}$  blockers, such as diltiazem or verapamil.

### Relaxation

Appropriate relaxation of the heart from each contraction is critical to proper functioning: Filling of the ventricles with blood returning from the systemic circulation and from the pulmonary circulation (via right and left atria, respectively) cannot occur until the ventricles have begun to relax. At the end of systole, the influx of  $Ca^{++}$  has stopped and SR  $Ca^{++}$  release has been terminated. At that time, the SR can effect a rapid net uptake of cytoplasmic  $Ca^{++}$ . As cytoplasmic  $[Ca^{++}]$  falls,  $Ca^{++}$  unbinds from troponin C, allowing crossbridge detachment and relaxation. Importantly, when catecholamines enhance myocardial contractile force, they also decrease the sensitivity of the contractile machinery to  $Ca^{++}$  by phosphorylating troponin I (see Fig. 13.4) which decreases the affinity of troponin C for  $Ca^{++}$ . This effect aids rapid relaxation, as it allows  $Ca^{++}$  to unbind more rapidly from troponin C once release has stopped. This effect is critical to allow diastolic filling during the rapid heart rates caused by catecholamine action. Extrusion of  $Ca^{++}$  by NCX1 (Fig. 16.6) during repolarization aids relaxation and the maintenance of  $Ca^{++}$  flux balance



• **Fig. 16.35** The cytoplasmic  $Ca^{++}$  transient and the force-interval relation of cardiac muscle. After a normal beat, a closely coupled beat (extrasystole, “a”) is strongly reduced in peak force. When the interval preceding the extrasystole is lengthened, recovery occurs back to the steady-state level, “b.” A “post-extrasystolic” beat, “a’,” occurring at the normal interval after an extrasystole, is much more forceful than normal, a phenomenon is known as “post-extrasystolic potentiation.” The cardiac force-interval relation is the result of (1) the interaction of all the time-dependent processes of cardiac E-C coupling and (2) the interval available for their operation. Redrawn from Fig. 1 of Wier WG, Yue DT. *J Physiol*. 1986;376:507–530.

### Force-Frequency Relationship

As described earlier, both L-type  $\text{Ca}^{++}$  current and SR  $\text{Ca}^{++}$  content are influenced by the rate and temporal pattern of the heartbeat. Thus, both contribute to the important dependence of cardiac contraction on the frequency and pattern of beating, known as the “force-frequency relationship” (Fig. 16.35 and see “Rate-induced Regulation” in Chapter 18). The action potential is also influenced by frequency or cycle length (Fig. 16.14) and the changes have several ionic mechanisms. At a constant heart rate, the strength of contraction of ventricular muscle tends to be greater at higher frequencies (see Fig. 18.14). Since heart rate may vary 3-fold in humans during a typical day (particularly if it includes dynamic exercise), the force-frequency relationship is normally one of the determinants of contractile strength of the heart. The force-frequency relationship is an expression of the regulation of all the mechanisms underlying electrical activity and E-C coupling.

### Contractility

Contractility defines cardiac muscle performance at a given preload and afterload (next section). Preload and afterload are physical factors that affect the heart's ability to contract, mostly independent of E-C coupling processes discussed earlier. In the whole heart, cardiac cell contractility determines the ability of the heart to generate force or shortening at a given initial cardiac cell (sarcomere length, which is determined by preload). Contractility can be augmented by catecholamines, such as norepinephrine, therapeutic agents (e.g., digitalis), or by an increase in contraction frequency via the force-frequency relationship. The increase in contractility (**positive inotropic effect**) produced by these interventions results in incremental increases in the force developed and in the velocity of contraction.

## Physical Factors Influencing Myocardial Contraction

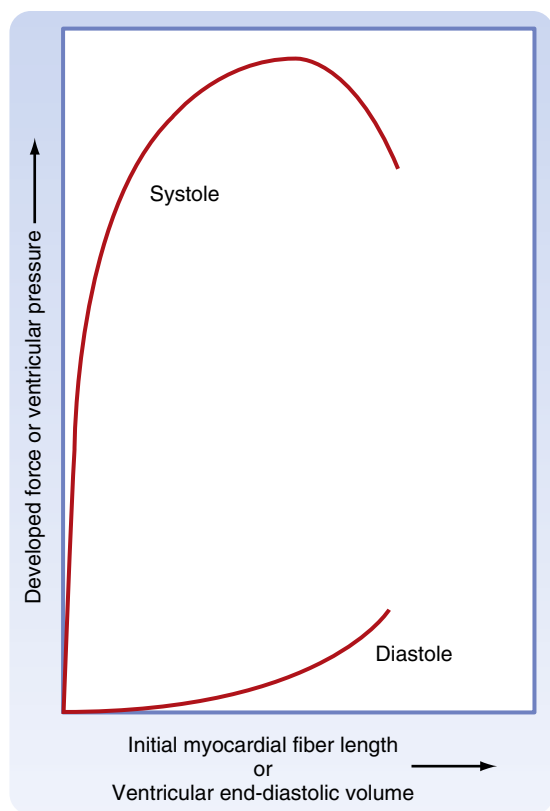
### Length Dependence of Cardiac Contraction

A key cellular property contributing to effective cardiac pump function is the *length dependence of cardiac contraction*. This property is expressed in the cardiac muscle length-tension relation. In the whole heart, it is expressed in volume-pressure relations. When cardiac chamber volume becomes greater due to physical stretch (filling), it can be inferred that myocardial cell length and sarcomere length are also greater. The length dependence of cardiac contraction is the mechanistic basis, at the cellular level, of the **Frank-Starling Law of the Heart**.

In cardiac muscle, as in skeletal muscle, generation of contractile force is the result of  $\text{Ca}^{++}$  activated, force-generating, myosin-actin cross-bridges (*viz.*, the sliding filament mechanism). In both skeletal and cardiac muscles, the number of cross-bridges that can form depends on the overlap of the myosin and actin filaments, which is determined by the sarcomere length. Accordingly, skeletal muscle and cardiac muscle show generally similar length-tension relationships, though with some key differences in form and cellular mechanisms (see Chapter 13). Developed force increases as sarcomere length is increased (the

ascending limb), until it reaches a maximum, and then declines at extreme long sarcomere lengths, according to the changing amount of thin (actin) and thick (myosin) filament overlap. A notable difference is that, in cardiac muscle, the affinity of troponin C for  $\text{Ca}^{++}$  increases with increasing sarcomere length, causing a steepening of the ascending limb of the length-tension relationship). The molecular interactions described in the sliding filament mechanism of muscle contraction, together with certain length-dependent mechanisms in cardiac muscle, provide the cellular basis of the Frank-Starling Law of the Heart, which describes the fact that the heart adjusts its output (stroke volume) to match its input (diastolic filling volume). The critical physiological role of the Frank-Starling law is discussed extensively in Chapters 18 and 19.

The volume-pressure relationships (reflecting sarcomere length-tension relationships) for the different cardiac chambers are different from each other, as the different chambers are capable of different maximum developed force or pressure. Typically, the LV is considered, as this is the chamber which performs the most work and which pumps blood into the systemic circulation. To construct this relationship for the LV (Fig. 16.36), peak left ventricular systolic pressure (or force) developed against a closed aortic valve (i.e., an isovolumic contraction) is plotted as a function of end-diastolic left ventricular volume (EDLV). Greater EDLV means greater sarcomere length. End-diastolic LV pressure may also be considered to be preload, as it is the force that stretches the cells, changing their length, and thus the LV volume. Note that the maximum pressure that the LV is capable of producing at a given EDLV (representing initial sarcomere length) is only obtained when the LV contracts entirely isovolumically (i.e., at the same volume). This can be arranged experimentally, but does not happen normally. However, the LV does normally contract (and relax) isovolumically for brief periods during each heartbeat, when both the mitral (AV) and the aortic valve are closed (see Fig. 16.40 for the normal isovolumic contraction and relaxation phases of a normal cardiac cycle in a human subject). In summary, the lower curve in Fig. 16.36 represents the sarcomere length achieved at the end of diastole, when the heart is filled to the maximum extent that it will be on a particular beat; sarcomeres are stretched at that time to the length that will determine (through the length dependence of cardiac contraction) the strength of the subsequent contraction. The upper curve represents the maximal *possible* force of active contraction that can be developed by the ventricle as a function of that initial sarcomere length: It is an expression of the length dependence of cardiac contraction. Finally, as alluded to above, the x-axis in this type of graph may alternatively be either end-diastolic pressure or end-diastolic volume, given the relation of these quantities to end-diastolic sarcomere length. Given a particular physiological state, the heart in the intact circulation always operates during each beat within the region of pressure and volume between these two curves. Because this operation occurs over a full cardiac cycle, these graphs are known as “pressure-volume” loops (see Figs. 16.42 and 16.43).



• **Fig. 16.36** Relationship of myocardial resting fiber length (sarcomere length) or end-diastolic volume to the force developed or peak systolic ventricular pressure during ventricular contraction in an intact heart. End-diastolic volume determines fiber length. End-diastolic volume is determined by end-diastolic pressure, according to ventricular compliance. See also [Chapter 17](#). (Redrawn from Patterson SW, et al. *J Physiol.* 1914;48:465.)

The pressure-volume curve during diastole is initially quite flat (compliant), which indicates that large increases in volume are produced by small increases in pressure. The active development of systolic pressure is considerable at the lower filling pressures however. This gives the heart the ability to contract strongly even when diastolic filling is low and initial sarcomere length is low. With greater filling, the ventricle becomes much less distensible, as evidenced by the sharp rise in the diastolic pressure curve at large intraventricular volumes. Over this range of filling volumes however, the heart has a rapidly increasing ability to generate contractile force, as shown by the upper curve. In a normal intact LV, peak force may be attained at a filling pressure of approximately 12 mm Hg. At this intraventricular diastolic pressure, which is near the upper limit observed in a normal heart, sarcomere length is near an optimal value of 2.2  $\mu\text{m}$ . Even at very high diastolic pressures (>50 mm Hg), sarcomere length is no greater than 2.6  $\mu\text{m}$ . This ability of the myocardium to resist stretch at high filling pressures probably resides in the noncontractile constituents of the heart tissue (connective tissue and pericardium), and it may serve as a safety factor against overloading of the heart in diastole. Usually, ventricular diastolic pressure is approximately 0–7 mm Hg, and the average diastolic sarcomere length is approximately 2.2  $\mu\text{m}$ . Thus, a normal heart operates on the steep

ascending portion of the Frank-Starling curve, as depicted in [Fig. 16.36](#).

### Preload and Afterload

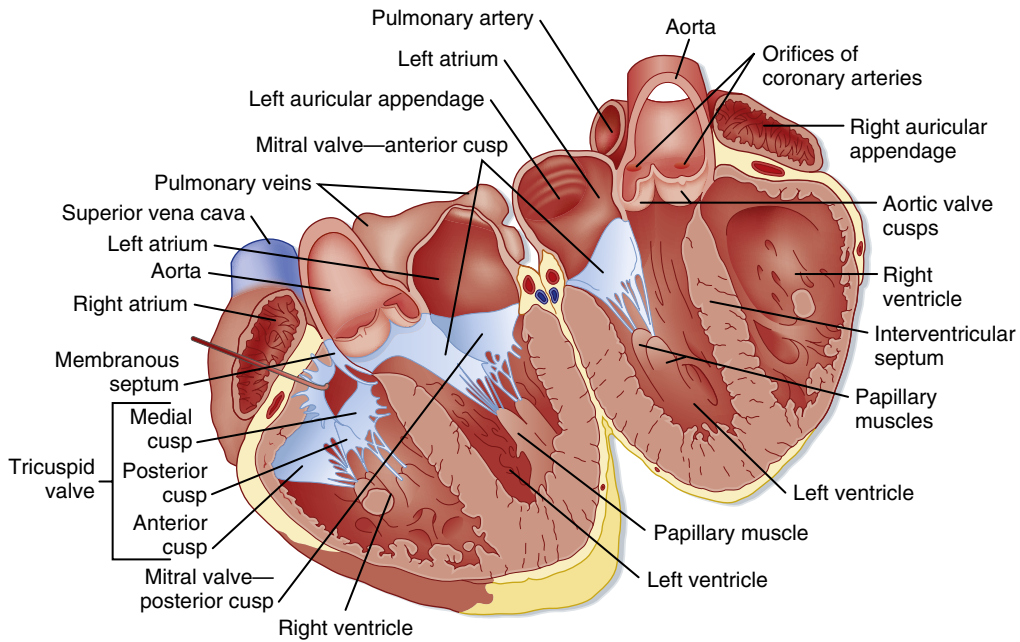
In addition to cellular E-C coupling processes, contraction of the whole heart is critically influenced by the “mechanical” or physical, factors termed **preload** and **afterload**. Preload can be measured in humans as a clinical parameter such as left ventricular end-diastolic pressure. It is a critical determinant of cardiac output. The dependence of cardiac output on preload is a manifestation of the length dependence of cardiac contraction and the Frank-Starling Law of the Heart. The concepts of preload, afterload, isometric contraction, isotonic contraction, and shortening velocity, all developed originally for skeletal muscle are also important for heart function, with essential modifications for the fact that the heart chambers are three-dimensional muscle structures from which blood must be ejected by muscle contraction. These concepts apply to the heart, but must be adapted for a three-dimensional chambered organ.

In the heart, preload of a particular heart chamber is the force that stretches that chamber to a greater volume during diastolic filling, thereby increasing the resting length of the cells comprising the wall of that chamber. In the LV, for example, the pressure of the blood filling the LV, and thus the stretching the LV wall during diastole, represents the preload of the LV. The lower curve in [Fig. 16.36](#) represents preload of the LV. Afterload, in the case of the LV, is the force, or pressure, against which the LV must contract as it shortens and ejects blood through an open aortic valve. Normally, in the LV, this force will be the pressure of the blood in the aorta, and thus arterial blood pressure is a major component of the afterload of the LV. However, afterload of the LV is not constant during ejection of blood, as the LV pressure changes throughout its shortening phase. The arterial blood pressure changes throughout ejection because of the compliance of the aorta, the arrival of reflected arterial pressure waves, and other factors. An increase in afterload tends to reduce ventricular muscle shortening velocity and hence, stroke volume.

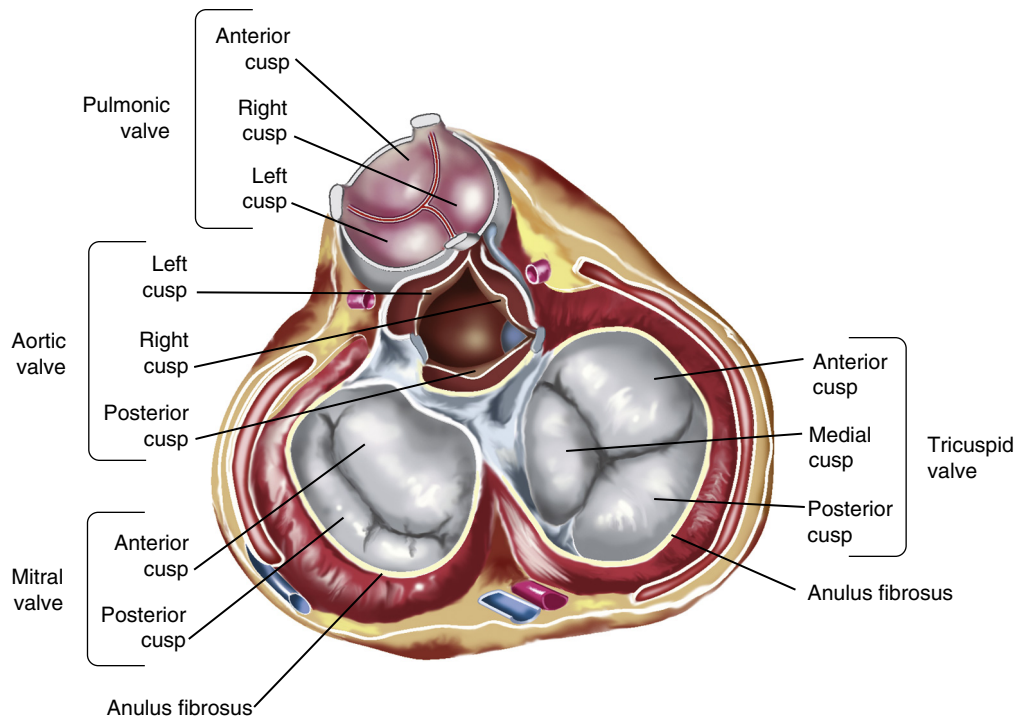
In the intact circulation, interacting cardiac and vascular factors affect preload and afterload and thus cardiac output. For example, venous pooling in the legs upon standing tends to reduce ventricular preload because it tends to reduce the pressure of venous blood returning to the heart. An increase in total peripheral resistance (TPR) tends to increase cardiac afterload. The interaction of vascular and cardiac factors in determining cardiac preload and afterload, and hence cardiac output, is discussed extensively in [Chapter 19](#).

### Structure of the Heart as a Pump

The mammalian heart is a four-chambered structure ([Figs. 16.37, 16.38](#)) that consists, from a functional standpoint, of two hearts in series. The “right heart” consists of the right atrium and right ventricle, receives deoxygenated blood from the systemic circulation and pumps it, at low pressure to the pulmonary circulation for oxygenation. The “left heart” consists of the left atrium and LV, receives



• **Fig. 16.37** Illustration of a heart split perpendicular to the interventricular septum to depict the anatomical relationships of the leaflets of the atrioventricular and aortic valves.



• **Fig. 16.38** Illustration of four cardiac valves as viewed from the base of the heart. Note how the leaflets overlap in the closed valves.

oxygenated blood from the pulmonary circulation, and pumps it, at high pressure, into the systemic circulation for distribution to all the organs and tissues.

### Cardiac Chambers

The atria are thin-walled, low-pressure chambers that function more as large-reservoir conduits of blood for their respective ventricles than as important pumps for the forward propulsion of blood. The ventricles comprise a continuum of muscle fibers originating from the fibrous skeleton at

the base of the heart (chiefly around the aortic orifice). These fibers sweep toward the cardiac apex at the epicardial surface. They pass toward the endocardium and gradually undergo a 180-degree change in direction to lie parallel to the epicardial fibers and to form the endocardium and papillary muscles.

At the apex of the heart, the fibers twist and turn inward to form papillary muscles. At the base of the heart and around the valve orifices, these myocardial fibers form a thick, powerful muscle mass that not only decreases the ventricular circumference to implement the ejection of blood

but also narrows the AV valve orifices, which aids in closure of the valve. Ventricular ejection is also accomplished by a decrease in the longitudinal axis as the heart begins to narrow toward the base. The early contraction of the apical part of the ventricles, coupled with the approximation of the ventricular walls, propels the blood toward the ventricular outflow tracts. The right ventricle, which develops a mean pressure that is approximately one-seventh that developed by the LV, is considerably thinner than the LV.

### Cardiac Valves

The cardiac valve leaflets consist of thin flaps of flexible, tough, endothelium-covered fibrous tissue that are firmly attached at the base to the fibrous valve rings. Movement of the valve leaflets is essentially passive, and the orientation of the cardiac valves is responsible for the unidirectional flow of blood through the heart. There are two types of valves in the heart: **atrioventricular** and **semilunar** (Figs. 16.37 and 16.38).

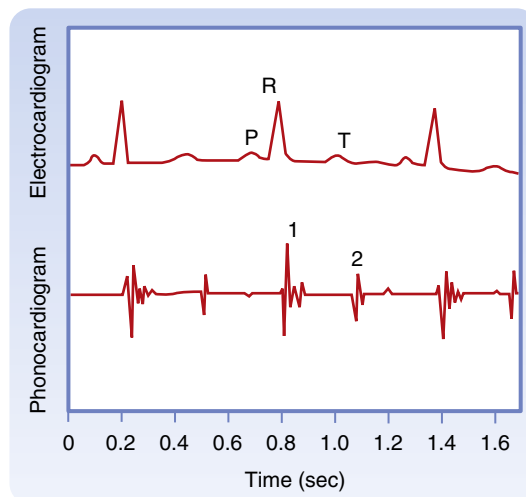
#### Atrioventricular Valves

The tricuspid valve, located between the right atrium and the right ventricle, is made up of three cusps, whereas the mitral valve, which lies between the left atrium and the LV, has two cusps. The total area of the cusps of each AV valve is approximately twice that of the respective AV orifice, and so considerable overlap of the leaflets occurs when the valves are in the closed position. Attached to the free edges of these valves are fine, strong ligaments (chordae tendineae cordis) that arise from the powerful papillary muscles of the respective ventricles. These ligaments prevent the valves from becoming everted during ventricular systole.

In a normal heart, the valve leaflets remain relatively close together during ventricular filling. The partial approximation of the valve surfaces during diastole is caused by eddy currents that prevail behind the leaflets and by tension that is exerted by the chordae tendineae cordis and papillary muscles.

#### Semilunar Valves

The pulmonic and aortic valves are located between the right ventricle and the pulmonary artery and between the LV and the aorta, respectively. These valves consist of three cup-like cusps that are attached to the valve rings. At the end of the reduced ejection phase of ventricular systole, blood flow briefly reverses toward the ventricles. This reversal of blood flow snaps the cusps together and prevents regurgitation of blood into the ventricles. During ventricular systole, the cusps do not lie back against the walls of the pulmonary artery and aorta; instead, they float in the bloodstream at a point approximately midway between the vessel walls and their closed position. Behind the semilunar valves are small out-pockets (sinuses of Valsalva) of the pulmonary artery and aorta. In these sinuses, eddy currents develop, which tend to keep the valve cusps away from the vessel walls. Furthermore, the orifices of the right and left coronary arteries are behind the right and the left cusps, respectively, of the aortic valve. Were it not for the presence of the sinuses of Valsalva and the eddy currents developed therein, the coronary ostia could be blocked by the valve cusps, and coronary blood flow would stop.



• **Fig. 16.39** The first and second heart sounds of the phonocardiogram (bottom tracing) are shown in regard to their relationship to the P, R, and T waves of the electrocardiogram (top tracing).

### The Pericardium

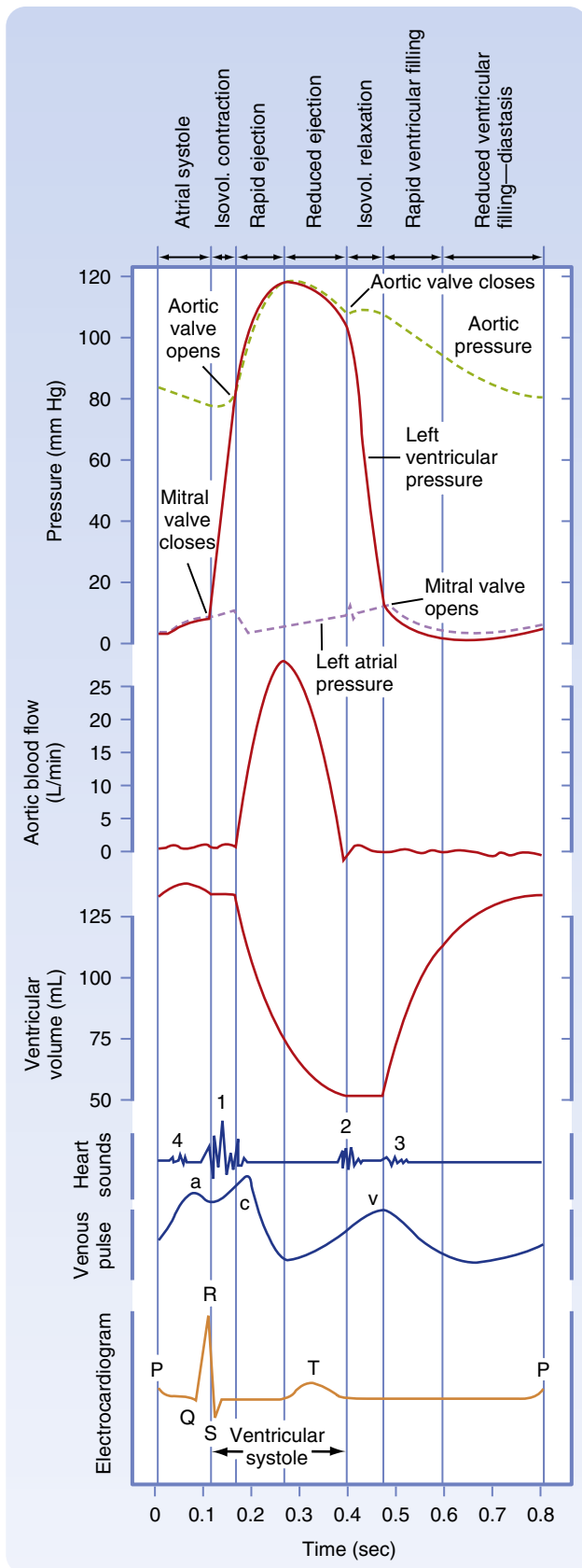
The pericardium invests the entire heart and the cardiac portion of the great vessels, and it is reflected onto the cardiac surface as the epicardium. The sac normally contains a small amount of fluid, which provides lubrication for the continuous movement of the enclosed heart. The pericardium is not very distensible; it strongly resists a large, rapid increase in cardiac size and hence prevents sudden overdistention of the chambers of the heart.

### Heart Sounds

Four sounds are usually generated by the heart, but only two are ordinarily audible through a stethoscope. With electronic amplification, the less intense sounds can be detected and recorded graphically as a phonocardiogram. This means of registering faint heart sounds helps delineate the precise timing of the heart sounds in relation to other events in the cardiac cycle.

The first heart sound is initiated at the onset of ventricular systole (Fig. 16.39) and reflects closure of the AV valves. It is the loudest and longest of the heart sounds, has a crescendo-decrescendo quality, and is heard best over the apical region of the heart. The tricuspid valve sounds are heard best in the fifth intercostal space just to the left of the sternum; the mitral sounds are heard best in the fifth intercostal space at the cardiac apex.

The second heart sound, which occurs with abrupt closure of the semilunar valves (see Fig. 16.38), is composed of higher frequency vibrations (higher pitch) and is of shorter duration and lower intensity than is the first heart sound. The portion of the second sound caused by closure of the pulmonic valve is heard best in the second thoracic interspace just to the left of the sternum, whereas that caused by closure of the aortic valve is heard best in the same intercostal space but to the right of the sternum. The aortic valve sound is generally louder than the pulmonic valve, but in cases of pulmonary hypertension, the reverse is true. The nature of the second heart sound changes with respiration. During expiration, a single heart sound is heard that reflects simultaneous closing of the pulmonic and



• **Fig. 16.40** Cardiac cycle (Wigger's diagram). Left atrial, aortic, and left ventricular pressure pulses correlated in time with aortic flow, ventricular volume, heart sounds, venous pulse, and the electrocardiogram for a complete cardiac cycle in a human subject. *Isovol.*, Isovolumic.

aortic valves. However, during inspiration, closure of the pulmonic valve is delayed, mainly as a result of increased blood flow from an inspiration-induced increase in venous return.<sup>a</sup> With this delayed closure of the pulmonic valve, the second heart sound can be heard as two components; this is termed **physiological splitting** of the second heart sound.

A third heart sound is sometimes heard in children with thin chest walls or in patients with left ventricular failure. It consists of a few low-intensity, low-frequency vibrations heard best in the region of the cardiac apex. The vibrations occur in early diastole and are caused by the abrupt cessation of ventricular distention and by the deceleration of blood entering the ventricles. A fourth, or atrial, sound consists of a few low-frequency oscillations. This sound is occasionally heard in individuals with normal hearts. It is caused by the oscillation of blood and cardiac chambers as a result of atrial contraction.

## The Cardiac Cycle

Cardiac cycle refers to the sequence of electrical and mechanical events that occur on each beat of the heart. Electrical events have been discussed extensively earlier in this chapter. The mechanical events are determined by chamber contraction after electrical activation. The opening and closing of the valves is determined passively (i.e., by the pressure and kinetic energy of the blood flowing between chambers or into pulmonary artery or aorta).

### Ventricular Systole

#### Isovolumic Contraction

The phase between the start of ventricular systole and opening of the semilunar valves (which occurs when ventricular pressure rises abruptly) is called the *isovolumic* (literally, “same volume”) *contraction period*. This term is appropriate because ventricular volume remains constant during this brief period (see Fig. 16.40). The onset of isovolumic



## IN THE CLINIC

In overloaded hearts, as in congestive heart failure, when ventricular volume is very large and the ventricular walls are stretched maximally, a third heart sound is often heard. A third heart sound in patients with heart disease is usually a grave sign. When the third and fourth (atrial) sounds are accentuated, as occurs in certain abnormal conditions, triplets of sounds resembling the sound of a galloping horse (called *gallop rhythms*) may occur. Mitral insufficiency and mitral stenosis produce, respectively, systolic and diastolic murmurs that are heard best at the cardiac apex. Aortic insufficiency and aortic stenosis, in contrast, produce, respectively, diastolic and systolic murmurs that are heard best in the second intercostal space just to the right of the sternum. The characteristics of the murmurs serve as an important guide in the diagnosis of valvular disease.

<sup>a</sup>With inspiration, intrathoracic pressure is reduced (see Chapter 21), which then increases venous blood flow to the right atrium.

contraction also coincides with the peak of the R wave on an ECG, initiation of the first heart sound, and the earliest rise in ventricular pressure on the ventricular pressure curve after atrial contraction.

### Ejection

Opening of the semilunar valves marks the onset of the ventricular ejection phase, which may be subdivided into an earlier, shorter phase (rapid ejection) and a later, longer phase (reduced ejection). The rapid ejection phase is distinguished from the reduced ejection phase by three characteristics: (1) a sharp rise in ventricular and aortic pressure that terminates at peak ventricular and aortic pressure, (2) an abrupt decrease in ventricular volume, and (3) a pronounced increase in aortic blood flow (see Fig. 16.40). The sharp decrease in left atrial pressure at the onset of ventricular ejection results from descent of the base of the heart and consequent stretching of the atria. During the reduced ejection period, runoff of blood from the aorta to the peripheral blood vessels exceeds the rate of ventricular output, and aortic pressure therefore declines. Throughout ventricular systole, the blood returning from the peripheral veins to the atria produces a progressive increase in atrial pressure.

During the rapid ejection period, left ventricular pressure slightly exceeds aortic pressure and aortic blood flow accelerates (continues to increase), whereas during the reduced ventricular ejection phase, aortic pressure is higher and aortic blood flow decelerates. This reversal of the ventricular-aortic pressure gradient in the presence of continuous flow of blood from the LV to the aorta is the result of storage of potential energy in the stretched arterial walls. This stored potential energy causes blood flow from the LV into the aorta to decelerate. The peak of the flow curve coincides with the point at which the left ventricular pressure curve intersects the aortic pressure curve during ejection. Thereafter, flow decelerates (continues to decrease) because the pressure gradient has been reversed.

Fig. 16.40 shows a tracing of a venous pulse curve recorded from a jugular vein. Three waves are apparent. The **a wave** occurs with the rise in pressure caused by atrial contraction. The **c wave** is caused by impact of the common carotid artery with the adjacent jugular vein and, to some extent, by the abrupt closure of the tricuspid valve in early ventricular systole. The **v wave** reflects the rise in pressure associated with atrial filling. Except for the c wave, the venous pulse curve closely resembles the left atrial pressure curve.

At the end of ventricular ejection, a volume of blood approximately equal to that ejected during systole remains in the ventricular cavities. This residual volume is fairly constant in normal hearts. However, residual volume decreases somewhat when the heart rate increases or when peripheral vascular resistance has diminished.

### Ventricular Diastole

#### Isovolumic Relaxation

Closure of the aortic valve produces the characteristic incisura (notch) on the descending limb of the aortic pressure curve, and it also produces the second heart sound (with some vibrations

evident on the atrial pressure curve). The incisura marks the end of ventricular systole. The period between closure of the semilunar valves and opening of the AV valves is termed *isovolumic relaxation*. It is characterized by a precipitous fall in ventricular pressure without a change in ventricular volume.

#### Rapid Filling Phase

The major portion of ventricular filling occurs immediately after the AV valves open. At this point, the blood that returned to the atria during the previous ventricular systole is abruptly released into the relaxing ventricles. This period of ventricular filling is called the *rapid filling phase*. In Fig. 16.40, the onset of the rapid filling phase is indicated by the decrease in left ventricular pressure below left atrial pressure. This pressure reversal opens the mitral valve. The rapid flow of blood from atria to relaxing ventricles produces transient decreases in atrial and ventricular pressures and a sharp increase in ventricular volume.

#### Diastasis

The rapid ventricular filling phase is followed by a phase of slow ventricular filling called *diastasis*. During diastasis, blood returning from the peripheral veins flows into the right ventricle and blood from the lungs flows into the LV. This small, slow addition to ventricular filling is indicated by gradual rises in atrial, ventricular, and venous pressures and in ventricular volume (see Fig. 16.40).



### IN THE CLINIC

An increase in myocardial contractility, as produced by catecholamines or by digitalis in a patient with a failing heart, may decrease residual ventricular volume and increase the stroke volume and ejection fraction, which are beneficial effects. In severely hypodynamic and dilated hearts, residual volume can become much greater than stroke volume.

### Atrial Systole

The onset of atrial systole occurs soon after the beginning of the P wave (atrial depolarization) of the ECG. The transfer of blood from atrium to ventricle achieved by atrial contraction completes the period of ventricular filling. Atrial systole is responsible for the small increases in atrial, ventricular, and venous pressure, as well as in ventricular volume. Throughout ventricular diastole, atrial pressure barely exceeds ventricular pressure. This small pressure difference indicates that the pathway through the open AV valves during ventricular filling has low resistance.

Because there are no valves at the junction of the venae cavae and right atrium or at the junction of the pulmonary veins and left atrium, atrial contraction may force blood in both directions. However, little blood is actually pumped back into the venous tributaries during the brief atrial contraction, mainly because of the inertia of the inflowing blood.

The contribution of atrial contraction to ventricular filling is governed to a great extent by the heart rate and the position of the AV valves. At slow heart rates, filling

practically ceases toward the end of diastasis, and atrial contraction contributes little additional filling. During tachycardia, however, diastasis is shortened and the atrial contribution can become substantial. Should tachycardia become so severe that the rapid filling phase is attenuated, atrial contraction assumes great importance in rapidly propelling blood into the ventricle during this brief period of the cardiac cycle. If the period of ventricular relaxation is so brief that filling is seriously impaired, even atrial contraction cannot provide adequate ventricular filling. The consequent reduction in cardiac output may result in syncope (fainting).



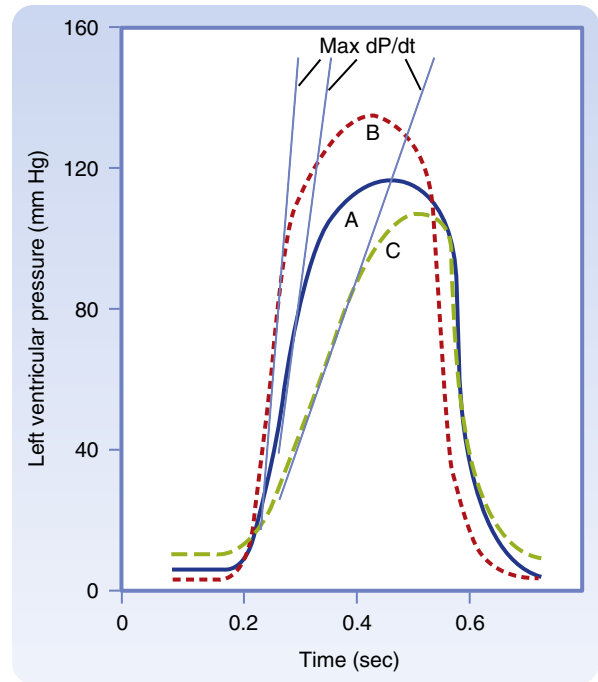
### IN THE CLINIC

Atrial contraction is not essential for ventricular filling, as can be observed in patients with atrial fibrillation or complete heart block. In atrial fibrillation, the atrial myofibers contract in a continuous, uncoordinated manner and therefore cannot pump blood into the ventricles. In complete heart block, the atria and ventricles beat independently of each other. However, ventricular filling may be normal in patients with these two arrhythmias. In certain disease states, the AV valves may be markedly narrowed (stenotic). In such conditions, atrial contraction plays a much more important role in ventricular filling than it does in a normal heart.

### Indices of Contractility in the Intact Heart

In the whole heart, a reasonable index of myocardial contractility can be derived from the contour of ventricular pressure curves (Fig. 16.41). A hypodynamic heart, of low contractility, is characterized by elevated end-diastolic pressure, slowly rising ventricular pressure, and a somewhat reduced ejection phase (curve C in Fig. 16.41). A hyperdynamic heart (curve B) is characterized by reduced end-diastolic pressure, fast-rising ventricular pressure, more rapid relaxation (in the case of catecholamine action), and a brief ejection phase. The slope of the ascending limb of the ventricular pressure curve indicates the maximal rate of force development by the ventricle. The maximal rate of change in pressure with time—that is, the **maximum  $dP/dt$** —is illustrated by the tangents to the steepest portion of the ascending limbs of the ventricular pressure curves in Fig. 16.41. The slope of the ascending limb is maximal during the isovolumic phase of systole. At any given degree of ventricular filling, the slope provides an index of the initial contraction velocity and hence an index of contractility.

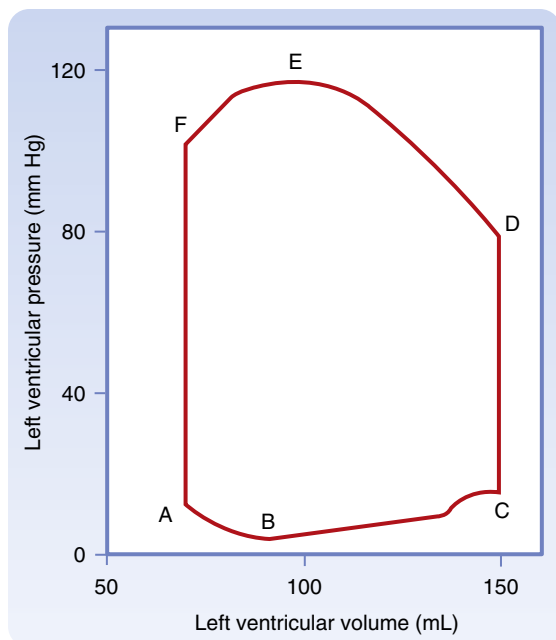
Similarly, the contractile state of the myocardium can be calculated from the velocity of blood flow that occurs initially in the ascending aorta during the cardiac cycle (Fig. 16.40). In addition, the **ejection fraction**, which is the ratio of the volume of blood ejected from the LV per beat (**stroke volume**) to the volume of blood in the LV at the end of diastole (end-diastolic volume), is widely used clinically as an index of contractility.



• **Fig. 16.41** Left ventricular pressure curves with tangents drawn to the steepest portions of the ascending limbs to indicate maximal rates of change in pressure with time ( $dP/dt$  values). **A** (blue curve), control; **B** (dashed red curve), hyperdynamic heart, as with administration of norepinephrine; **C** (green dashed curve), hypodynamic heart, as in cardiac failure.

### Pressure-Volume Relationship, Left Ventricle

The changes in left ventricular pressure and volume that occur throughout each cardiac cycle are visualized in a pressure-volume “loop” (Fig. 16.42). Diastolic filling starts when the mitral valve opens (point A in Fig. 16.42), and it terminates when the mitral valve closes (point C). The initial decrease in left ventricular pressure (from points A to B), despite the rapid inflow of blood from the left atrium, is attributed to progressive ventricular relaxation and distensibility. During the remainder of diastole (from points B to C), the increase in ventricular pressure reflects ventricular filling and changes in the passive elastic characteristics of the ventricle. Only a small increase in pressure accompanies the substantial increase in ventricular volume during diastole (from points B to C), and this is because the LV is normally highly compliant. The small increase in pressure just before the mitral valve closes (to the left of point C) is caused by the contribution of left atrial contraction to left ventricular filling. With isovolumic contraction (from points C to D), LV pressure rises steeply, but ventricular volume does not change because the mitral and aortic valves are both closed. When the aortic valve opens (point D), and during the first (rapid) phase of ejection (from points D to E), the large reduction in volume is associated with a steady increase in ventricular pressure. This reduction in volume is followed by reduced ejection (from points E to F) and a small decrease in ventricular pressure. Closure of the aortic valve (point F) is followed by isovolumic relaxation (from points F to A), which is



• **Fig. 16.42** Schematized pressure-volume loop of the left ventricle for a single cardiac cycle.

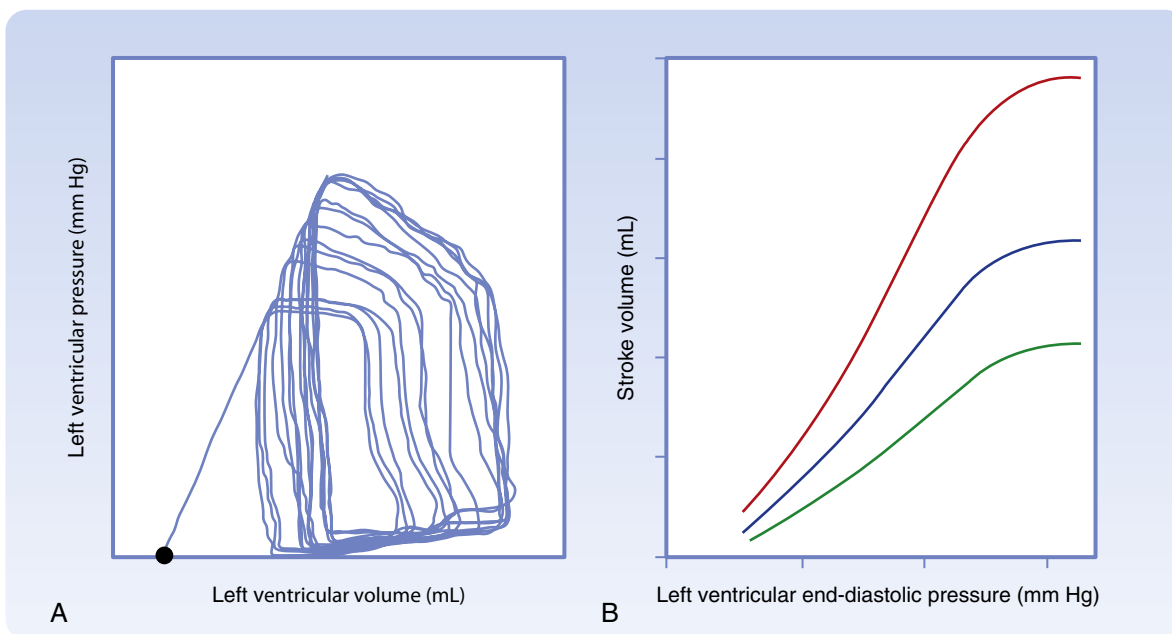
characterized by a sharp drop in pressure. Ventricular volume does not change during the interval between closing of the aortic valve and opening of the mitral valve (from points F to A) because both the mitral and aortic valves are

closed. The mitral valve opens (point A) to complete one cardiac cycle.

Several key cardiovascular system parameters are evident on a left ventricular pressure-volume loop (P-V loop), or may be calculated from it. End-diastolic volume is obtained at mitral valve closure (point C in Fig. 16.41) and the end-systolic volume at mitral valve opening (point A). The stroke volume is then apparent as the “width” of the P-V loop and is calculated as follows:

$$\text{Stroke volume} = \text{end - diastolic volume} \\ - \text{end - systolic volume}$$

The preload of the LV, considered here as left ventricular end-diastolic pressure, is the pressure coordinate when the mitral valve closes (point C in Fig. 16.42). The approximate “diastolic” arterial blood pressure may be read when the aortic valve opens (point D), and the approximate “systolic” arterial blood pressure is read during systole (point E). Left ventricular P-V loops recorded from a human (Fig. 16.43A) are similar to the schematized version (see Fig. 16.41). The slope of the end-systolic P-V relation (line extending from the dot in Fig. 16.43A) defines contractility; a steeper slope indicates increased contractility. In this subject, partial occlusion of the inferior vena cava reduced the preload of the LV on successive beats (as the inflow of blood to the LV was reduced) and the effect of the reduced preload was successively smaller



• **Fig. 16.43 A**, Left ventricular pressure-volume loops recorded in a human. The left ventricle was subjected to different preloads by transient occlusion of blood flow in the inferior vena cava. As preload (left ventricular end-diastolic pressure [LVEDP]) was decreased, both end-diastolic volume and end-systolic volume decreased, but end-diastolic volume decreased more, which resulted in decreased stroke volume. **B**, Cardiac function curves when stroke volume is plotted as a function of LVEDP for a normal heart in the basal state (*blue line*), a heart with increased contractility (*red line*), and a heart with reduced contractility (*green line*). At any given preload, stroke volume is higher in hearts with increased contractility and lower in hearts with decreased contractility than stroke volume in the normal basal state. (**A**, From Senzaki H, et al. Single-beat estimation of end-systolic pressure-volume relation in humans. A new method with the potential for noninvasive application. *Circulation*. 1996;94[10]:2497-2506.)

stroke volume of the LV. This experiment illustrated, in humans, the operation of the Frank-Starling law of the heart, whereby changes in preload changed myocardial fiber length, and thus the strength of the subsequent contraction. This changed the stroke volume produced. This important phenomenon is characterized graphically by the cardiac function curve (Fig. 16.43B). As preload increases, stroke volume increases (solid blue line). If contractility of the heart is increased, as in the action of norepinephrine, the slope of the end-systolic P-V relation becomes steeper, and the entire cardiac function curve shifts upward (solid red line), which reflects the fact that the ventricle is now able to produce a larger stroke volume at a given preload. The increased stroke volume at any given preload is largely produced by a decreased end-systolic volume: Hearts with increased contractility are able to “squeeze down” to a greater extent. Conversely, if the ventricle is damaged, as after cardiac ischemia, or if its contractility is otherwise reduced from normal (as after calcium channel blockade), the cardiac function curve is shifted downward (green line), which reflects a reduced stroke volume at any given preload. The cardiac function curve is also known as *ventricular function curves* or *Starling curves*. To assess the integrated functioning of the cardiovascular system (see Chapter 19), cardiac output, rather than stroke volume, is usually measured; preload of the heart is considered to be the filling pressure of the right ventricle, typically measured as mean right atrial pressure ( $\bar{P}_{ra}$ ), or central venous pressure.

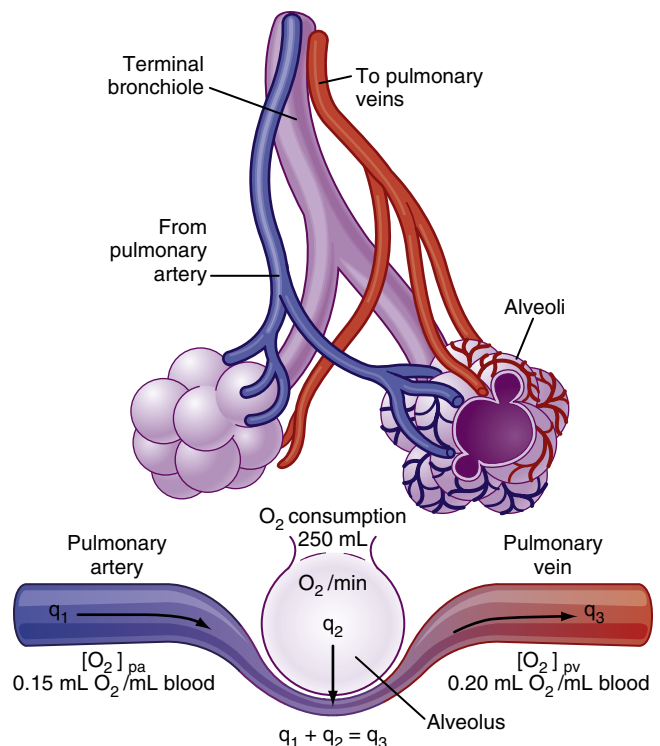
## Measurement of Cardiac Output

### The Fick Principle

Cardiac muscle must contract repetitively for a lifetime, and hence it requires a continuous supply of  $O_2$ . Cardiac muscle is very rich in mitochondria, as these organelles (see Fig. 13.1B) have the enzymes necessary for oxidative phosphorylation. Rapid mitochondrial oxidation of substrates and synthesis of ATP sustains the myocardial energy requirements, particularly for muscle contraction and  $Ca^{++}$  cycling. To provide adequate  $O_2$  and substrate for its metabolic machinery, the myocardium is also endowed with a rich capillary supply, approximately one capillary per fiber. Thus, diffusion distances are short, and  $O_2$ ,  $CO_2$ , substrates, and waste material can move rapidly between the myocardial cell and capillary.

In 1870, the German physiologist Adolf Fick contrived the first method for measuring cardiac output in intact animals and people. The basis for this method, called the **Fick principle**, is simply an application of the law of conservation of mass. The principle is derived from the fact that the quantity of  $O_2$  delivered to the pulmonary capillaries via the pulmonary artery, plus the quantity of  $O_2$  that enters the pulmonary capillaries from the alveoli, must equal the quantity of  $O_2$  that is carried away by the pulmonary veins.

The Fick principle is depicted schematically in Fig. 16.44. The rate of  $O_2$  delivery to the lungs ( $q_1$ ) equals the  $O_2$  concentration in pulmonary arterial blood ( $[O_2]_{pa}$ ), multiplied



• **Fig. 16.44** Schema illustrating the Fick principle for measuring cardiac output. The change in color from pulmonary artery to pulmonary vein represents the change in color of the blood as venous blood becomes fully oxygenated.

by pulmonary arterial blood flow ( $Q$ ), which equals cardiac output; that is,

#### Equation 16.1

$$q_1 = Q [O_2]_{pa}$$

If  $q_2$  is the net rate of  $O_2$  uptake by the pulmonary capillaries from the alveoli, then at steady state,  $q_2$  equals the  $O_2$  consumption of the body. The rate at which  $O_2$  is carried away by the pulmonary veins ( $q_3$ ) equals the  $O_2$  concentration in pulmonary venous blood ( $[O_2]_{pv}$ ), multiplied by total pulmonary venous flow, which is virtually equal to pulmonary arterial blood flow ( $Q$ ); that is,

#### Equation 16.2

$$q_3 = Q [O_2]_{pv}$$

From the law of conservation of mass,

#### Equation 16.3

$$q_1 + q_2 = q_3$$

Therefore,

#### Equation 16.4

$$Q [O_2]_{pa} + q_2 = Q [O_2]_{pv}$$

When this is solved for cardiac output,

#### Equation 16.5

$$Q = q_2 / ([O_2]_{pv} - [O_2]_{pa})$$

Eq. 16.5 is the statement of the Fick principle.

To determine cardiac output by this method, three values must be known: (1)  $O_2$  consumption of the body, (2) the  $O_2$  concentration in pulmonary venous blood ( $[O_2]_{pv}$ ), and (3) the  $O_2$  concentration in pulmonary arterial blood ( $[O_2]_{pa}$ ).  $O_2$  consumption is computed from measurements of the volume and  $O_2$  content of expired air over a given interval. Because the  $O_2$  concentration of peripheral arterial blood is essentially identical to that in the pulmonary veins,  $[O_2]_{pv}$  is determined with a sample of peripheral arterial blood withdrawn by needle puncture. The compositions of pulmonary arterial blood and mixed systemic venous blood are virtually identical to one another. Samples for  $O_2$  analysis are obtained from the pulmonary artery or right ventricle through a catheter.

With the values depicted in Fig. 16.44, cardiac output can be calculated as follows: If the  $O_2$  consumption is 250 mL/minute, the arterial (pulmonary venous)  $O_2$  content is 0.20 mL of  $O_2$  per milliliter of blood, and the mixed venous (pulmonary arterial)  $O_2$  content is 0.15 mL of  $O_2$  per milliliter of blood, cardiac output equals  $250/(0.20 - 0.15) = 5000$  mL/minute. In the clinic today however, cardiac output is most commonly measured noninvasively with Doppler echocardiography.

### Cardiac Oxygen Consumption and Work

Consumption of  $O_2$  by the heart depends on the amount and type of activity that the heart performs. Under basal conditions, myocardial  $O_2$  consumption ( $\dot{V}_{O_2}$ ) is approximately 8 to 10 mL/minute/100 g of heart. It can increase severalfold during exercise and decrease moderately in such conditions as hypotension and hypothermia. The  $O_2$  content of cardiac venous blood is normally low ( $\approx 5$  mL/dL), and the myocardium can receive little additional  $O_2$  by further extraction of  $O_2$  from coronary blood. Therefore, increased  $O_2$  demands of the heart must be met mainly by an increase in coronary blood flow (see Chapter 17). In experiments in which the heartbeat is arrested but coronary perfusion is maintained,  $O_2$  consumption falls to 2 mL/minute/100 g or less, which is still six to seven times greater than the  $O_2$  consumption of resting skeletal muscle.

Cardiac work has external and internal components. Left ventricular work per beat (stroke work) is approximately equal to the product of stroke volume and the mean aortic pressure against which the blood is ejected by the LV. External cardiac work ( $W_e$ ) may be defined as follows:

$$\text{Equation 16.6} \\ W_e = \int_{t_1}^{t_2} P dV + \rho v^2 / 2$$

That is, each small increment in volume that is pumped ( $dV$ ) is multiplied by the associated pressure ( $P$ ), and the products ( $PdV$ ) are integrated over the time interval of interest ( $t_2 - t_1$ ) to calculate total work. Added to this is kinetic work due to the velocity ( $v$ ) of blood flow and the density ( $\rho$ ) of blood. The mean pressure during expulsion is used to simplify this to

$$\text{Equation 16.7} \\ W_e = PV + \rho v^2 / 2$$

At resting levels of cardiac output, the kinetic energy component is negligible. However, with high cardiac output, as in strenuous exercise, the kinetic energy component can account for up to 50% of total cardiac work.

The internal work ( $W_i$ ) of the heart can be written as

$$\text{Equation 16.8} \\ W_i = \alpha \int T dt$$

where  $\alpha$  is a proportionality constant that converts  $T dt$  into units of work,  $T$  is wall tension, and  $dt$  is time. Clinically,  $\dot{V}_{O_2}$  and left ventricular power are difficult to measure; however, both are closely related to the systolic pressure-time index, the integral of left ventricular pressure, and time during systole. Such measurements are important because internal work is a large determinant of myocardial  $O_2$  need. An alternative approach to evaluate cardiac work and its relation to  $O_2$  consumption has been developed in which P-V loops (see Fig. 16.43A) are examined in conditions with varied pre-load and afterload; contractility is maintained constant.

Simultaneously halving aortic pressure and doubling cardiac output, or vice versa, result in the same value for cardiac work. However, the  $O_2$  requirements are greater for any given amount of cardiac work when a major proportion of the work is pressure work, as opposed to volume work. An increase in cardiac output at a constant aortic pressure (volume work) is accompanied by only a small increase in left ventricular  $O_2$  consumption, whereas increased arterial pressure at constant cardiac output (pressure work) is accompanied by a large increase in myocardial  $O_2$  consumption. Thus myocardial  $O_2$  consumption may not be well correlated with overall cardiac work. The magnitude and duration of left ventricular pressure are correlated with left ventricular  $O_2$  consumption. The work of the right ventricle is one-seventh that of the LV because pulmonary vascular resistance is much less than systemic vascular resistance.

### Cardiac Efficiency

The efficiency of the heart may be calculated as the ratio of the work accomplished to the total energy used. If the average  $O_2$  consumption is assumed to be 9 mL/minute/100 g for the two ventricles, a 300-g heart will consume 27 mL of  $O_2$  per minute. This value is equivalent to 130 small calories when the respiratory quotient is 0.82. Together, the two ventricles do approximately 8 kg-m of work per minute, which is equivalent to 18.7 small calories. Therefore, the gross efficiency of the heart is approximately 14%:

$$\text{Equation 16.9} \\ 18.7/130 \times 100 \cong 14\%$$



### IN THE CLINIC

The greater energy demand of pressure work than of volume work is clinically important, especially in aortic stenosis. In this condition, left ventricular  $O_2$  consumption is increased, mainly because of the high intraventricular pressure developed during systole. However, coronary perfusion pressure (and hence  $O_2$  supply) is either normal or reduced because of the pressure drop across the narrow orifice of the diseased aortic valve.

The actual gross mechanical efficiency of the heart is slightly higher (18%) than the value calculated and is determined through subtracting the  $O_2$  consumption of a non-beating heart ( $\approx 2$  mL/minute/100 g) from the total cardiac  $O_2$  consumption in the calculation of efficiency. During physical exercise, efficiency improves because mean blood pressure does not change appreciably, whereas cardiac output and work increase considerably, without a proportional increase in myocardial  $O_2$  consumption.

### Myocardial Adenosine Triphosphate and Its Relation to Mechanical Function

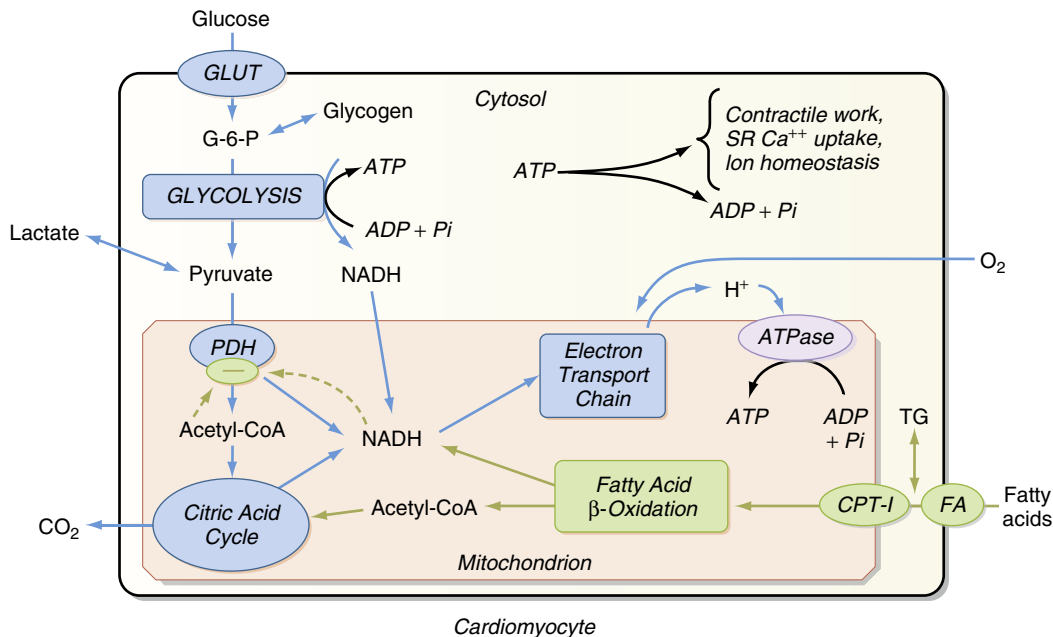
The chemical energy that fuels cardiac contractile work and relaxation is derived from ATP hydrolysis (Fig. 16.45). The healthy heart has a relatively constant level of ATP ( $\approx 5 \mu\text{mol/g}$  wet weight) despite an extremely high rate of ATP hydrolysis ( $\approx 0.3 \mu\text{mol/g}^{-1}/\text{second}^{-1}$ ). The tissue content of ATP is low in relation to the rate of breakdown and production; complete turnover of the myocardial ATP content occurs approximately every 12 seconds in the heart at rest. ATP hydrolysis (see Fig. 16.45) provides energy for contractile work (actin-myosin interaction and cell shortening), pumping  $Ca^{++}$  back into the SR at the end of systole and maintaining normal ion gradients (low  $Na^+$  and high  $K^+$  in the cell). Approximately two-thirds of the ATP hydrolyzed by the heart is used to fuel contractile work, and the remaining third is used for ion pumps and “housekeeping” functions such as synthesis of proteins and nucleic acids. The  $Ca^{++}$ -ATPase of the SR is the primary ion pump consuming ATP.

ATP resynthesis occurs primarily through oxidative phosphorylation in mitochondria ( $>98\%$ ) and, to a

small degree, through glycolysis ( $<2\%$ ). Oxidative phosphorylation requires  $O_2$  and  $H_2$ . The  $O_2$  is delivered to the myocardium and consumed in the mitochondria to make  $H_2O$ , and the  $H_2$  is from the metabolism of carbon fuels (mainly fatty acids, glucose, and lactate) and the generation of the reduced form of nicotinamide adenine dinucleotide (NADH). Pyruvate dehydrogenase (PDH) regulates the oxidation of glucose and lactate. Of importance is that the rates of ATP formation and breakdown depend on an adequate delivery of  $O_2$  to the myocardium, which is a function of myocardial blood flow and oxygenation of arterial blood. An increase in ATP breakdown in the myocardium, such as occurs when heart rate, systolic blood pressure, and contractility are increased (as during exercise), necessitates an increase in  $O_2$  delivery to the myocardium so that the mitochondria can generate sufficient ATP by oxidative phosphorylation to meet the demand for ATP. Thus, the rate of myocardial  $O_2$  consumption is tightly linked to the work rate (or power) of the myocardium.

### Substrate Utilization

The heart is versatile in its use of substrates, and within certain limits, uptake of a particular substrate is directly proportional to its arterial concentration. The use of one substrate by the heart is also influenced by the presence or absence of other substrates. For example, the addition of lactate to the blood that perfuses a heart metabolizing glucose leads to a reduction in glucose uptake and vice versa. At normal blood concentrations, glucose and lactate are consumed at approximately equal rates.



• **Fig. 16.45** Overall scheme for production and utilization of adenosine triphosphate (ATP) within a cardiac myocyte. Pathways for utilization of glucose, fatty acids (FA), and lactate are indicated, as are the requirements for  $O_2$  and  $H^+$  by the electron transport chain in mitochondria. ADP, Adenosine diphosphate; CoA, coenzyme A; CPT-I, carnitine palmitoyltransferase; G-6-P, glucose-6-phosphate; GLUT, glucose transporter; NADH, nicotinamide adenosine dehydrogenase; PDH, pyruvate dehydrogenase; Pi, inorganic phosphate; SR, sarcoplasmic reticulum; TG, triglyceride.

Of the total cardiac  $O_2$  consumption, only 35%–40% can be accounted for by the oxidation of carbohydrate. Thus, the heart derives the majority of its energy from the oxidation of noncarbohydrate sources: namely, esterified and nonesterified fatty acids. These account for approximately 60% of the myocardial  $O_2$  consumption in people in the postabsorptive state. Ketone bodies, especially acetoacetate, are readily oxidized by the heart, and they are a major source of energy in diabetic acidosis.

## Key Points

- The transmembrane action potentials recorded from fast response fibers contain the following five phases:
  - Phase 0: The action potential upstroke is initiated when a suprathreshold stimulus rapidly depolarizes the membrane by activating the voltage-dependent  $Na^+$  channels.
  - Phase 1: The notch is an early partial repolarization that is achieved by the efflux of  $K^+$  through channels that conduct the transient outward current ( $I_{to}$ ).
  - Phase 2: The plateau represents a balance between the influx of  $Ca^{++}$  through calcium channels and the efflux of  $K^+$  through several types of potassium channels.
  - Phase 3: Final repolarization is initiated when the efflux of  $K^+$  exceeds the influx of  $Ca^{++}$ . The resultant partial repolarization rapidly increases  $K^+$  conductance and restores full repolarization.
  - Phase 4: The resting potential of the fully repolarized cell is determined by conductance of the cell membrane to  $K^+$ , mainly through  $I_{K1}$  channels.
- Fast-response action potentials are recorded from atrial and ventricular myocardial fibers and from ventricular specialized conducting (Purkinje) fibers. Such an action potential is characterized by a large amplitude, a steep upstroke, and a relatively long plateau. The effective refractory period of fast-response fibers begins at the upstroke of the action potential and persists until midway through phase 3. The fiber is relatively refractory during the remainder of phase 3, and it regains full excitability soon after it is fully repolarized (phase 4).
- Slow-response action potentials are recorded from normal SA and AV nodal cells and from abnormal myocardial cells that have been partially depolarized. The action potential is characterized by a less negative potential during diastole (phase 4), a less steep upstroke, a smaller amplitude, and a shorter duration than is typical of the fast-response action potential. The upstroke in slow-response fibers is produced by the activation of calcium channels. Slow-response fibers become absolutely refractory at the beginning of the upstroke, and partial excitability may not be regained until very late in phase 3 or until after the fiber is fully repolarized.
- Normally, the SA node serves as the pacemaker to initiate the cardiac impulse. This impulse is propagated from the SA node to the atria and ultimately reaches the AV node. After a delay in the AV node, the cardiac impulse is propagated throughout the ventricles. Ectopic foci in the AV node or the His-Purkinje system may initiate propagated cardiac impulses if the normal pacemaker cells in the SA node are suppressed or if the rhythmicity of the ectopic automatic cells is abnormally enhanced.
- Under certain abnormal conditions, afterdepolarizations may be triggered by an otherwise normal action potential. EADs arise in phase 3 of a normal action potential. They are more likely to occur when the basic cycle length of the initiating beat is very long and when the cardiac action potentials are abnormally prolonged. DADs appear in phase 4. They are more likely to occur when cells are overloaded with  $Ca^{++}$ .
- Reentrant arrhythmias occur when a cardiac impulse traverses a loop of cardiac fibers and reenters previously excited tissue. This can happen when there is an area of unidirectional block and conduction of the impulse around the remainder of the loop is slow.
- The ECG, which is recorded from the surface of the body, traces the conduction of the cardiac impulse throughout the heart. The ECG may be used to detect and analyze cardiac arrhythmias and other aspects of cardiac function.
- On excitation, voltage-gated calcium channels open to admit extracellular  $Ca^{++}$  into the dyadic space of cardiac myocytes. The influx of  $Ca^{++}$  activates the release of  $Ca^{++}$  from the sarcoplasmic reticulum (a “ $Ca^{++}$  spark”).  $Ca^{++}$  sparks summate to produce the total change in cytoplasmic  $[Ca^{++}]$  that elicits contraction of the myofilaments. This process constitutes the “local control theory of cardiac E-C coupling.”
- In ventricular contraction, preload is stretch of the fibers by blood during ventricular filling. Afterload is the arterial pressure against which the ventricle ejects the blood. An increase in myocardial fiber length, as occurs with augmented ventricular filling (preload) during diastole, produces a more forceful ventricular contraction. This is known as the Frank-Starling law of the heart.
- Contractility is an expression of cardiac performance at a given preload and afterload. Contractility can be modulated by the autonomic nervous system, and rate and pattern of beating.
- In the normal heart, the rate of ATP hydrolysis is matched by the rate of ATP synthesis. ATP is generated by oxidative phosphorylation of fatty acids and glucose, a process that requires  $O_2$ . The rate of  $O_2$  utilization is coupled to the rate of cardiac work. The myocardium functions only aerobically.